Antal Kerpely Doctoral School of Materials Science and Technology

Improved Corrosion Resistance for Reinforced Concrete Using Environmentally Friendly Inhibitors

A dissertation submitted in partial fulfillment of the requirements for the degree of Doctor of Philosophy in Metallurgy as a part of Stipendium Hungaricum Scholarship in Material Science and Technology

By

Shaymaa Abbas Abdulsada

Supervisor

Dr. Tamás I. Török, Professor Emeritus

Head of the doctoral school
Prof. Dr. Zoltán Gácsi

Institute of Metallurgy
Faculty of Material Science and Engineering
University of Miskolc
Miskolc, Hungary
2021

RECOMMENDATION FROM THE SUPERVISOR TO

Shaymaa Abbas Abdulsada

PhD Candidate at University of Miskolc Antal Kerpely Doctoral School of

Materials Science and Technology

Mrs. *Shaymaa Abbas Abdulsada* had joined our Kerpely Doctoral School at University of Miskolc bringing with her a quite well thought out research topic from her home workplace at University of Kufa, Materials Engineering Department, Najaf-Iraq. Upon her affiliation in our Doctoral School it also became possible to extend our former traditional chemical metallurgical research fields with a scientifically rather complex as well highly technology oriented novel one.

In the past years Mrs. *Shaymaa Abbas Abdulsada* has shown great progress both in pursuing her PhD study courses quite successfully and also in designing, managing and completing her mostly experimental research program. She was able to co-operate quite efficiently with supporting teams she found in the relevant regional industries (Wanhua BorsodChem Ltd., CRH Magyarország Kft.), and also in a leading domestic research institute Zoltan Bay Nonprofit Kft. as well as in several well equipped laboratories at the two most traditional Faculties of University of Miskolc.

As her research topic is a rather interdisciplinary one it was also necessary to initiate and built up several internal collaborations between the laboratories at the Institutes of Polymers and Ceramic Engineering and that of the Physical Metallurgy, Metal Forming and Nanotechnology in addition to the host Institute of Metallurgy with its Laboratory of Surface Treatments and Surface Technologies dealing also with metals corrosion studies.

At the Faculty of Materials Science and Engineering Mrs. *Shaymaa Abbas Abdulsada* could manage quite independently and progress well with her PhD research work. She was also studious and successful in publishing her results regularly in several scientific international journals and is still planning to present her research results at international conferences as, for example, at the EUROCORR 2021 event.

All in all, in my view, her overall achievements can be highly valued based on the requirements of the Antal Kerpely Doctoral School of Materials Science and Technology, and having observed through the years her persistent enthusiasm and persevering endeavors in further developing herself, I can only wish her reaching her goals both in the successful completion of her PhD studies and fulfilling her dreams in her future academic and personal life.

Miskolc, 5 April, 2021

Dr. Tamás I. Török

Professor Emeritus

ACKNOWLEDGEMENTS

I am very thankful to *Mr. Kovács Árpád* for kind helping with the SEM+EDS measurements, thanks to *Ms. Márkus Zoltánné* for helping me in polishing the samples, both of them works at the Institute of Physical Metallurgy, Metal Forming and Nanotechnology in the Faculty of Materials Science and Engineering at University of Miskolc.

I would like to thank *Bioekotech Hungary Kft.* for supplying the superplasticizer type Oxydtron.

I am grateful for the advice and assistance that colleagues *Mr. Ferenczi Tibor* and Mr. *Gál Károly* have given me during work; they work in the Faculty of Materials Science and Engineering at University of Miskolc.

I owe a very special thanks to the Institute of Metallurgy's efforts, University of Miskolc, in providing all the possibilities available to us to make the work successful.

Finally, I am very grateful to my father and my mother for supporting me during the time of the study, and every day, they contact me to encourage and pray to complete this way. I don't forget the support from my brothers and my sisters; I am very thankful for them.

Shaymaa,
01 February 2021

List of papers

[**1**] A. Shaymaa Abbas, Ferenc Kristály, and Tamás I. Török, Distribution of corrosion products at the steel-concrete interface of XD3 concrete samples, Magazine of Civil Engineering. 2020. 100(8). Article No. 10005. DOI: 10.18720/MCE.100.5

[**2**] S. A. Abdulsada, T. I. Török, Investigations on the resistivity of XD3 reinforced concrete for chloride ions and corrosion with calcium nitrate inhibitor and superplasticizers, Cement Wapno, Beton, 25 (2020) 330-343. https://doi.org/10.32047/cwb.2020.25.4.7

[**3**] Abdulsada S. A., Bak R., Heczel A., Török T. I, Corrosion studies on XD3 reinforced concrete samples prepared by using calcium nitrate as inorganic corrosion inhibitor with different superplasticizers, Koroze a ochrana materiálu 64 (2020) 11-18. https://doi.org/10.2478/kom-2020-0002

[**4**] S. Abbas Abdulsada, Tamás I. Török, Studying chloride ions and corrosion properties of reinforced concrete with a green inhibitor and plasticizers, Structural Concrete, WILEY, 21(5), 1894-1904, 2020. https://doi.org/10.1002/suco.201900580

[**5**] S. Abbas Abdulsada, Tamás I. Török, Studying compression strength of XD3 concrete samples after addition of calcium nitrate inhibitor and superplasticizers, építőanyag-Journal of Silicate Based and Composite Materials 72 (2020) 16-19. https://doi.org/10.14382/epitoanyag-jsbcm.2020.3

[**6**] S. Abbas Abdulsada, Tamás I. Török, Studying effect of addition green inhibitor on compression strength of reinforced concrete, IOP Conference Series: Materials Science and Engineering 613 (2019) 012024 https://doi.org/10.1088/1757-899X/613/1/012024

[**7**] S. Abbas Abdulsada, É. Fazakas, Tamás I. Török, Corrosion testing on steel reinforced XD3 concrete samples prepared with a green inhibitor and two different superplasticizers, Materials and Corrosion, 70 (2019) WILEY, 1262-1272. https://doi.org/10.1002/maco.201810695

[**8**] Shaymaa Abbas Abdulsada, Tamás I. Török, Measurements and Studying Corrosion Potential of Reinforced Concrete Samples Prepared with and without a Green Inhibitor and Immersed in 3.5%NaCl Solution, Materials Science And Engineering, *MultiScience - XXXII. microCAD International Multidisciplinary Scientific Conference, University of Miskolc, 5-6 September, 2018*, 44 (2019) 5–13.

[**9**] S. Abbas Abdulsada, T.I. Török, É. Fazakas, Preliminary Corrosion Testing of Steel Rebar Samples in 3.5%NaCl Solution with and without a Green Inhibitor, építőanyag-Journal of Silicate Based and Composite Materials 70 (2018) 48-53. https://doi.org/10.14382/epitoanyag-jsbcm.2018.10

[**10**] S. Abbas Abdulsada, É. Fazakas, T.I. Török, Corrosion studies of steel rebar samples in neutral sodium chloride solution also in presence of a bio-based (green) inhibitor, International Journal of Corrosion and Scale Inhibition, 7 (2018) 38-47. http://dx.doi.org/10.17675/2305-6894-2018-7-1-4

Abstract

The breakthrough and diffusion of chloride ions into reinforced concrete structures is the major contributing factor for inducing corrosion of the steel reinforcement; therefore, this work focused on demonstrating the beneficial effects of green inhibitor (orange peels extract) and calcium nitrate on chloride-induced corrosion. Another reason for choosing and testing these types of inhibitors was to study their effectiveness in more depth by utilizing several distinct scientific approaches and using many different and highly sophisticated laboratory and materials testing techniques. In this way the chosen eco-friendly inhibitor (so-called green inhibitor) could also be compared with at least a less harmful inorganic one, namely calcium nitrate as that is also cheap and normally effective to mitigate the corrosion of iron in the given environment. Moreover, calcium nitrate can also be considered as a kind of replacement to the well-established nitrite inhibitor which latter one is also targeted by some toxicity concerns.

This work presented a study of the compressive strength and the porosity for concrete samples and focused on studying and analyzing the corrosion processes and the total chloride contents in concrete by testing electrical resistivity, half-cell potential, chloride ions concentration, and electrochemical polarization curves of concrete samples. The analysis was based on an experimental investigation of the samples with the time of immersion (during 18 months) in 3.5 wt.% NaCl aqueous solutions at room temperature according to European Standards. For this work, different mixtures of concrete were prepared by added corrosion inhibitors (orange peels extract and calcium nitrate) with concentrations of 1% and 3% by weight of cement to the concrete mix in addition to two different admixtures (superplasticizer admixture and water-resisting admixture). The results showed that low porosity, low chloride ion, and the more reduction in the chloride induced corrosion rate were observed in samples at 3 wt.% corrosion inhibitors (orange peels extract and calcium nitrate) with water-resisting admixture.

Összefoglaló

Vasbeton szerkezeteknél a betonacél erősítő szálak korróziós károsodásának egyik legveszélyesebb kiváltó oka klorid ionok beszüremkedése a betonba és diffúziója az acélbetét felületéhez. A kutatómunka éppen ezért irányult a kloridionok kiváltotta acélkorrózió gátlását célzó, azaz hatásos inhibiálására képes újfajta 'zöld' inhibitor és kalcium-nitrát inhibitor viselkedésének részletes tanulmányozására, amihez változatos tudományos módszertani megközelítést és különböző élvonalbeli nagyműszeres laboratóriumi anyagvizsgáló technikákat használtam. A kiválasztott környezetbarát, ún. zöld inhibitort, ilyen módon és az adott körülmények között, össze tudtam hasonlítani egy viszonylag olcsó és ugyancsak kevéssé káros szervetlen inhibitor-adalék, a kalcium-nitrát korrózió-gátló hatásával a beágyazott acélbetétre, arra is figyelemmel, hogy a kalcium-nitrát a korábban már kipróbáltnak és beváltnak tekinthető, de toxicitását tekintve mégis kedvezőtlen, nitrit inhibitort is kiválthatja.

Ebben a kutatómunkában a beton minták nyomószilárdságát és porozitását is vizsgáltam, de legnagyobb figyelmet a minták klorid-tartalmának és a korróziós folyamatok időbeli lefolyásának a tanulmányozására fordítottam, vizsgálva a vasbeton minták elektromos ellenállását, félcella potenciálját, a kloridion tartalmakat, továbbá felvéve az elektrokémiai polarizációs görbéket. A vizsgálatokat a vonatkozó európai szabványokban rögzített eljárások szerint, 3,5%(m/m) NaCl tartalmú vizes oldatokban, szobahőmérsékleten és 18 hónap időtartamig végeztem el. A vasbeton tesztminták narancshéj extraktum (zöld) inhibitort, illetve kalcium-nitrát inhibitort 1, illetve 3 %(m/m) mennyiségben tartalmaztak, külön-külön, a betonkeverék cement tartalmára vonatkoztatva, s emellett még kétféle betonadalékot is, egy szuper-plaszticizáló, illetve egy vízállóság-javító hatásút. Az eredmények csekély porozitást, alacsony klorid-tartalmat és az acélbetét kloridionok által kiváltott korróziója sebességének jelentős csökkenését mutatták a 3%(m/m) inhibitor (narancshéj extraktum, ill. kalcium-nitrát) tartalmú mintáknál, különösen azoknál, amelyek vízállóság-javító adalékot is tartalmaztak.

Symbols and Abbreviations

ACI	Admixed Corrosion Inhibitors
C2S	Dicalcium silicate (belite)
C_3A	Tricalcium aluminate
C_3S	Tricalcium silicate (alite)
C_4AF	Tetracalcium aluminoferrite
C_{cl}^-	Chloride concentration
Cr. Rate	Corrosion rate
CSF	Condensed Silica Fume
CSH	Calcium silicate hydrates
CTV	Chloride threshold value
D	Diffusion coefficient
E	Potential
$E_{0,Fe}$	Standard equilibrium potential
EDS (or EDAX)	Energy-dispersive X-ray spectroscopy
$E_{eq,Fe}$	Thermodynamically reversible potential
F	Faraday's constant
FA	Fly ash
FTIR	Fourier-transform infrared spectroscopy
GGBS	Ground granulated blast furnace slag
HDPE	High-Density Polyethylene
I_{corr}	Corrosion current
ICP-OES	Inductively Coupled Plasma - Optical Emission Spectroscopy
ITZ	Interfacial Transition Zone in Concrete
MCI	Migrating corrosion inhibitors
OPC	Ordinary Portland Cement
R	universal gas constant
RCS	Reinforced concrete structures
RH	Relative humidity
SEM	Scanning electron microscope
SF	Silica fume
T	Absolute temperature
t	time
w/c	water/cement ratio
W_{dry}	Weight of dry sample
W_{sat}	Weight of saturated sample
x	Thickness of concrete cover
XRD	X-ray diffraction
β	Tafel slope
β_a	Tafel slope for anodic reaction
β_c	Tafel slope for the cathodic reaction
a_{Cl}^-	chlorides activity

List of Figures

List of Tables

Table of Contents

Chapter One: Introduction

1.1 Background Information

The corrosion of steel reinforcement is one of the main causes of premature deterioration of reinforced concrete, leading to significant economic losses. Chloride ions in the marine zone or the use of thawing salts or carbonation in urban areas can cause rapid deterioration [1]. In general, for steel reinforcement, good quality concrete offers excellent protection. Because of the high alkalinity of concrete pore fluid, steel in concrete stays in a passive state initially and, in most instances, for long periods. Corrosion is initiated either due to a drop in alkalinity resulting from carbonation or the breakdown of the passive layer by chloride ion attack [2]. The concrete porosity and exposure class are decisive too from the point of view of rebar corrosion.

When ice accumulates on bridges during cold weather in countries like the United States, Canada, and Europe, salt is typically used to melt the ice. And when the concrete structures are and have been exposed to chemically aggressive agents such as chloride ions, either from deicing salts or the marine environment or chloride contaminated aggregates, the defensive passive steel stratum will be dissolved locally in the presence of chloride, so that the unprotected steel areas can and will begin to dissolve [3-7].

The corrosion of a reinforced concrete structure's steel reinforcement is an electrochemical process (as shown in Fig.1.1) and occurs when the concentration of dissolved ions inside the concrete varies, forming electrochemical potential cells or corrosion cells characterized by electrons and ions flowing between the cathodic and anodic regions [1].
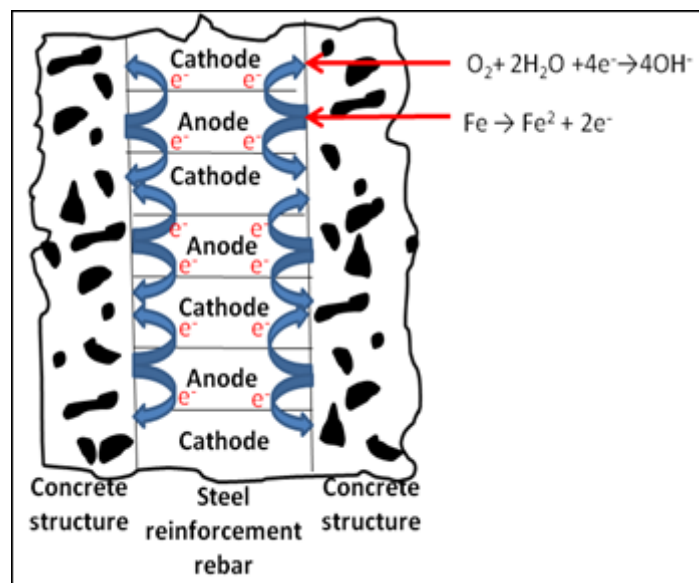
Figure 1.1 Representation of the corrosion process [1]

By using corrosion-resistant steels, cathodic safety, fusion-bonded epoxy coatings, corrosion inhibitors, and admixtures, steel corrosion can be alleviated. Corrosion inhibitors are the most commonly used of these approaches, with high cost-effectiveness and easy use. Inhibitors prevent corrosion from occurring by increasing concrete pH or fixing harmful ions that can cause steel corrosion [8].

The inhibitors often form a hydrophobic film on the reinforcement surface by adsorbing inhibitor ions or molecules on the surface. It decreases reinforcement corrosion by blocking cathodic or anodic reactions. The use of inhibitors with strong inhibiting effects is easy and economical [9].

Concerning corrosion inhibitors, the environmental issues caused by most chemicals in general and those used in corrosion protection, in particular, have favored the production of so-called 'green inhibitors.' According to the US Environmental Protection Agency, green inhibitors consist of chemicals and chemical processes intended to minimize or remove harmful impacts on the environment. Reduced waste materials, non-toxic elements, and increased performance may be involved in the use and processing of these chemicals. This form of corrosion inhibitor is referred to as environmentally safe inhibitors [10].

Plant extracts contain a large range of organic compounds. The natural constituents of these extracts include N, O, and S containing heterocyclic macromolecules, which can form protective layers to eliminate water molecules and inhibit the ingression of destructive species such as Cl^-, SO_4^{-2} and CO_2 when they meet the steel surface by diffusion and are adsorbed at the steel-concrete interface by secondary molecular interaction with metal and metal oxide [11]. Another group [12] used compounds such as carboxylates, distinguished by the inclusion of the carboxylic acid (-COOH) group, as organic inhibitors. These compounds, similar to amines, have the ability to bind to the metal surface, thereby forming an organic coating and shielding the steel from corrosion. Carboxylate-based inhibitors appear to decrease cement hydration rate by increasing setting time and slowing the increase in resistance rate, among the effects produced in concrete [12].

Inorganic and organic inhibitors are widely used corrosion inhibitors to investigate a new corrosion inhibitor class to replace the effective calcium nitrite inhibitor that caught on in the late 1980s when European regulations started to limit its use due to toxic and environmental concerns. Organic and inorganic inhibitors have been tested as alternatives to address these disadvantages. The need to integrate a non-toxic and environmentally

friendly inhibitor into concrete structures to avoid rebar corrosion phenomena led to the study of nitrate-based compounds [13].

1.2 Summary of Previous Research

In the literature, general steel corrosion mechanisms in concrete and all related subjects (protection, monitoring, repair) have been reported and have focused on many conferences, books, and journals. It follows a review that illustrates some of the possible shortcomings of the previous researches.

The slow corrosion process quickly became evident and was an apparent setback when researchers started paying attention to concrete corrosion. Correspondingly, many of the researchers concentrated on corrosion inhibitors, and today they are widely used in reinforced concrete corrosion research. The efficacy of commercial migration organic inhibitors for steel reinforcement corrosion in concrete was studied by Bolzoni F. et al. (2006). Two organic migratory inhibitors (based on amine and alkanolamine) were added to the concrete surface, and for more than four years, Bolzoni F. et al . were regularly monitored the free corrosion potential and corrosion rate of the steel reinforcing bars. The results show that migration inhibitors are not effective in reducing the corrosion rate, either for corrosion induced by chloride or carbonation, although some effect has been observed in delaying the initiation of corrosion in the case of penetration of chloride [14].

The effect of the addition of calcium nitrite on the passive rebar films was investigated by Yanbing Tang et al. (2017) to discover what allows calcium nitrite to further extend the service life of reinforced concrete structures. The concrete mix inhibitor was applied and the findings showed that the passivation behavior of rebar was drastically altered by the addition of calcium nitrite after measurement. In other words, the passive film produced in the 10 g/L $Ca(NO_2)_2$ samples had less donor density (Nd), more positive plate potential, smoother surface area and lower Fehydrox content than that produced without $Ca(NO_2)_2$ [15]. The influence of amino-alcohol-based corrosion inhibitors on concrete durability by admixed form and surface-applied form was presented by Congtao Sun et al. (2019). The findings showed that after the two types of corrosion inhibitors were added, the anti-penetrability, compactness, and hydration of concrete were improved. The penetration of chloride ions and water into concrete was mitigated by using corrosion inhibitors, effectively delaying the reinforcing bar's corrosion. The surface-applied corrosion inhibitor showed better efficiency in the concrete specimens compared to the admixed form [16].

Some researchers have used green inhibitors (extracted from plants) to minimize corrosion problems in reinforced concrete because it is also very inexpensive and less harmful to

humans and the environment. Eyu D. G et al. (2013) studied the green inhibitor's effect on the corrosion activity of reinforced carbon steel in concrete and compared it with calcium nitrite and sodium nitrite by using vernonia amygdalina extract. After the measurements, they found that the vernonia amygdalina (bitter leaf) extract acts as an excellent corrosion inhibitor for rebar steel, with improved dose efficiency increases, and the physical adsorption mechanism was the inhibition mechanism responsible for shielding the specimen from the corrosive atmosphere [17].

Organic inhibitors used by Herbert Sinduja et al. (2019) were isolated from Azadirachta indica (neem) powder and dehydrated Aloe-vera powder, and calcium nitrate was the inorganic inhibitor used. Inhibitors were applied during concrete mixing (2% of cement weight) and then the samples were immersed in the corrosion induction solution of sodium chloride (NaCl). The inhibitors' results showed that compared to Aloe-vera inhibitor and calcium nitrate inhibitor, Azadirachta indica has superior corrosion inhibition ability [18]. Varvara Shubina H. et al. (2019) researched Rhamnolipids (RLs) as an eco-friendly rebar corrosion inhibitor in a simulated concrete pore solution. Two application methods were tested: applying RLs as a steel coating (conditioning method) and adding the RLs directly to the hostile setting (addition method). Two application methods were tested. In a simulated concrete pore solution containing 0.5 M NaCl, both methods were tested for their ability to protect steel [19]. Rajan Anitha et al. (2019) tested extracts of Rosa damascena (R. damascena) leaves on reinforced steel rebar as a green corrosion inhibitor. Electrochemical tests have shown that the charge transfer resistance increases as the concentration of acid and ethanol extracts of R. damascena increases. Tafel polarisation curves indicate that the potential is moved to the positive side, illustrating the inhibitor's nobility [20].

Chapter Two: Concrete

Concrete is a composite material characterized by aggregates and porous cement paste, the reaction product of cement with additional mixing water. It is usually reinforced with embedded carbon steel rebars: the incorporation of reinforcements into the cement paste allows the steel to be shielded from violent atmospheric conditions, avoiding different kinds of deterioration and corrosion.

2.1 Concrete general aspects

A mixture of limestone and clay raw materials is the constitutive element of cement: the primary components are calcium silicates and aluminates. The mineral powder forms colloidal, hydrated products of very poor solubility in the presence of water. Cement paste solidification is primarily caused by the hydration of first-reacting aluminates; hydration of silicates contributes to the formation of calcium silicate hydrates, a hard gel known as CSH gel. It is characterized by very small particles with a thin-spaced layer structure of less than 2 nm and a wide surface area (100-700 m^2/g): the CSH gel can give the cement paste considerable strength due to this conformation [21]. An aqueous solution of calcium , sodium and potassium hydroxides ($Ca(OH)_2$, NaOH, KOH) is formed during hydration and accumulates within the pores. The chemical composition of the pore solution depends on the concrete materials, but due to the high alkalinity of the dissolved species, the solution pH ranges from 12 to 14 [22].

Carbon steel passivates in aerated, chloride-free, alkaline solutions at pH > 9.2 since a protective oxide film forms [23]. This is what happened in rebars within concrete: the pore solution's alkalinity is sufficient to guarantee a stable passivity condition and a virtually zero metal corrosion rate. The passive layer is just a few nanometers thick and is likely to be part of metal oxide hydroxide and part of cement mineral; it is a thin, impenetrable film that can prevent corrosion instauration [24]. The passivating environment, however, is not always preserved: concrete carbonation and chloride attack are the two conditions which compromise the integrity of the protective layer. A physical shield, called a concrete cover, is an additional defensive effect of cement on rebars that prevents the metal from slowing down the penetration of aggressive animals. The diffusion from the atmosphere to the carbon steel surface of oxygen, water or aggressive ions (such as chlorides) will lead to the introduction of metal corrosion, hence concrete degradation.

The transport mechanisms of fluids and ions inside concrete are a key factor in their longevity; the diffusion of these substances is connected to their concrete properties

(porosity and presence of cracks), their binding to cement paste, and the environmental conditions of the concrete surface [21].

During cement paste hydration, interconnected pores of different sizes are often created: the durability of concrete is strictly related to the dimension and distribution of these voids. Pores are divided into macropores, pores of the capillary and pores of the gel (Fig. 2.1). The above constitute the CSH gel interlayer spaces and do not impact cement permeability because they vary in dimension from a few nm to many nm.
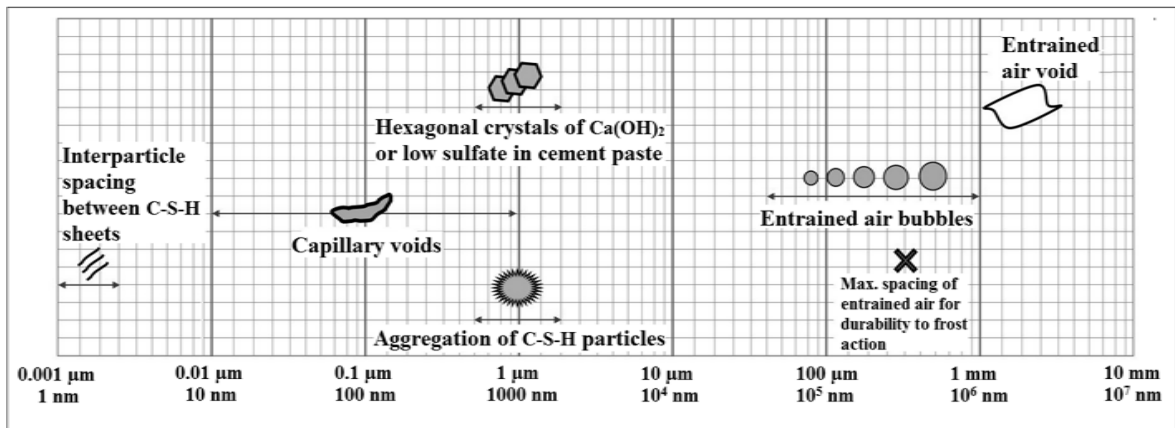
Figure 2.1 Dimensional range of solids and pores in hydrated cement paste [5]

Bigger voids are defined by capillary pores, not by solid hydrate products that fill space. According to the water/cement ratio (w/c) adopted, they may have different sizes: low ratios are favored because they ensure voids of tens of nm, not a crucial dimension for penetration by aggressive conditions. Macropores, on the other hand, are critical for concrete durability and rebar safety because they can exceed a few mm in size; they are usually induced during mixing by trapped air and not removed by fresh concrete compaction [25]. The size and distribution of pores as well as the amount of aqueous solution contained in them are important; the diffusion into concrete of aggressive species depends on the water's transport properties. The water content within the pores of the concrete exposed to the atmosphere is related to the relative humidity of the environment, in the absence of humidity and under conditions of equilibrium. Water is first adsorbed on its surface within capillary voids and then, as the relative humidity increases, it fills up the pores, beginning with the smallest and then progressing to the larger ones, as shown in Fig.2.2. The diffusion in the gaseous process of aggressive conditions is related to the water content within the pores. Gas diffusion is impeded in the presence of full water-filled pores, intertwined with each other; on the other hand, voids with water only adsorbed on the surface encourage it.
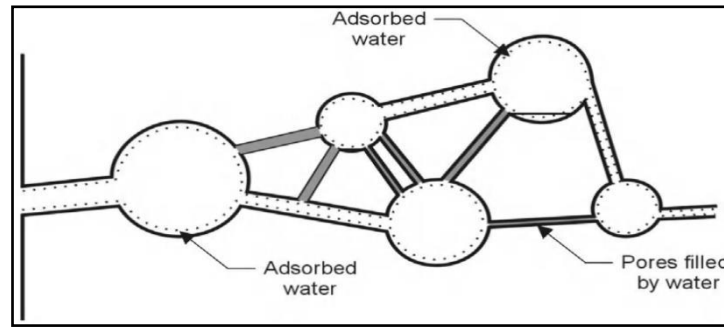
Figure 2.2 Representation of water present in capillary pores [21]

As regards the kinetic diffusion of ions, the presence of water free from surface capillary tensions is encouraged: its transport properties are identical to those of a bulk solution [21]. The most important steps to be taken to improve concrete durability are based on the good dimensioning of the concrete cover and the right choice of mix design: the correct choice of water/cement ratio, cement form, dimension and aggregate size distribution is included [26].

2.1.1 Exposure classes for designing durable concrete

Published in 2000, European Standard EN 206-1 classified exposure groups based on various degradation mechanisms [27]. This was, in fact, one of the first attempts to break away from the hitherto arbitrary division of groups of exposure and base the class description on a more logical basis. Details of the European exposure groups are given in Table 2.1, which is divided into the following six major categories:

• No risk of corrosion or attack

• Corrosion induced by carbonation

•Corrosion induced by chlorides other than from sea water

•Corrosion induced by chlorides from sea water

•Freeze/thaw attack with or without de-icing salts

• Chemical attack.

Such groups are further sub-divided into sub-classes, totaling 18, thereby extending their meanings. Table 2.1 also contains standard examples that illustrate various sub-classes. The idea of 'intended service life' was also adopted by the European Standard, which offered guidelines on the limiting values of the concrete composition, based on the assumption of the intended working life (indicative design working life displayed in Table 2.2 according to EN 1990: 2010 [28]) of a 50-year structure. Limitation values are shown in Table 2.3. These values apply to the use of cement type CEM I in compliance with EN

197-1 [29] OPC (Ordinary Portland Cement) and of aggregates with a nominal maximum size of 20-32 mm. It is possible that concrete will be subject to more than one mechanism of degradation. In such a case, the standard notes that it may also be appropriate to express 'environmental conditions to which it is exposed as a combination of exposure classes' [27]. It further notes that "it is possible that various concrete surfaces will be subjected to different environmental behavior for a given structural component."

Table 2.1 Exposure class related to environmental conditions in accordance with EN 206-1 [27]

Class designation	Description of the environment	Informative examples where exposure classes may occur
1	**No risk of corrosion attack**	
X0	For concrete without reinforcement or embedded metal: all exposure except where there is freeze/thaw, abrasion or chemical attack. For concrete with reinforcement or embedded metal: very dry	Concrete inside buildings with very low air humidity
2	**Corrosion induced by carbonation**	
XC1	Dry or permanently wet	Concrete inside building with low air humidity. Concrete permanently submerged in water
XC2	Wet, rarely dry	Concrete surfaces subject to long-term water contact. Many foundations
XC3	Moderate humidity	Concrete inside buildings with moderate or high air humidity. External concrete sheltered from rain
XC4	Cyclic wet and dry	Concrete surfaces subject to water contact, not within the exposure class XC2
3	**Corrosion induced by chlorides**	
XD1	Moderate humidity	Concrete surfaces exposed to airborne chlorides
XD2	Wet, rarely dry	Swimming pools. Concrete components exposed to industrial waters containing chlorides
XD3	Cyclic wet and dry	Parts of bridges exposed to spray containing chlorides. Pavements. Car park slabs

4	Corrosion induced by chlorides from sea water	
XS1	Exposed to airborne salt but not in direct contact to sea water	Structures near to or on the coast
XS2	Permanently submerged	Parts of marine structures
XS3	Tidal, splash and spray zones	Parts of marine structures
5	Freeze/Thaw attack	
XF1	Moderate water saturation, without de-icing agent	Vertical concrete surfaces exposed to rain and freezing
XF2	Moderate water saturation, with de-icing agent	Vertical concrete surfaces of road structures exposed to freezing and air-borne de-icing agents
XF3	High water saturation, without de-icing agents	Horizontal concrete surfaces exposed to rain and freezing
XF4	High water saturation, with de-icing agents or sea water	Road and bridge decks exposed to de-icing agents Concrete surfaces exposed to direct spray containing de-icing agents and freezing Splash zone of marine structures exposed to freezing
6	Chemical attack	
XA1	Slightly aggressive chemical environment according to EN 206-1, Table 2.3	Natural soils and ground water
XA2	Moderately aggressive chemical environment according to EN 206-1, Table 2.3	Natural soils and ground water
XA3	Highly aggressive chemical environment according to EN 206-1, Table 2.3	Natural soils and ground water

Table 2.2 Indicative design working life in accordance with EN 1990: 2010 [28]

Design working life category	Indicative design working life (years)	Examples
1	10	Temporary structures [1]
2	10-25	Replaceable structural parts, e.g. gantry girders, bearings
3	15-30	Agricultural and similar structures
4	50	Building structures and other common structures
5	100	Monumental building structures, bridges, and other civil engineering structures

[1] Structures or parts of structure that can be dismantled with a view to being re-used should not be considered as temporary

Table 2.3 Recommended limiting values for composition and properties of concrete in accordance with EN 206-1 [27]

	Exposure classes																		
	No risk of corrosion or attack	Carbonation-induced corrosion				Chloride-induced corrosion						Freeze/ thaw attack				Aggressive chemical environments		
						Sea water			Chloride other than from sea water									
	X0	XC1	XC2	XC3	XC4	XS1	XS2	XS3	XD1	XD2	XD3	XF1	XF2	XF3	XF4	XA1	XA2	XA3
Maximum w/c	-	0.65	0.60	0.55	0.50	0.50	0.45	0.45	0.55	0.55	0.45	0.55	0.55	0.50	0.45	0.55	0.50	0.45
Minimum strength class	C12/15	C20/25	C25/30	C30/37	C30/37	C30/37	C35/45	C35/45	C30/37	C30/37	C35/45	C30/37	C25/30	C30/37	C30/37	C30/37	C30/37	C35/45
Minimum cement content (kg/m^3)	-	260	280	280	300	300	320	340	300	300	320	300	300	320	340	300	320	360
Minimum air content (%)	-	-	-	-	-	-	-	-	-	-	-	-	4.0[a]	4.0[a]	4.0[a]	-	-	-
Other require-ments												Aggregate in accordance with EN 12620 with sufficient freeze/thaw resistance					sulfate-resisting cement [b]	

[a] Where the concrete is not air entrained, the performance of concrete should be tested according to an appropriate test method in comparison with a concrete for which freeze/thaw resistance for the relevant exposure class is proven

[b] When SO_4^{2-} leads to exposure classes XA2 and XA3, it is essential to use sulfate-resisting cement. Where cement is classified with respect to sulfate-resisting cement, moderate or high sulfate-resisting cement should be used in exposure class XA2 (and in exposure class XA1 when applicable) and high sulfate-resisting cement should be used in exposure class XA3.

2.1.2 Cements and hydration

There are different forms of cement, most of them based on clinkers of Portland cement. It consists, to a large extent, of tricalcium and dicalcium silicates and, to a limited extent, of aluminates of calcium and iron calcium, gypsum and other minor constituents, such as alkaline oxides (Na_2O, K_2O) [30]. It reacts to calcium silicate hydrates, abbreviated as CSH, when combined with water, a gel consisting of particles with a layer structure [30]. Calcium hydroxide ($Ca(OH)_2$) is another Portland cement hydration substance that is important to the corrosion behavior of embedded steel.

One of the major factors impacting on the compressive strength of concrete is the hardening phase of concrete. In concrete, the binder is cement. During the hydration process, the cement matrix is formed and binds the aggregates together.

Limestone ($CaCO_3$), silica (SiO_2), alumina (Al_2O_3), iron oxide (Fe_2O_3) and other substances in minor amounts are the essential elements in the manufacture of Portland cement. The raw materials are mixed, ground and burned in a rotary kiln at about 1450°C for the production of cement clinkers. To form new minerals, the constituents react. Tricalcium silicate (C_3S), dicalcium silicate (C_2S), tricalcium aluminate (C_3A) and tetracalcium aluminoferrite (C_4AF) are the four principal minerals in cement clinkers.

When water is added, the minerals in the clinker start reacting. This sequence of chemical reactions is called the process of hydration, and consists of different phases. It begins immediately, and on the first day [31,32] the dominant reactions occur. Chemical reactions, however, persist for months or even years, eventually slowing down. In engineering practice, after about 28 days when the representative intensity is achieved, the hydration process is always expected to be 'finished'. It is described according to Locher [33] schematically in Fig.2.3.
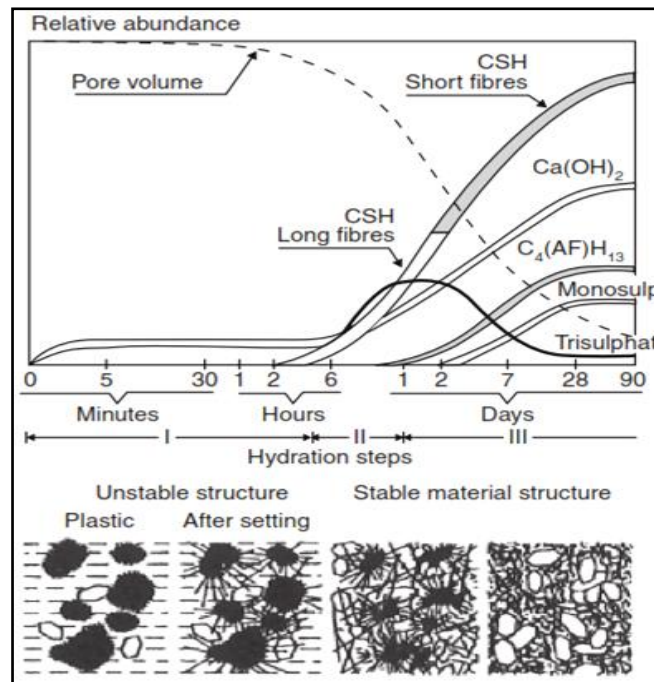
Figure 2.3 Scheme of the hydration process according to Locher [33]. (Top) The development of the individual components and (bottom) schematic sketches of the material structure at four corresponding stages in time

Some siliceous materials are also able to react with water and calcium hydroxide to produce calcium silicate hydrates. These materials are referred to as pozzolanic or pozzolanic materials, and the so-called pozzolanic reaction [30] is the reaction leading to CSH. When blended with Portland cement, the calcium hydroxide content in the hydrated cement paste(as consumed in the pozzolanic reaction) is reduced, but the amount of CSH is increased. Moreover, they are typically associated with lower energy use during processing (as they are waste products from other manufacturing processes) and/or lower emissions that adversely impact the environment.

Fly ash (FA, a by-product of coal combustion in thermal power plants), condensed silica fume (SF, a waste product of the silicon or ferro-silicon processing industry), and natural pozzolanas, such as volcanic ashes, are pozzolanic materials widely used in the cement industry to partially replace ordinary Portland cement. Portland cement is mixed with other mineral additions, such as ground granulated blast furnace slag (GGBS, a by-product of the steel industry) or limestone filler, in addition to pozzolanic materials.

The EN 197-1 [29] European standard distinguishes the following forms of cement:

• Portland cement (CEM I), with >95% clinker.

• Portland-composite cements (CEM II) with up to 35% of another single mineral constituent (GGBS, SF, FA, natural pozzolanas, burnt shale, or limestone).

• Blast furnace slag cement (CEM III) with 36–95% GGBS.

• Pozzolanic cement (CEM IV) with 11–55 % of a pozzolanic material (SF, FA, or natural pozzolanas).

• Composite cement (CEM V) with 18–50% GGBS and 18–50% FA or natural pozzolanic material.

Pozzolanas (and other mineral additions) may also be applied at the concrete plant in addition to blended cements, where binders and mineral additions are blended by the cement manufacturer.

2.1.3 Moisture content

Chemically bound water (combined in hydration products), interlayer water (held in gel pores, the gel-pores water cannot be removed. A T-relative humidity curve would be very informative), adsorbed water (on pore walls), capillary water (held in capillaries), and water in macro pores and air vacuums may be found in concrete in various ways. The quantity of chemically bound water depends on the degree of hydration; its quantity is normally assumed at 0.23–0.25 g water / g cement at maximum hydration (alpha= 1).

Only when cement paste is ignited and decomposed (at temperatures up to > 1000°C) is chemically bound water released [34].

On the other side, interlayer water, adsorbed water, capillary water, and water are evaporative in macro pores. A film of adsorbed water, regardless of pore size, is present on the pore walls when water has evaporated from the pores. The thickness of the adsorbed layer depends on the relative humidity of the pores and the volume of adsorbed water in the cement paste pore system is proportional to the surface of the inner pore. Capillary pores, by capillary powers, retain water. The radius of the capillaries filled with stable water depends, among other factors, on the ambient temperature and relative humidity. According to this theory, the stable radius of a cylindrical pore is in the range 3-10 nm for relative humidities of 70 percent to 90 percent at a temperature of 20°C [34].

2.1.4 Permeability and transport properties

Permeability is known as the property of concrete that measures how easily when pressure is applied a fluid can flow through concrete. There may be an external water pressure in some kinds of construction, such as dams and tunnel lining, but in others it may be absorption processes that generate differential pressure.

The importance of a high permeability to a structure may not be merely the ability of water to penetrate it; chlorides and sulphates dissolved in the water may cause more serious damage, which can then affect the reinforcement and the concrete itself. Diffusion is a

mechanism by which an ion can pass without the flow of water through saturated concrete. Diffusion is guided by the gradient of concentration. They would also lead for the same concentration if a strong solution is in contact with a weak solution. Thus, for example, if a pile of salt is put in one corner of a container full of water diffusion, it will be the mechanism that ensures that a uniform concentration in the water is assumed when the salt has dissolved [35].

With certain exceptions (e.g. lightweight aggregates), aggregates typically have low permeability and thus transport mechanisms occur basically through the pore structure of the cement paste, the ITZ, and concrete cracks or fissures. Since gel water and adsorbed water are under the control of surface forces, it is commonly assumed that they do not contribute significantly to transport processes. Therefore, transport characteristics can be associated with the quantity and interconnectivity of capillary pores. This is evident in Fig.2.4a, which indicates the coefficient of permeability for the stationary transport of water in cement paste vs. the capillary porosity volume fraction. The pore structure, and in particular the existence of capillaries, depends strongly on the w/c ratio and degree of hydration, as discussed above, and it would therefore not be surprising if permeability was associated with the w/c ratio. Fig.2.4b shows that this is indeed the case (for hydrated cement paste) and that permeability increases markedly and non-linearly with the w/c ratio rising, particularly above w/c ≈ 0.5 [34].
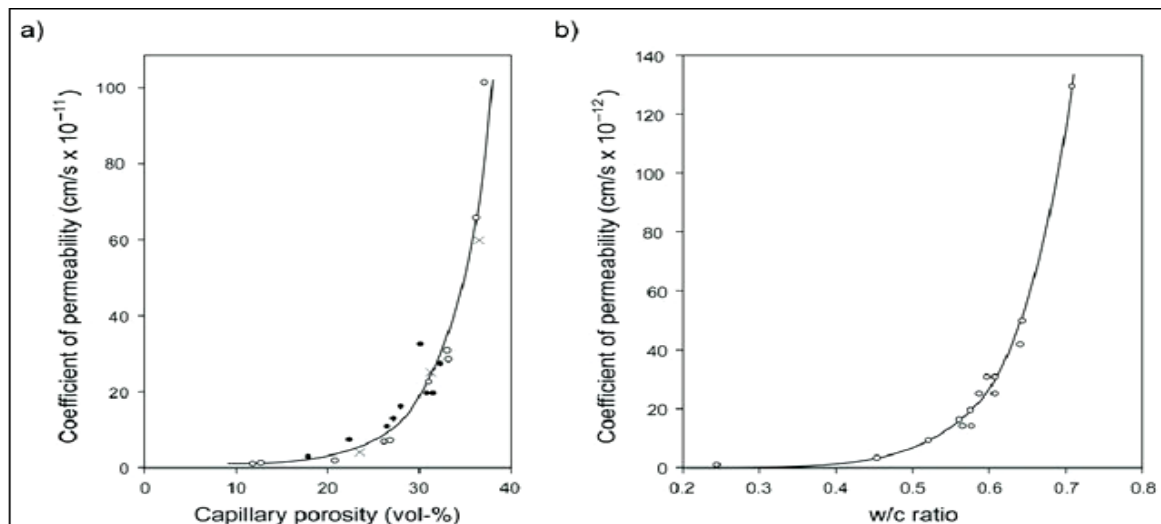
Figure 2.4 a) Relationship between water permeability and capillary porosity, according to Powers, different symbols represent different cement pastes; b) permeability vs. w/c ratio of mature cement paste ($\alpha = 0.93$), according to Powers et al. [34]

2.1.5 Chloride ingress into concrete

The most prevalent method associated with reinforced concrete degradation is the entry of chloride-contaminated water either from deicing salt used for winter maintenance purposes

for snow and ice prevention on roads or from the marine environment where, for example, bridges span tidal estuaries. Although the use of deicing salt is likely to continue for the near future and concrete structures will still be put in the marine environment or close to it, nothing can be done to avoid the exposure of structures to chloride salts. The premature degradation of concrete structures due to the ingress of chloride and subsequent corrosion of the steel reinforcement is a global issue and imparts a major drain on maintenance resources, not only in terms of the required remedial work, but also in terms of the costs associated with routine inspections and testing along with indirect costs [36].

Performance-related approaches that are more applicable to corrosion resistance consider each applicable degradation process, the working life of the part or structure and the parameters determining the end of this working life (e.g. time to initiation of corrosion) in a quantitative manner [36]. It is necessary to acknowledge the Fig.2.4 is valid for cement paste; for concrete, which also includes aggregates, ITZ (Interfacial Transition Zone in Concrete) and cracks, transport properties and permeability are distinct. In the water process, transport of hostile ionic molecules, such as chloride ions, occurs primarily through the following mechanisms: capillary suction, diffusion, permeation and migration [34].

2.1.6 Durability aspects

The durability of concrete is distinguished by its resistance to weathering, chemical attacks and other processes of degradation [37]. Concrete durability depends on the degree of exposure, the grade (or strength) of concrete and the content of cement. The effects of moisture penetration can be best resisted by a high density. Since concrete is a porous material, if precautions are not taken, reinforcing bars inside the concrete will be subject to potential corrosion. The requirements should provide sufficient concrete 'cover' for the reinforcement in order to avoid moisture or salts entering the rebar. If the rebar corrodes, the rebar expands and the major forces involved cause the concrete to crack [38].

2.1.7 Superplasticizers

In concrete preparation, superplasticizers are chosen for their ability to minimize the need for water while retaining workability and allowing strength to be improved. The working mechanism of the superplasticizer is shown in Fig.2.5. Cement particles are distributed by the repulsive force generated by negatively charged superplasticizers (Fig. 2.5 / b), as in our case , for example, by the modified Mapei Dynamon SR 31 acrylic polymer, and the trapped water is released. The flow characteristics of concrete are also enhanced [39].
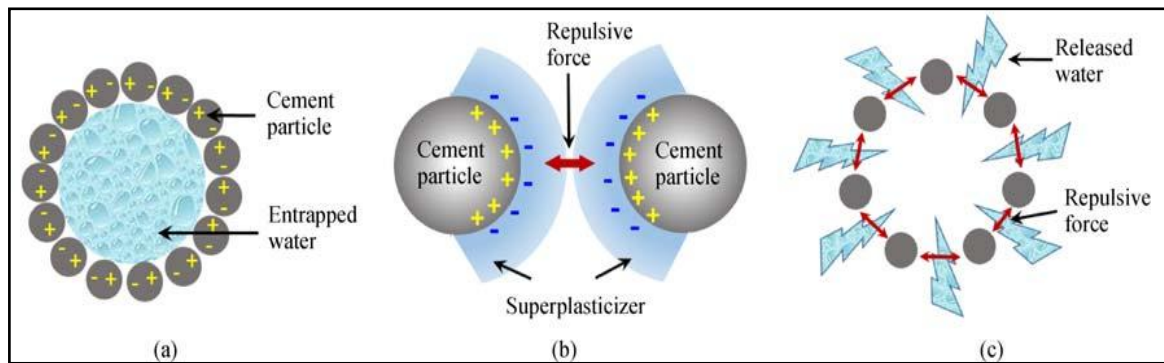
Figure 2.5 Action of superplasticizer on cement particles. (a) Flocculated cement particles; (b) dispersing cement particles by the repulsive force generated by negatively charged superplasticizer; (c) releasing of entrapped water [39]

2.2 Steel embedded in concrete

2.2.1 Alkaline environment and passivity

The alkaline condition of the concrete, through the creation of a passive film of iron oxides, provides natural protection for steel reinforcement against corrosion. By carbonation or by chloride attack, passivation of steel can be killed. Corrosion, in the presence of moisture and oxygen, can begin once the passive film breaks down. Steel corrosion is defined as an electrochemical process involving: (i) an anode where iron is removed from steel, Fe^{2+}, (ii) a cathode where OH-hydroxyl ions are formed, (iii) an electrical conductor for transmission of electrons, and (iv) an ion transfer electrolyte. The released hydroxyl ions migrate through the electrolyte at the cathode to react with the ions at the anode, generating rust [40]. Concrete retains water in the pore structure in normal environmental conditions. The chemistry of this water, hereinafter referred to as concrete pore solution, is largely dependent on the concrete hydration products in the concrete as they are in equilibrium with the pore solution.

The alkalinity is usually high due to the presence of $Ca(OH)_2$ as well as alkali metal ions Na^+ and K^- [34].

Steel is capable of passivity due to its elevated alkalinity (Fig. 2.6). As long as the pH stays at a high level, the passive film is stable, according to Fig.2.6 above pH~9. Leaching, e.g. in the outer cover zone exposed to rain, or carbonation, i.e. the reaction of calcium hydroxide with CO_2 from the atmosphere, may affect the alkalinity of concrete pore solution. Although the pH in the presence of pozzolanas is usually not reduced to levels that make it difficult to shape a passive layer, the resistance to alkalinity loss due to contact with the environment is lower when pozzolanas are used [41].
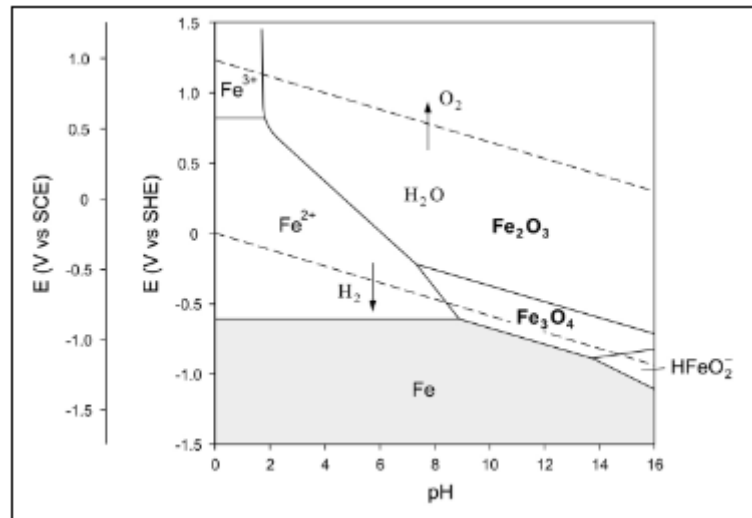
Figure 2.6 Pourbaix diagram for iron in water (for ion concentration 10^{-6} mol/l and 25°C). Only Fe, Fe_3O_4, Fe_2O_3 as solid products considered [41]

2.2.2 Chloride threshold value

One of the significant causes of premature deterioration of reinforced concrete structures (RCS) is known to be chloride-induced steel corrosion. Marine environments and the extensive use of de-icing salts can cause the passive layer to rupture, allowing the steel surface to work as a combined anodic and cathodic reaction cell where corrosion processes may take place [42-44]. Chloride-induced concrete reinforcement corrosion has been extensively studied under various conditions in the last five decades, often in relation to the chloride threshold value (CTV) or critical chloride content [45-47]. The chloride content associated with reinforcement de-passivation in non-carbonated alkaline concrete [48] is known as CTV. This just takes the initial corrosion stage into consideration.

CTV can be expressed either as the total content of chloride as a cement / concrete percentage by weight, or as the molar ratio between $[Cl^-]$ and $[OH^-]$. In a solution environment, the $[Cl^-]/[OH^-]$ ratio represents the ratio of aggressive ions to inhibitive ions that lead to corrosion initiation. In addition, the $[Cl^-]/[OH^-]$ ratio has the benefit of being simple to calculate. The corrosion danger of bound chloride and the inhibitive effect of cement hydration products are also taken into account [49].

The high alkalinity of the concrete pore solution, significantly above the pH needed for iron passivation (Fig. 2.6), is thus a major explanation for the corrosion-induced resistance to chloride. This must be taken into account when reducing the pH due to the use of pozzolanic material [41].

2.2.3 Concrete cover and service life

One of the most critical parameters in the manufacture of reinforced concrete components is the concrete cover, as the concrete cover must ensure that:

1-Firm transfer of adhesive forces between reinforcement and concrete;

2-Sufficient resistance of a structure to fire;

3-Sufficient protection against corrosion of steel reinforcement.

The minimum requirements for concrete cover according to the increase in exposure class and concrete strength class according to EN 206-1[27] are provided in Table 2.4.

Table 2.4 Dependence of the concrete cover on exposure class and concrete strength class [27]

Exposure class	XC0	XC1	XC2, XC3	XC4	XD1, XS1, XF1, XA1	XD2, XS2, XF2, XA2	XD3, XS3, XF3, XF4, XA3
Concrete class	<C30/C37	<C30/C37	<C35/C45	<C40/C50	<C40/C50	<C40/C50	<C45/C55
Min. concrete cover (mm)	10	10	15	20	25	30	35
Concrete class	≥C30/C37	≥C30/C37	≥C35/C45	≥C40/C50	≥C40/C50	≥C40/C50	≥C45/C55
Min. concrete cover (mm)	10	10	10	15	20	25	30

To protect the rebar against corrosion and to provide resistance against fire, concrete reinforcement cover is required. Cover thickness depends on the environmental conditions and the structural member type. The minimum thickness of the reinforcement cover shall be indicated or extracted from the applicable code of practice in the drawings [50].

2.2.4 Corrosion initiation and propagation stage

Initiation and production of corrosion are both affected by factors and environmental factors related to concrete. One of the key environmental factors is the availability of oxygen: because corrosion can only occur when oxygen is available, the very low corrosion kinetics for underwater concrete are clarified. As with relative air humidity, the external concentration of hostile agents (chloride ions) is a crucial factor because humidity favors transport mechanisms through concrete. Carbonation in concrete pores almost only

occurs at a relative humidity (RH) between 40% and 90%. When the relative humidity in the pores is higher than 90% carbon dioxide is not able to enter the pore, and when RH is lower than 40% the carbon dioxide can not dissolve in the water. This dependency on environmental conditions for the production of corrosion can give rise to difficulties in assessing the material quality, since the measurements at the time of investigation are also highly dependent on temperature and humidity [51-53].

The two key variables for concrete are the cover depth and the porosity of the concrete. Cover plays a simple role; since both carbonation and chloride entry are processes of diffusion, their rate of development is a time power function, with an exponent of about 0.5. This implies the doubling of the cover multiplies the time before initiation by a factor of four. This offers an easy way to increase the durability of concrete. Porosity constitutes the second aspect.

The rate of any phase of transport depends on the pores' volume fraction, tortuosity and connectivity. This is measured by factors such as the ratio of water to cement (w/c), the content of cement, the fineness of cement, the form of cement, the use of materials to replace cement (such as ground granulated blast furnace slag, pulverized fuel ash or silica fume), the compaction of concrete and the degree of hydration. As the matrix can bind some of the chlorides and thus decrease the pH loss, the concrete mix also has an effect on the input of chlorides [37].

The corrosion rate is controlled by the kinetics of the reaction steps once stable pitting corrosion has been created, viz. As shown in Fig. 2.7 [34], the anodic reaction, the cathodic reaction and the ionic current flow in the macro-cell.
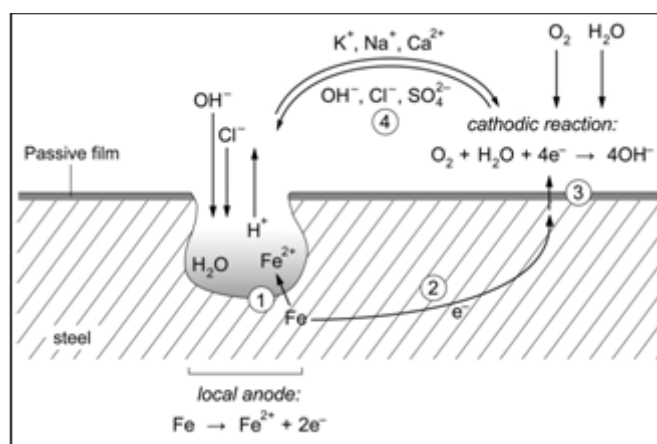
Figure 2.7 Schematic illustration of chloride induced pitting corrosion and reaction steps: 1. Anodic iron dissolution; 2. Flow of electrons through metal; 3. Cathodic reduction reaction; 4. Ionic current flow through the electrolyte [34]

Chapter Three: Fundamentals of Steel Reinforcement Corrosion

This section deals with fundamental concerns related to concrete reinforcement corrosion, including corrosion processes and inhibitors of corrosion.

3.1 Corrosion processes

Reinforcement corrosion in concrete is primarily related to the concrete or chloride penetration carbonation into the concrete. Both of these cause the steel to become (i.e. de-passivated-see later) thermodynamically unstable and thus to corrode. When the steel begins to corrode aggressively, the concrete framework is deteriorated and can endanger its structural performance [54]. Three phases are involved in the degradation of RC structures due to steel corrosion, as shown in Fig. 3.1 [55]:

(i) An initiation period before the beginning of corrosion, during which there is little to no damage. However, the introduction of harmful substances such as chlorides and carbon dioxide takes place during this time, which can ultimately lead to de-passivation of the steel reinforcement and eventually cause corrosion of the reinforcement. Concrete permeability, pore solution chemistry, environmental exposure conditions, cover depth, and potential cracking of the concrete primarily influence the intake of hazardous substances and the progress of carbonation.

(ii) A process of propagation after activation of corrosion that generates expansive products of corrosion, causing the cover concrete to crack.

(iii) An acceleration stage where the rate of corrosion increases due to easy access through cracks and spalls of oxygen, moisture and violent agents. Harm is clearly evident, steel cross-section loss occurs, and due to significant cracking and spalling, the concrete cover can be of little use in managing corrosion.
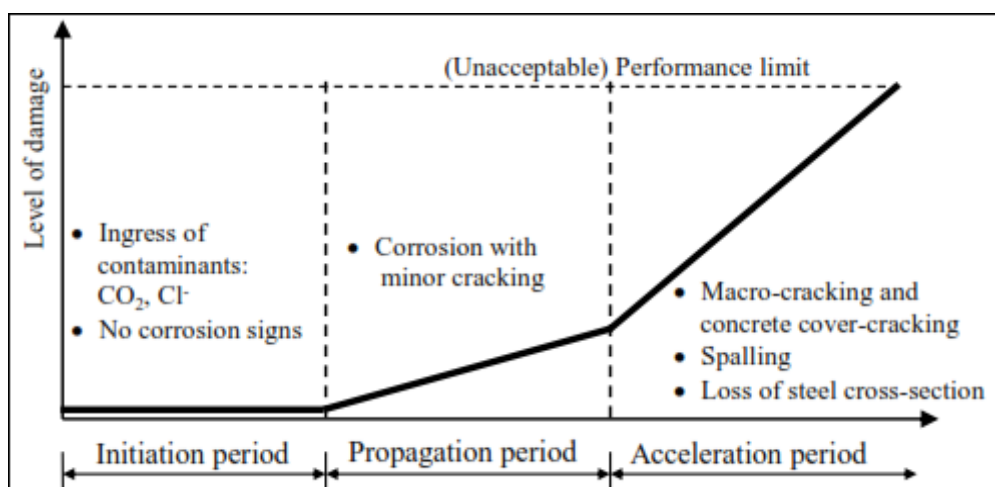
Figure 3.1 Three-stage corrosion damage model [55]

Reinforcement corrosion may be triggered if the protective layer is weakened (see Fig. 3.2a) or de-passivated. An electrochemical process of two half-cell reactions is the corrosion of steel in concrete. (I) Electrons are produced at the anode site , i.e. iron is oxidized to form ferrous ions (Fig . 3.2b) (oxidation reaction (iron dissolution)):

$$Fe \rightarrow Fe^{2+} + 2e^-$$
(3.1)

In the presence of water, free electrons absorb oxygen at the cathodic site (Fig . 3.2b) and form OH- hydroxyl ions (reduction reaction (reduction of oxygen)):

$$2H_2O + O_2 + 4e^- \rightarrow 4 OH^-$$
(3.2)

The hydroxyl ions react with the ferrous ions (Fig. 3.2c) forming the iron(II)-hydroxide:

$$Fe^{2+} + 2OH^- \rightarrow Fe(OH)_2$$
(3.3)
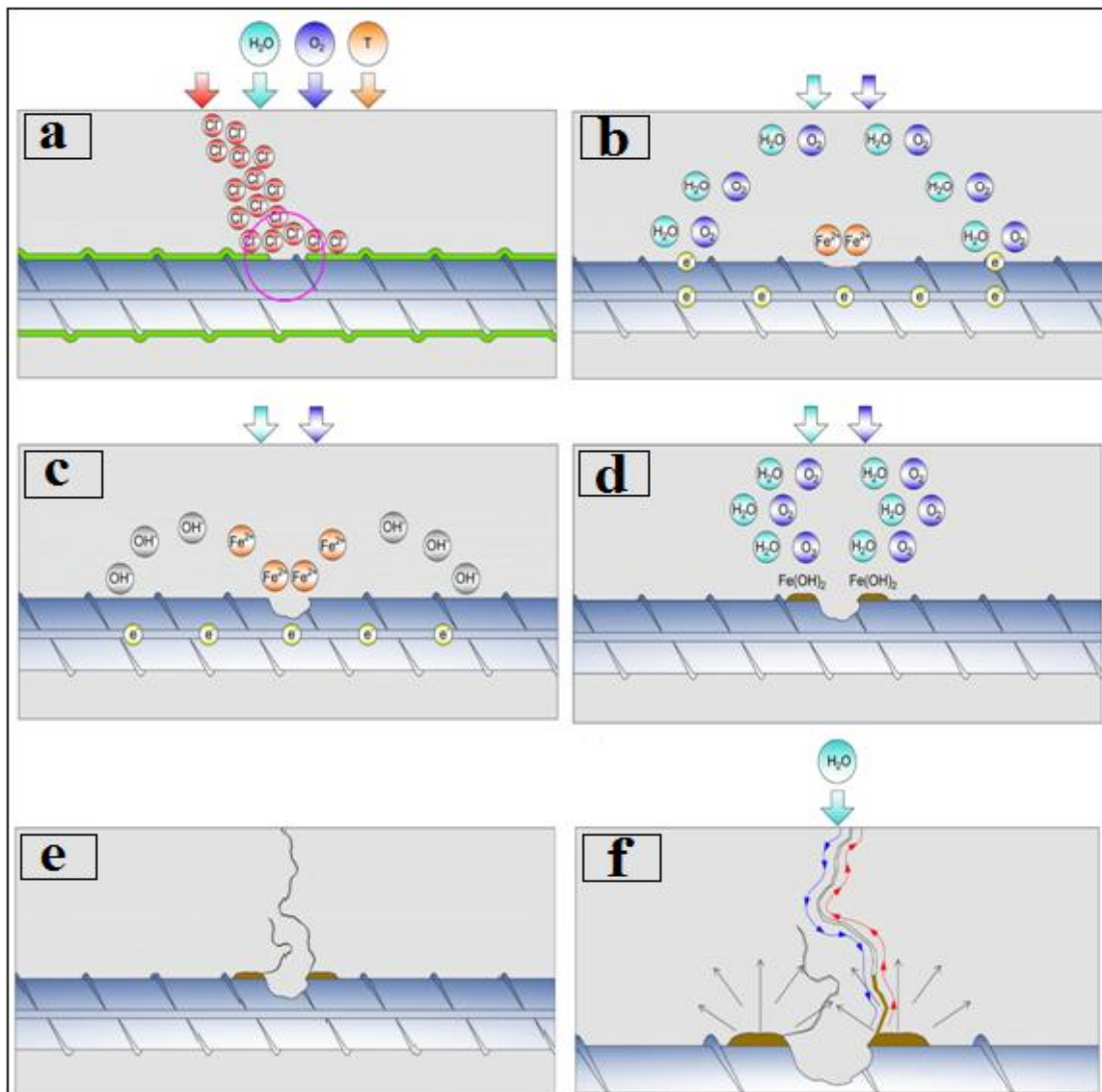
Figure 3.2 Corrosion in concrete: depassivation of reinforcement because of chlorides (a); forming of ferrous and hydroxyl ions (b); forming of the iron(II)-hydroxide (c); production of iron(III)-oxide (d); cracking of concrete cover (e) and transport of corrosion products (f) [56]

The environmental conditions and available chemical reactants depend on the further reactions and development of corrosion products. The formation of iron(III)-oxide or red rust (Fig. 3.2d) in the presence of oxygen and water is one of the possible occurring reactions:

$$4Fe(OH)_2 + O_2 + 2H_2O \rightarrow 4Fe(OH)_3 \qquad\qquad (3.4)$$
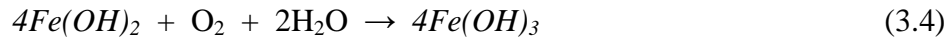
Considering that the specific volume of the corrosion materials is greater than regular material, due to the strain due to the rise in volume, corrosion-induced cracks are formed in the surrounding concrete (Fig. 3.2e). The expansion of the formed rust is highly affected by the existence of concrete pores and voids and the efficacy of the expansion of the products depends greatly on their diffusion through concrete itself. Corrosion products can migrate/diffuse not only in pores and voids but also in cracks (Fig. 3.2f) and that wetting drying cycles and subsequent outer solution entry also affect their transport. Due to this effect, the slowing of corrosion damage in time is generally noted [56].

3.1.1 Electrode potentials

Whenever a metal (electrode) is immersed in a solution, a metal/solution phase boundary is determined and metal ions dissolve. Thus, charges are transferred into the solution in the form of metal ions and electrons are left behind. As it contains dissolved metal ions (and possibly also other ions), the solution is considered an electrolyte and is therefore electrically conductive. With electrons in the metal and (solvated) metal ions in the electrolyte, an electric double layer is formed.

At the phase boundary, the charge separation gives rise to an electric potential gap across the double sheet. This potential depends on both the metal form and the electrolyte and is a measure of the metal 's ability to ionize, that is, to dissolve into the electrolyte. The capacity of a reaction of half a cell, such as the one defined by eq. (3.1), vs. another half-cell or reference electrode, may be measured.

These potentials are called normal electrode potentials, commonly named E^o, under standard conditions. Normal conditions mean 25°C temperature, 1 bar pressure and 1mol/L electrolyte concentration of metal ions. The electrode potential varies under other conditions, e.g. at various concentrations of metal ions in the solution, which can be measured with the Nernst equation, in the case of iron which reaction:

$$\boldsymbol{E}_{Fe/Fe^{2+}} = \boldsymbol{E}^{o}_{Fe/Fe^{2+}} + (RT/2F) * \ln c(Fe^{2+}) \qquad\qquad (3.5)$$

Here, R is the gas constant, T temperature, F the Faraday constant (see symbols and abbreviations) and $c(Fe^{2+})$ is the concentration of iron ions in the electrolyte [34] .

3.1.2 Potential-pH diagrams (thermodynamic stability)

The relationship between potential and pH value is usually given by the Pourbaix diagram. The state of the passive layer is assessed on the basis of thermodynamic conditions by the Pourbaix diagram, where steel corrodes, areas where protective oxides are formed, the region of corrosion immunity depending on the pH and the potential for steel reinforcement (Fig. 3.3). The Pourbaix diagrams can usually be used for various function forms. One is the diagram of the predominance field, in which the dominant aqueous species will be given as a pH and E function, where pH means -log $a(H^+)$ and E is the corresponding electrical potential variable. In terms of convex polygons, the resulting region of each aqueous species can be represented [57].
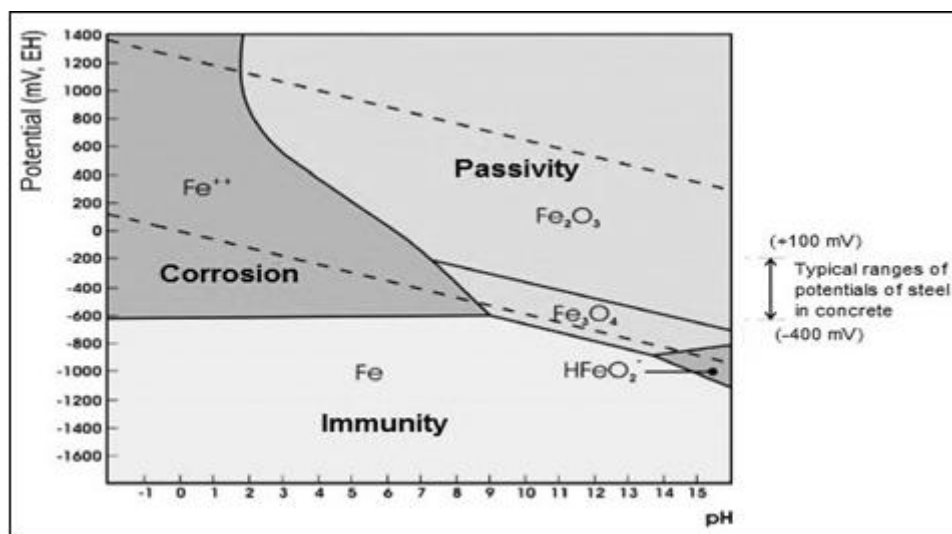
Figure 3.3 Iron-water system, without chloride, at 25 °C Pourbaix diagram [57]

3.1.3 Theory of Passivation

By acting as a shield, concrete offers physical corrosion resistance to steel reinforcement and, as a result of its high pH, chemical corrosion resistance. Concrete that is not subjected to any external interference typically exhibits a pH between 12.5 and 13.5. As shown in the Pourbaix diagram (Fig. 3.3), which describes the range of electrochemical potential and pH for the Fe-H_2O system in an alkaline setting, a protective passive layer forms on the steel surface at potentials and pHs normally found within the concrete. This coating is assumed to be an ultra-thin (< 10 nm) protective oxide or hydroxide film that reduces steel's dissolution rate to negligible levels.

However, partial or absolute passive layer failure referred to as depassivation, results in the aggressive corrosion of steel bars. The corrosive iron products are expansive, and their the

formation can lead to concrete cracking and further degradation. On the formation and breakdown of the passive layer, limited research has been carried out. It has been observed that the iron passive layer's oxidation state differs across the layer. The outer layer, which is primarily composed of Fe^{3+} rich oxides and hydroxides, is presumed to be non-protective, and the inner oxide layer adjacent to the Fe^{2+} rich steel is protective. It is also understood that in the presence of chloride ions, the Fe^{3+}/Fe^{2+} ratio increases.

It was hypothesized that when chloride ions diffuse through the nonprotective outer layer and come into contact with the inner layer, they convert some Fe^{2+} oxides / hydroxides to Fe^{3+} oxides / hydroxides that reduce the protective nature of the inner layer. Two major factors that can crack the passive film on the steel surface and cause corrosion are chloride ions that come mainly from deicing salts or seawater, and carbon dioxide from the atmosphere [58].

3.1.4 Pitting corrosion (chloride induced corrosion)

In the case of chlorides, a combination of capillary action, evaporation, absorption and diffusion allows the chloride ions to permeate the concrete cover by depositing water bearing the chloride ions on the concrete surface. When chloride ions reach the steel surface, their combination with hydrogen ions in the pore water produces acids that neutralize the alkalinity of the concrete in sufficient concentration and facilitate the passive layer breakdown that allows localized corrosion to be established. Corrosion appears to proceed in a very particular form known as "pitting" as a result of the localized nature of the chloride attack. Pitting is probably the most insidious form of corrosion because relatively little weight loss can lead to a significant reduction in the size of the section and it can be difficult to detect its localised attack before serious deterioration has occurred [59].

A very aggressive environment is produced inside pits when pitting corrosion has begun, while the protective film on the surrounding passive surface is retained (and even reinforced by alkalinity produced by the cathodic process). Inner pit corrosion can reach very high penetration rates (up to 1 mm/year in wet and heavily chloride-contaminated structures), leading rapidly to an unacceptable decrease in cross-sectional reinforcement [60].

3.1.5 Electrochemical Kinetics

Thermodynamics provides an indication of the propensity of electrode reactions to occur, whereas the rates of such reactions are addressed by electrode kinetics. The reactions of concern are primarily corrosion reactions, so it is more fitting to call corrosion kinetics the

kinetics of such reactions. In order to understand the theory of aqueous corrosion, it is important to establish a complete understanding of the kinetics of reaction proceeding on an electrode surface in contact with an aqueous electrolyte [61]. A current passes through the circuit within the formed macro-cell. Since there must be consistency in the currents, according to Kirchhoff 's law, the following four steps must take place at the same space:

- Anodic iron dissolution and electron release according to eq. (3.1).

- Transporting electrons from the anodic to the cathodic sites through the metal.

- Cathodic reactions to electron consumption; in the case of steel corrosion in concrete, oxygen reduction is primarily reduced according to eq. (3.2) is pertinent.

- Electric current flows between anodic and cathodic sites through the electrolyte, carried by ion flux.

The relation between an electrode 's potential and current is referred to as the polarization curve. In general, as the anode potential is increased to more positive values, the corrosion current increases; the reaction rate of the cathodic half-cell reaction increases with the potential to decrease (to more negative values).

In Fig. 3.4b, in alkaline as well as acidic environments, polarisation curves for steel are schematically depicted and related to the Pourbaix diagram. At high pH, where the anodic current (iron dissolution) is at a low level, almost independent of potential, a wide range of passivity is visible; at low pH, the anodic current logarithm rises linearly with the potential. The dotted line representing cathode kinetics in Fig. 3.4b is drawn at high pH as the cathodic reaction occurs on metal surfaces outside the pit. The logarithm of the cathodic current increases linearly as the potential decreases to more negative values [34].
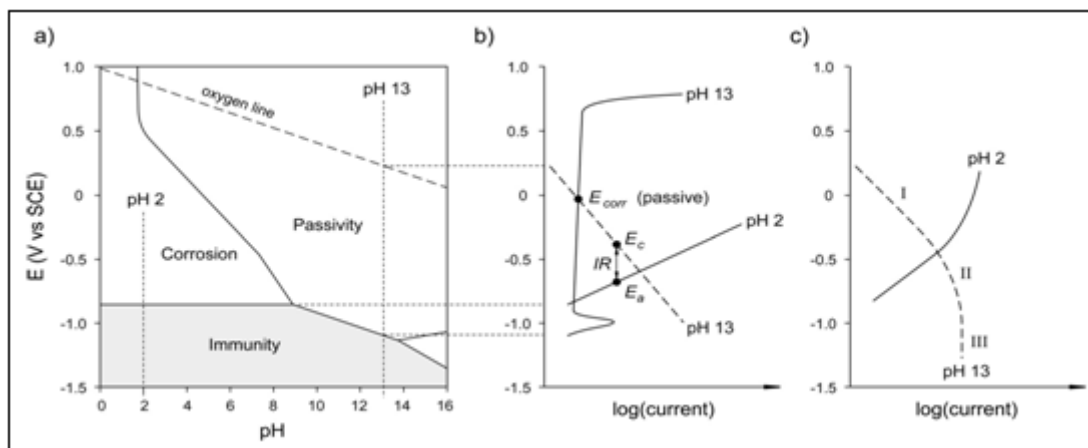
Figure 3.4 Simplified Pourbaix diagram for iron (a) and schematic anodic (solid line) and cathodic (dashed line) polarisation curves in active and passive regions (b); effect of diffusion control (c). The ordinate is the same for all three graphs [34]

3.2 Corrosion inhibitors

The corrosion of steel reinforcement is one of the main causes of premature deterioration of reinforced concrete, leading to significant economic losses. Chloride ions in the marine zone, or the use of thawing salts or carbonation in urban areas, may cause rapid deterioration. Several products known as corrosion inhibitors have been used in recent years in order to provide extra protection and improve the life span of reinforced concrete structures. Corrosion inhibitors have been gaining more attention in recent years because of the benefits they offer. A promising way to improve the resilience of concrete structures exposed to chloride ions and carbonation is to use inhibitors.

Inhibitors are chemicals that decrease the corrosion rate when present at certain concentrations, without substantially altering the concentration of any other corrosive agent. Compared to other traditional methods of safety and repair, corrosion inhibitors can be a reasonable option, because of their lower cost and ease of implementation. Furthermore, it is possible to apply inhibitors preventively or as a corrective step.

Corrosion inhibitors may be categorized according to their methods of application, safety mechanism or structure, which may be organic and inorganic, by inhibiting the corrosive process by forming passivating film (anodic inhibitors) or by raising polarity and reducing the potential for corrosion (cathodic inhibitors). Inhibitors that work both ways are also present. These products may be applied directly to the reinforcement, pretreated by immersion of the reinforcement in an inhibitor solution, added to the mixing water during the mixing of concrete, or applied to the surface of the reinforced concrete structure by capillary penetration of the inhibiting solution into the concrete [62].

The substances used as inhibitors may be organic as well as inorganic in nature; they may be categorized according to the method of application:

- Admixed Corrosion Inhibitors (ACI)-As an additive, they are applied to the fresh concrete.

- Migrating corrosion inhibitors (MCI)-During the initiation phase, they are added to the surface of hardened concrete; their penetration through the concrete cover is necessary for the safety of reinforcements, promoting corrosion rate reduction [21].

3.2.1 The concrete – reactions of cement with inhibitors

3.2.1.1 Initial set of concrete

Cement is a finely ground calcium silicate and calcium aluminate mixture that reacts in stages with water. Within a few minutes, tricalcium aluminate ($3CaO. Al_2O_3$, or, in cement

terminology, C_3A) and calcium aluminoferrite ($4CaO. Al_2O_3. Fe_2O_3$ or C_4AF, of somewhat variable composition) start to react with water. A few percent of gypsum ($CaSO_4. 2H_2O$) or plaster ($CaSO_4. 1/2H_2O$) is applied to regulate the fluidity before tricalcium silicate can begin to hydrate (after a few hours). These compounds absorb water and do not produce much strength, but can stiffen the mix and decrease workability. Then much later, dicalcium silicate contributes to the strength. The initial set is a stiffening that makes it possible to finish after a few hours, but it is only the beginning of the concrete strength growth, which is conventionally measured at 7, 14 and 28 days, and even at higher ages, especially when pozzolans are used. The gypsum content in the cement also has a key role in controlling of setting time of the cement. By using admixtures, the rate of cement hydration reactions may be, and sometimes is, deliberately altered. Admixtures that typically do more than just prevent corrosion are corrosion inhibitors. Admixtures may affect the influence initial set, the later gain of strength or other properties. The results they generate in the field depend on conditions there, which may not be the same as those used in the laboratory. Changes in the period when an admixture is added or in the order when two admixtures are added may offer different set times [63].

3.2.1.2 Air entrainment

Expansion may open cracks already started by corrosion processes due to freezing wet concrete, and vice versa. Then, cracked concrete allows water and chloride to penetrate at a faster pace than uncracked concrete. The use of deicing salt means freezing temperatures, so air would be intentionally applied for safety when salt is used on concrete. Admixtures that prevent corrosion can have an impact on the air content or its characteristics, and this will be taken into account by a well-designed concrete mix [64].

3.2.1.3 Permeability and diffusion

Low permeability, resulting from a low water/cement ratio used in high-strength concretes, decreases the input of external sources of chloride ions. When high-strength concrete offers improved corrosion resistance, lower permeability is the cause of the reduced corrosion hazard, rather than mechanical strength. By determining the minimum desired compressive strength, concrete permeability could be preserved at relatively low values [65].

Using water reducers or superplasticizers, lower water/cement ratios can be achieved without loss of workability. Pozzolanic materials such as silica fume, slag and fly ash (which are not in themselves corrosion inhibitors) can also achieve lower permeability and increased strength [66]. The permeability reduction can be a factor of 5 or 10. To create

more silicate binder, Pozzolans react with calcium hydroxide; thus, pozzolanic concretes typically contain less cement of the same strength than ordinary portland cement concrete. Concrete permeability can also be decreased by applying chemical water barriers or hydrophobic agents such as calcium stearate emulsion, butyl stearate emulsion or butyl oleate emulsion to an admixture that has other corrosion preventives. These esters are stable as an aqueous admixture, but are hydrolyzed into an alcohol plus an insoluble, hydrophobic calcium salt in alkaline concrete (Eq. (3.6)). If the reaction occurs at the optimum time, the

$$2C_4H_9\text{-}fatty\ carboxylate + Ca(OH)_2 = 2C_4H_9OH + Ca(fatty\ carboxylate)_2 \qquad (3.6)$$
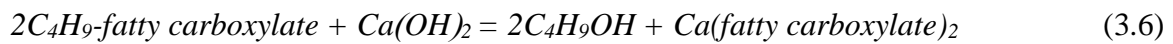
precipitate will line the pore walls, or block them entirely, with a layer of hydrophobic salt that resists further water penetration. For steady-state conditions, Fick's first law of diffusion (the volume of a fluid diffusing is proportional to the difference of concentration) applies. In real corrosion conditions, Fick 's second law (Eq. (3.7), [67]) is more useful (the rise in chloride concentration at the rebar divided by the time interval equals the diffusion coefficient times the concrete surface concentration of chloride divided by the thickness of the concrete cover squared:

$$\mathrm{d}C_{cl}^- / \mathrm{d}t = D.\ \mathrm{d}^2 C / \mathrm{d}x^2 \qquad (3.7)$$

where: C = chloride concentration, D = diffusion coefficient, x = thickness of concrete cover, t = time.

The chloride ion diffusion coefficient (typically in the range of 10^{-11}- 10^{-13} m^2/s) increases by a factor of about 7 as the w/c ratio increases from 0.3 to 0.6. With an activation energy of ~35 kJ/mol, it often increases as temperature rises, similar to chemical reactions in general. However it decreases with time, as the cement begins to hydrate, about a factor of two after ten years. For corrosion, ion permeability is important because the electrochemical character of corrosion has two components: the electronic path (electrons pass through steel from anode to cathode) and the ionic path (which helps the excess cathode-formed anionic species (hydroxyl ions) to balance electric charges with the anode-formed ferrous cations). If the porosity of the concrete is low, or if it is very dry, the corrosion current will be much reduced [63].

3.2.2 Effect on the service life

Inhibitors of corrosion have the potential to improve the service life of a concrete system operating on its time of initiation and rate of propagation. The service life of the structure

can be seen in Tuutti's diagram [68], which indicates that, in the presence of corrosion inhibitors, they are modified by their operation, as shown in Fig. 3.5.
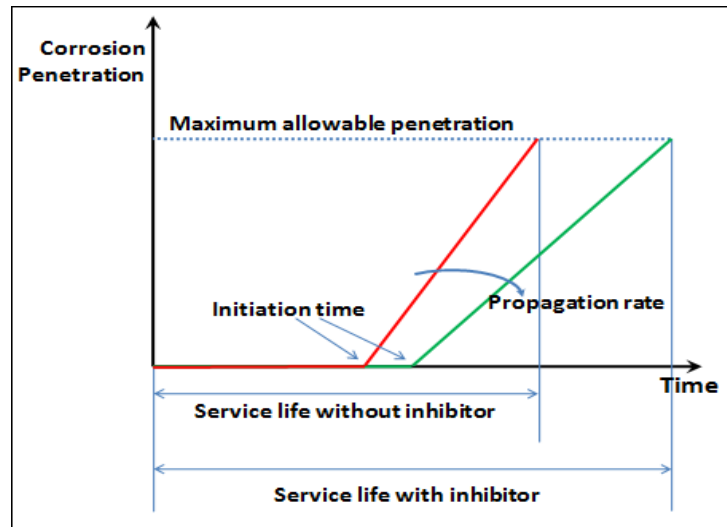
Figure 3.5 Influence of the inhibitor on the service life [68]

First of all, the inhibitor can work on the corrosion initiation time: a barrier effect, caused by its presence within the concrete matrix, can restrict the diffusion towards the reinforcements of aggressive conditions. A strengthening mechanism of the rebar passive layer may also be correlated with the delay in initiation time; the chloride threshold value can thus be increased. The corrosion inhibitor will further affect the stage of corrosion propagation by creating a reduction in the rate of corrosion of the rebars after initiation. Therefore, the effect of corrosion inhibitors is to ensure that the concrete structure has a service life equal to or greater than the intended one. To do this, the compatibility of an efficient inhibitor with the concrete matrix must be satisfied, without affecting the properties of both fresh and hardened concrete and the environment: there must be no toxicity and environmental impact problems [69].

3.2.3 Effect on chloride-induced corrosion

The initiation of the chloride contamination-related rebar corrosion process is triggered by overcoming the threshold concentration of chloride capable of breaking down the passive oxide film on the surface of the steel. A very fast propagation rate begins with localized corrosion (pitting), which can be called autocatalytic. Therefore, chloride-induced attack corrosion inhibitors only act on the initiation time: once the steel passive layer is locally destroyed, no inhibition will act on the propagation of corrosion [70].

According to Elsener [71], the pitting potential of the anodic potential at which localized corrosion begins is related to the concentrations of chloride ions:

$$E_{pit} = C - B log(a_{Cl^-}) \qquad (3.8)$$

Where: C and B constants and a_{Cl-} chlorides activity. The pitting potential is improved by effective corrosion inhibitors, hitting values higher than the corrosion potential, preventing pitting initiation. They thus decrease the concentration of chloride on the steel surface and prevent the creation of pits with various mechanisms: for example, they can adsorb on the steel surface to avoid the accumulation of chlorides; instead, they can increase or buffer the concrete pH near the reinforcements, hindering the production of the pit [71].

3.2.4 Inhibition mechanism

The inhibition of corrosion of steel reinforcements within concrete structures focuses on the hindrance of the phase of electrochemical corrosion: if there is no chemical reaction or transport mechanism, the phenomenon of corrosion is absolutely blocked. The corrosion inhibitor defense mechanism works precisely on these processes; according to the reaction they impede, they can be categorized into:

(i) adsorption inhibitors, specifically acting on the anodic or cathodic partial corrosion reaction or both reactions (mixed inhibitor),

(ii) film-forming inhibitors that more or less fully block the surface, and

(iii) passivators that favor the passivation reaction (e.g. hydroxyl ions) of steel.

A totally different condition has to be addressed in the case of the inhibition of corrosion of steel in concrete. Steel in concrete is therefore normally passive, being covered by a thin film of spontaneously formed oxy-hydroxides in the alkaline pore solution (passive film). Consequently, the mechanistic action of corrosion inhibitors is not to counteract uniform corrosion (see above), but to locate or pit passive metal corrosion resulting from the presence of chloride ions or from a drop in pH. Therefore, it is clear that the long and proven track record of general corrosion inhibitors in acidic or neutral media cannot provide a justification for (tacitly) believing that similar compounds can function for concrete steel as well. For pitting corrosion, chloride ions are responsible, with the pitting potential depending on the behavior of the chloride. Corrosion pitting inhibitors are able to act:

- by a competitive method of inhibitor and chloride ion surface adsorption (reducing the efficient passive surface chloride content).
- Via pH buffering in the local pit area.
- Competitive migration of inhibitor and chloride ions into the pit so that it is impossible to produce the low pH and high chloride content required to maintain pit development [71].

Chapter Four: Mitigation of Steel Rebar Corrosion by Inhibitors – a Critical Review

Corrosion inhibitors can avoid or at least delay the de-passivation of steel and/or decrease the corrosion rate of steel in concrete in new reinforced concrete structures, concrete repair systems or surface-applied liquids. For an effective and durable inhibitor action, several fundamental requirements have to be fulfilled [72]:

1.Unique properties (strength, freeze thaw resistance, porosity etc.) should not be adversely affected by the inhibitor and should be environmentally friendly.

2.With respect to hostile (chloride) ions, the inhibitor must be present at a sufficiently high concentration in the reinforcing steel.

3. The concentration of the inhibitor should be sustained over a long period of time.

4. The effect of an inhibitor on steel corrosion in concrete should be observable.

4.1 Green (plant extract) corrosion inhibitor, effectiveness, effect on concrete properties

Natural inhibitors are more effective and extremely beneficial to the environment in the corrosion process than other corrosion inhibitors. As natural inhibitors, certain plant sources are used, such as polyphenols, terpenes, alkaloids, flavonoids, etc. These also met all the criteria for the features of natural inhibitors. Sugar parts of vegetable concentrate have been tested in reinforced concrete as a natural inhibitor [73].

Plant extracts are seen to be an extremely rich source of naturally synthesized chemical compounds that are biodegradable in nature and can be extracted by simple, low-cost processes [74].

The use of plant extract as a green inhibitor due to toxicity and the environmental hazards of chemical inhibitors. Therefore, there is an attempt to make use of environmentally safe , non-toxic extracts as corrosion inhibitors of natural plant materials. The inhibitors developed from naturally occurring plant extracts are commonly referred to as green inhibitors of corrosion. A broad range of organic compounds are present in extracts of plant materials. Most of them contain hetero atoms such as P, N, S, O. Through their electrons, these atoms coordinate with the corroding metal atom (its ions). Protective films are then produced on the surface of the metal and corrosion is therefore prevented.

Green corrosion inhibitors are derived from plant extracts that are readily available, inexpensive, environmentally safe, cheap and sustainable. Green inhibitors are more environmentally friendly and reduce environmental risks than conventional and inorganic

inhibitors. There is increasing interest in the use of green corrosion inhibitors due to the toxicity of chemical inhibitors [75].

Inhibiting mechanism

A dual 'active-passive mechanism' is the green inhibitor mechanism: the active portion of this organic inhibitor is the adsorption of a film-forming amine on the reinforcing steel and the creation of a physical barrier against the action of aggressive agents such as chloride ions. The decrease of concrete permeability is the passive component of the mechanism, thereby decreasing the intake of chloride ions, humidity and other violent chemicals.

The forming of fatty acids and their calcium salts by the waterproofing ester process results in the development of a hydrophobic coating within the pores, limiting the input of water and chloride ions [66].

4.2 Nitrate-based inhibitors, effectiveness

A new class of corrosion inhibitors to replace an efficient calcium nitrate inhibitor was studied at the end of the 1980s, when European regulations began to restrict its use due to toxic problems and environmental requirements [76]. Organic and inorganic inhibitors have been studied as alternatives to overcome these disadvantages. The necessity to integrate a non-toxic and environmentally friendly inhibitor into concrete structures to avoid phenomena of rebar corrosion led to the study of nitrate-based compounds.

Nitrate is a polyatomic ion with the NO_3^- molecular formula (Fig. 4.1) and, due to its high solubility and biodegradability, is primarily produced for agricultural use as fertilizer. As food preservatives, the second main use of nitrates is [77].
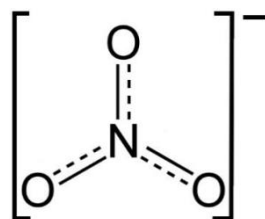
Figure 4.1 Nitrate ion [77]

Nitrates are cheaper and less toxic to the environment compared to nitrite compounds; they are often widely used as set accelerators, showing their perfect compatibility with concrete mixtures[78][79]. Since calcium nitrite was the most popular inorganic admixed corrosion inhibitor with widely assessed efficacy, the study focused on calcium nitrate ($Ca(NO_3)_2$) as an alternative nitrate-based inhibitor.

The first study on these inhibitors dates back to 1987: D'yachenko et al . investigated the inhibitory efficiency of the chloride-induced corrosion of abandoned concrete samples by nitrate and nitrite mixes [80]. The latter work was so basic and inexperienced that it was appropriate to wait until 1994 for a full study on the inhibitor of calcium nitrate [81]: Justnes et al. drafted the first hypothesis on the mechanism of inhibition, gathering all the previous findings.

4.2.1 Inhibiting mechanism

The inhibitory function of calcium nitrate for the corrosion of concrete steel was first suggested by Justnes in 1994 and then further explained in 2000 [82]. Like nitrite, it is known to be an anodic corrosion inhibitor: the usual mechanism of inhibition is characterized by the suppression of anodic reactions aiding the passivation of spontaneous metals or the creation of compounds of barrier deposition [83].

The behavior of nitrate as a corrosion inhibitor can be understood by the well known mechanism of the associated nitrite ion. The anodic activity of the oxidation of ferrous ions to form a protective oxide surface layer was characterized by nitrite-based inhibition, thus competing with the violent chloride ions. Justnes exploited this process and applied it to the actions of nitrate; he believed, in particular, that nitrate's oxidation action is the consequence of its simple reduction to nitrite. The two half-reactions illustrate the mechanism:

$$\text{Reduction: } 2NO_3^- + 2H_2O + 4e^- \rightarrow 2NO_2^- + 4OH^- \tag{4.1}$$

$$\text{Oxidation: } 4Fe(OH)_2 + 4OH^- \rightarrow 4Fe(OH)_3 + 4e^- \tag{4.2}$$

They are combined to give the total reaction:

$$2Fe(OH)_2 + NO_3^- + H_2O \rightarrow 2Fe(OH)_3 + NO_2^- \tag{4.3}$$
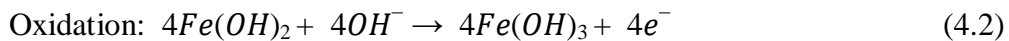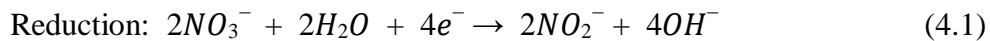
The comparison between the equation (4.3) and the corresponding nitrite mechanism $(Fe(OH)_2 + NO_2^- + H_2O \rightarrow Fe(OH)_3 + NO + OH^-)$ suggests that nitrate (NO_3^-) should be an even better inhibitor than nitrite (NO_2^-), since the amount of moles of ferrous oxide that reacts with one mole of inhibitor is doubled with respect to the nitrite reaction. Therefore, theoretically, the effectiveness of nitrate as a corrosion inhibitor would be twice as high as nitrite [82]. This indicated that the kinetics of nitrate redox reactions may be slower than nitrite. The delay in the evolution of this inhibition mechanism was assessed during the years by Justnes himself and other studies [81][84][85].

An alternative and more recent theory was suggested in 2011 by Saura et al. on the inhibitory function of nitrate [86]; in particular, the behavior and efficacy of sodium nitrate

(NaNO$_3$) was studied in neutral and acidic environments. With the creation of an oxide layer, insoluble in pore water, which creates a precipitation barrier on the steel surface, the starting point of this theory was still referred to as the nitrite inhibition mechanism. In comparison to Justnes, however, the authors found a different compound generation of ferrous oxide: γ-Fe$_2$O$_3$, so they referred to the corresponding nitrite equation (4.6). The mechanism is described by two half-equations:

$$\text{Reduction: } NO_3^- + H_2O + 2e^- \rightarrow NO_2^- + 2OH^- \qquad (4.4)$$

$$\text{Oxidation: } 2Fe^{2+} + 3OH^- \rightarrow \gamma\text{-}Fe_2O_3 + 2e^- + 3H^+ \qquad (4.5)$$

They are combined to give the total reaction:

$$2Fe^{2+} + NO_3^- + H_2O + OH^- \rightarrow \gamma\text{-}Fe_2O_3 + NO_2^- + 3H^+ \qquad (4.6)$$
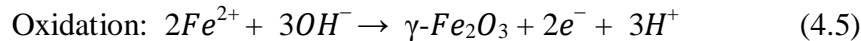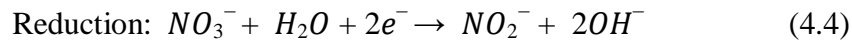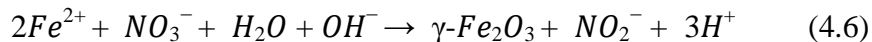
In the simulation of concrete pore solution, the above mechanism was assessed and the γ-Fe$_2$O$_3$ shaped layer was shown to be stable in alkaline environments, causing a strong protective effect on the surface of the steel. Passive film stability issues have nevertheless been found in neutral or low pH solutions; as a result, nitrate protective effects in carbonation-induced corrosion have been presumed to be limited [86].

4.2.2 Effect on concrete properties

Since the 1980s, when the formulation of the chloride-free set accelerator was needed to replace the commonly used calcium chloride compound, the use of calcium nitrate as a concrete admixture setting accelerator was developed [79]. As a basic component for a fixed accelerating admixture, calcium nitrate was proposed in 1981 and was widely studied in combination with amine as a scientific calcium nitrate over the years. Justnes has long studied the effect of calcium nitrate additions on the setting properties of cement: the results showed that it usually has a good efficiency between 7°C and 20°C; however, the set accelerating effects are highly dependent on the form of cement [81][87]. Additional side effects on concrete properties have been reported and tend to be linked to changes in concrete porosity after calcium nitrate has been added: enhancements in compressive strength and improvements in freeze-thaw resistance have been found [88].

In particular, several case studies focused on improving the compressive strength due to the nitrate admixture; they decided on a linear dependence of the compressive strength of the early age on the calcium nitrate admixed concentration. However, its reinforcing effect is, in the long term, insufficient to regard it as a hardening accelerator [89][90].

Chapter Five: Knowledge Gaps and Major Research Aims

5.1 Knowledge gaps

Studying the interactions between the corrosion inhibitors and admixtures (superplasticizer and water-resisting admixture) together because most of the researchers were just interested either in the effect of the corrosion inhibitors or that of the admixtures.

Consequently, the recent dissertation's main topic was chosen to analysis the reinforced concrete samples' properties after mixing orange peels inhibitor with water-resisting admixture and, for comparison, preparing also another mix with the same admixture (water-resisting admixture) and calcium nitrate inorganic inhibitor. Moreover, the construction of the previous procedure was repeated using superplasticizer admixture as well. In this way it became possible to draw new conclusions about the determinative effects of both types of admixtures (i.e. the selected two kinds of inhibitors combined with the two different admixtures).

Finally, it also became possible to figure out each inhibitor's individual behavior with the two types of admixtures used in this work and describe their effectiveness in mitigating the risk of corrosion in reinforced concrete.

5.2 Major research aims

The main objectives of the PhD research program are as follows:

1- Using orange peels extract or calcium nitrate as suitable and more environmental-friendly and less harmful to health type alternative inhibitors to the traditional chemical corrosion inhibitors.

2- Demonstrating the potential and advantages of using orange peel extract 'green' inhibitor in the prepared concrete mixtures to prove that certain kinds of food wastes as well can be transformed into useful engineering materials and so reducing the environmental pollution of our precious planet Earth.

3- Improving plasticity of fresh concrete mixes by using carefully chosen superplasticizer and water-resisting admixtures together with the selected two corrosion inhibitors.

4- Performing laboratory studies and material testing analysis on the ability of inhibitor containing hardened steel reinforced concrete mixtures' resistance to chloride induced corrosion in 3.5wt.% NaCl aqueous solution for 18 months at room temperature.

Chapter Six: Experimental Work

In this part, the details of the experimental program of the work during the period of the study are presented, these include the materials used, specimens preparation and the tests carried out.

6.1 Materials

6.1.1 Cement

Portland slag cement CEM II/A-S 42,5 R was used in this study conforming to the EN 197-1 [29] and it received from CRH Magyarország Kft. company in Miskolc, Hungary. It was kept in the laboratory and stored at a dry place. The chemical composition and physical properties of this cement are given in Tables 6.1 and 6.2 respectively [91].

Table 6.1 Physical characteristics of cement [91]

Physical properties	Achieved value	Standard EN 197-1
Compressive strength after 2 days (MPa)	25.1 – 29.1	≥ 20
Compressive strength after 28 days (MPa)	52.5 – 57.6	$\geq 42.5 \leq 62.5$
Setting time (min.)	160 - 216	≥ 60
Additive content (%)	9 - 13	6-20
Volume stability Le-Chatelier (mm)	0 – 1.5	≤ 10

Table 6.2 Chemical composition and main compounds of cement [91]

Chemical properties	Achieved value	Standard EN 197-1
SO_3 content (%)	3.5 – 3.7	≤ 4.0
Cl^- content (%)	0.04 – 0.07	≤ 0.10

6.1.2 Aggregate

Aggregates was used according standard EN 12620 [92] and it received from CRH Magyarország Kft. company in Miskolc, Hungary.

6.1.2.1 Fine Aggregate

Fine aggregate includes the particles that all passes through 4 mm sieve. Graded sand used in this study (0/4 mm).

6.1.2.2 Coarse Aggregate

Coarse aggregate includes the particles that retain on 4 mm sieve. Graded gravel will be used in this study (4/8 mm).

6.1.3 Water

Tap water was used throughout this work for both making and curing the specimens.

6.1.4 Corrosion Inhibitor

6.1.4.1 Green Inhibitor

In this work were used orange peels as a green inhibitor. Fresh leaves of orange peels were washed under running water, shade-dried in a furnace at 50˚C for 3 hours and ground into powder in the workshop of the Institute of Metallurgy. The extraction was carried out using the Soxhlet extraction process in Wanhua BorsodChem company in Hungary. The powder of about 50g was placed in the Soxhlet apparatus and was continuously extracted using condensed solvent (methanol) for 6 hours. The total amount of methanol used in this process was about 250 ml. The result of the extraction process was the methanol extract with the amount of about 338.8g. The extracts from Soxhlet apparatus were rotary-evaporated to expel the methanol by using vacuum evaporation in laboratories of Institute of Metallurgy at (max.) temperature 40˚C and pressure 60 mbar. After evaporation of the methanol off the extract I obtained a viscous orange yellow colored material that was then dissolved in pure water before adding to the fresh concrete mix. The total amount of water-orange peel extract after the process of extraction was about 100 ml (~108g). The process of extraction of orange peels is illustrated and explained in Fig. 6.1.
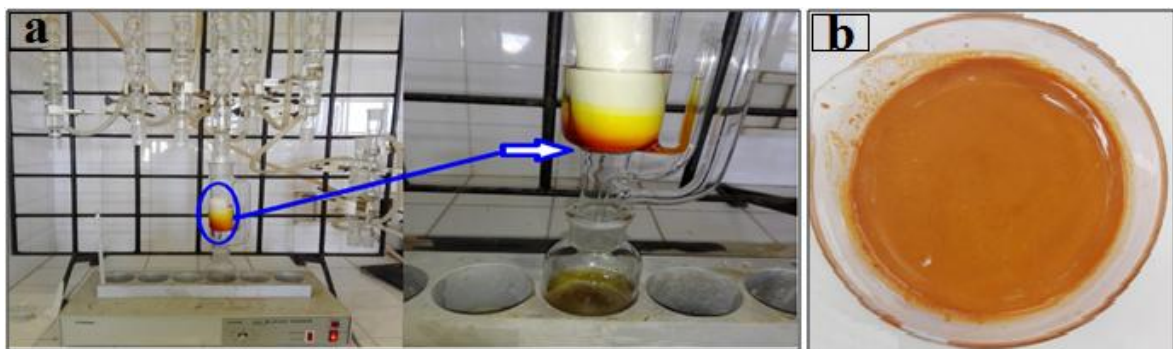
Figure 6.1 a: Extraction of orange peels process, b: Water-orange peel extract after the process of extraction

6.1.4.2 Inorganic Inhibitor

In this work were used calcium nitrate as inorganic inhibitor with the formula $Ca(NO_3)_2$ (as shown in Fig. 6.2) and it is a colorless salt absorbs moisture from the air and is commonly found as a tetrahydrate. This inhibitor use with concrete and mortar is based on two effects.

The calcium ion accelerates formation of calcium hydroxide and thus precipitation and setting. This effect is used also in cold weather concreting agents as well as some combined plasticizers. The nitrate ion leads to formation of iron hydroxide, whose protective layer reduces corrosion of the concrete reinforcement.
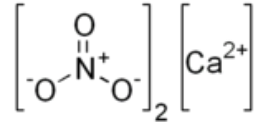
Figure 6.2 Formula of calcium nitrate

For this study calcium nitrate was received from Minerals-water Ltd company in the United Kingdom as a very strong HDPE bottle with net-weight 500g as shown in Fig. 6.3.
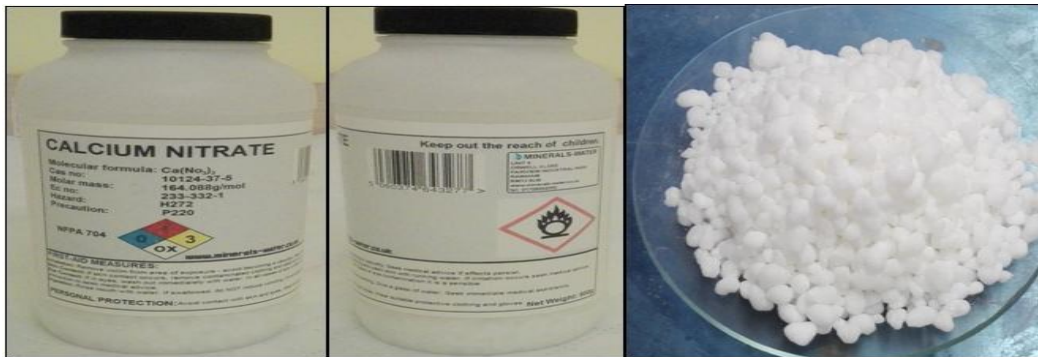
Figure 6.3 Calcium nitrate that used in this work

6.1.5 Admixtures

The properties of the freshly mixed then hardened concrete can be modified by adding liquid or mineral admixtures to the concrete during batching .In this work two types of admixtures according to EN 934-2 [93] were used:

1. Superplasticizer admixture.   2. Water-resisting admixture.

6.1.5.1 Superplasticizer Admixture

The superplasticizer that was used in this work (product name was Dynamon SR31 and it brown liquid as shown in Fig. 6.4) is an admixture based on modified acrylic polymers specially designed for ready-mixed concrete and it received from CRH MagyarországKft. company in Miskolc, Hungary. Concretes manufactured with superplasticizer have a high level of workability according to EN 206-1 [27], and are consequently easy to apply when fresh. At the same time they offer excellent mechanical performance when hardened. Typical properties of superplasticizer shown in Table 6.3.
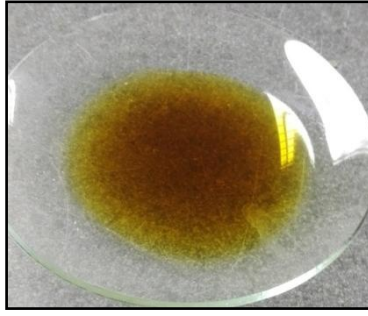
Figure 6.4 Superplasticizer admixture that used in this work

Table 6.3 Typical properties of superplasticizer admixture [94]

PRODUCT IDENTITY	
Consistency	liquid
Color	brown
Density according to ISO 758 (g/cm³)	1.06 ± 0.02 at +20°C
Main action	increase workability and/or reduction of mixing water,
Classification according to EN 934-2	long slump retention
Classification according to ASTM C494	set retarding, high range water reducing
Classification according to ASTM C1017	superplasticizer
Chloride content according to EN 480-10 (%)	type G
Alkali content (Na_2O equivalent) according to EN 480-12 (%)	type II
pH content according to ISO 4316	< 0.1 (absent according to EN 934-2)

6.1.5.2 Water-resisting Admixture

This admixture as a nanocement and it's effect mechanism is based on the changes in the chemical processes of concrete bonding which were examined on the level of physics (elemental level). It was experienced that water is unable to convey to reach the necessary energy for the elemental balance (100% micro crystal structure). This missing energy is conveyed by the water-resisting mineral admixture which results in the increase of micro crystals. The components of water-resisting admixture in presence of water have an effect on the structure of old concrete and other pore structured mineral building materials used in the building industry triggering secondary crystallizing processes [95]. The water-resisting admixture was used in this work (as shown in Fig.6.5) it received from Bioekotech Hungary Kft.
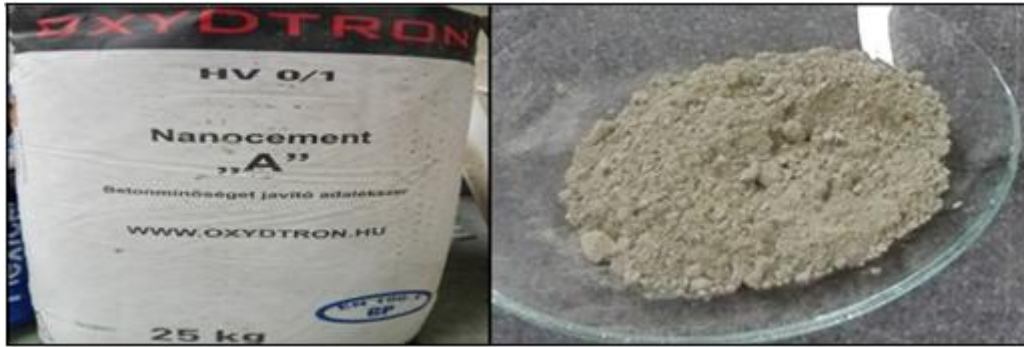
Figure 6.5 Water-resisting admixture that used in this work

6.1.6 Steel Reinforcement

Steel rebar samples (with diameter of 8mm) were obtained from the ÓAM steel producing company operating in Ózd city, Hungary. Before start the work these rebar samples were cleaned with wetted grinding paper (rough then smooth) then coated with epoxy in certain areas (for masking) as shown in Fig. 6.6.
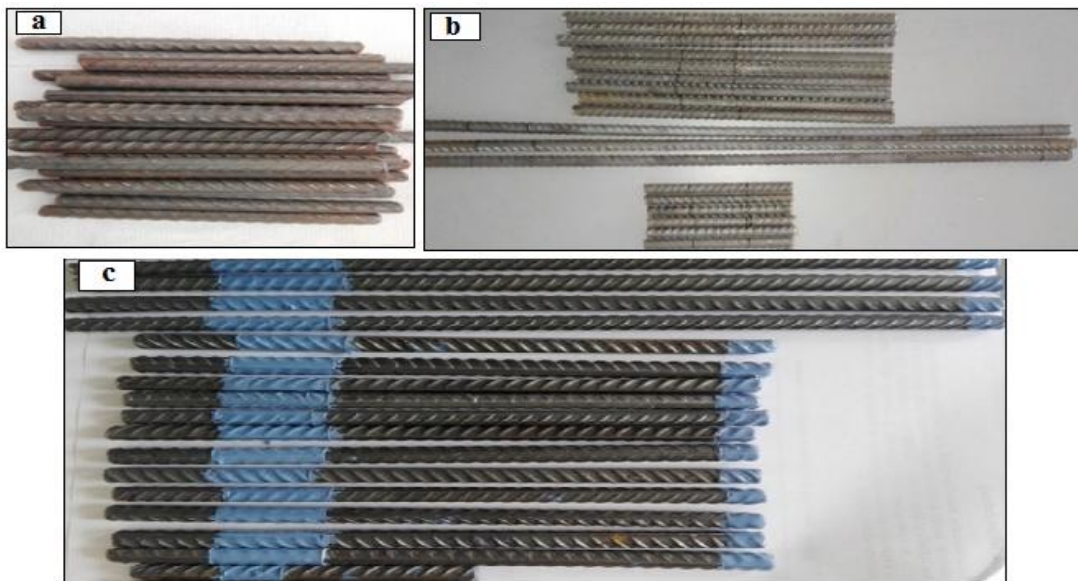
Figure 6.6 Steel reinforcing wires a) before cleaning, b) after cleaning, c) after masking (blue coating) certain areas

6.2 Concrete Mixes

Concrete mixes were designed in accordance with the European mix design method (XD3 class) to have a compressive strength C35/45 at age of 28 days, by the cover depth of concrete I select the structure class type S2 with depth 35mm have service life of 10 to 25 years (application examples for such working life span: Pavements or Car park slabs) according to the EN 1990 [28]. The composition of the mix prepared for casting the specimens was as follows:

Cement: 400 kg/m^3 (CEM II/A-S 42.5 R), Water: 172 kg/m^3 (w/c = 0.43 planned/targeted value)

Admixtures: 2.4 kg/m^3, Aggregate: 1815 kg/m^3 (sand 0/4: 60%   1089 kg/m^3)

(gravel 4/8: 40%   726 kg/m^3).

Ten types of concrete mixes were prepared throughout this study as shown in Table 6.4:

Table 6.4 The concrete mixtures (specimens) prepared for the experiments

Symbol of Mix	Type of Mix		
	Type of Admixture	% of Adding Orange Peels Extract Inhibitor	% of Adding Calcium Nitrate Inhibitor
A1=A3 Reference	Superplasticizer admixture	without	without
B1	Superplasticizer admixture	1% by weight of cement	-
C1	Superplasticizer admixture	3% by weight of cement	-
A2=A4 Reference	Water-resisting admixture	without	without
B2	Water-resisting admixture	1% by weight of cement	-
C2	Water-resisting admixture	3% by weight of cement	-
B3	Superplasticizer admixture	-	1% by weight of cement
C3	Superplasticizer admixture	-	3% by weight of cement
B4	Water-resisting admixture	-	1% by weight of cement
C4	Water-resisting admixture	-	3% by weight of cement

6.3 Preparation, Casting and Curing of the Test Specimens

In this work were prepared for both types of inhibitors 30 cubes of 70mm*70mm for compressive strength test, 30 cubes of 70mm*70mm for testing the resistance of concrete to chloride ion ingress, 10 reinforced concrete prisms of 70*70*250 mm^3 for half-cell corrosion potential test, 10 reinforced concrete cubes of 70mm*70mm for linear polarization resistance (Tafel) test and 10 reinforced concrete cubes of 150mm*150mm for electrical resistivity tests. The molds were thoroughly cleaned and oiled before casting to avoid adhesion with the concrete surface as shown in Fig. 6.7. The samples preparation and casting (as shown in Fig. 6.8) were done in the laboratories of Institute of Ceramics and Polymers Engineering at Faculty of Materials Science and Engineering. Mixing of

materials was done manually after that water was added to the mix with continued mixing, then the mix was put into the molds and it was homogenized.

Figure 6.7 Molds were cleaned and oiled
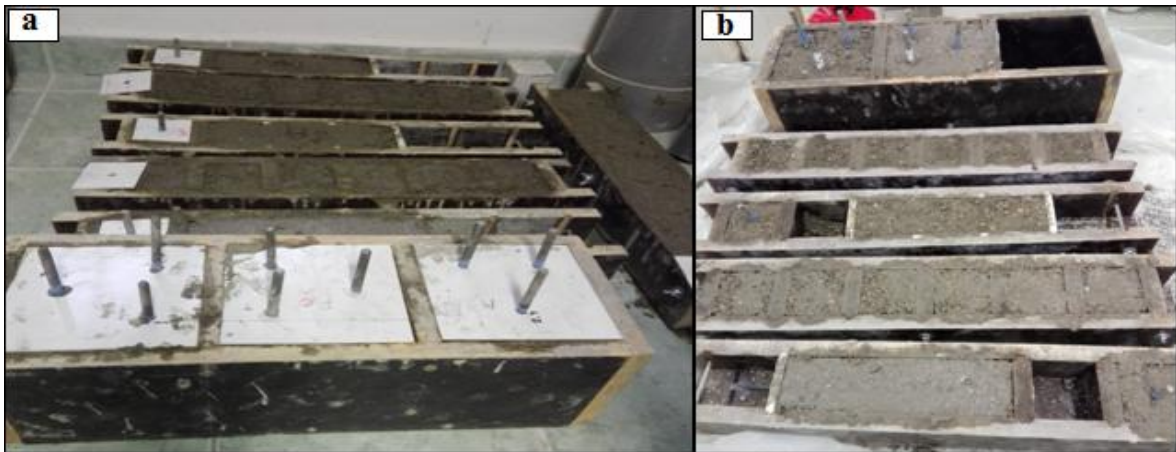
Figure 6.8 Casting of the specimens a) samples with green inhibitor, b) with calcium nitrate

The test specimens were taken out from the molds after 24 hours of casting (as shown in Fig. 6.9) and then they were completely immersed in tap water for a period of 28 days aging. These specimens were then compressive strength tested (see Fig. 6.10). The reinforced concrete samples (prepared for the electrical resistivity testes, half-cell corrosion potential tests and linear polarization resistance tests) were partially immersed in 3.5% NaCl solution during 18 months, while the concrete samples prepared for the chloride ion ingress tests were completely immersed in 3.5% NaCl solution for one month, 3 months and 6 months (as in Fig. 6.11).
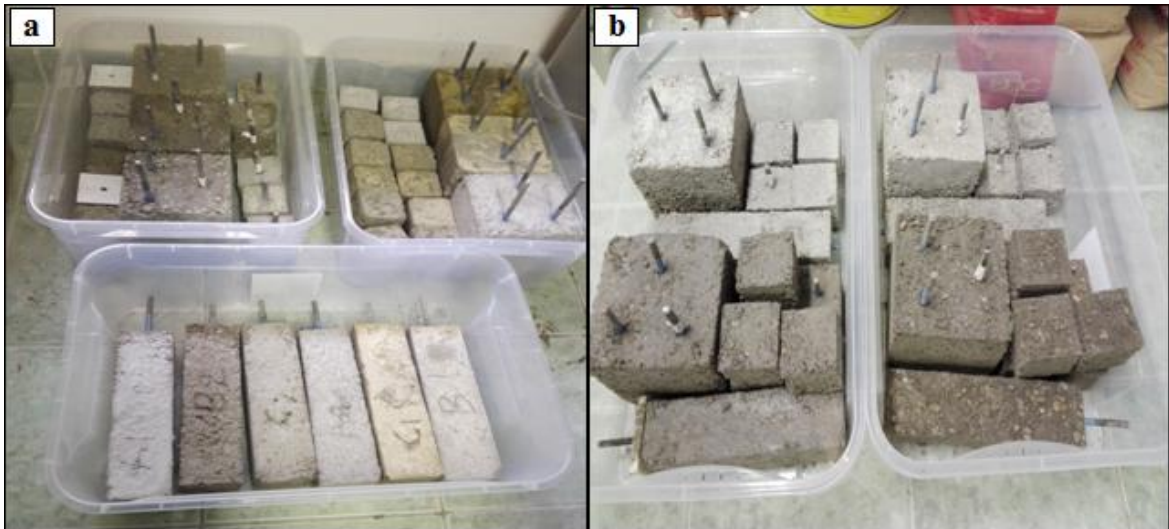
Figure 6.9 Specimens after taken out from the molds after 24 hours of casting a) samples with green inhibitor, b) with calcium nitrate
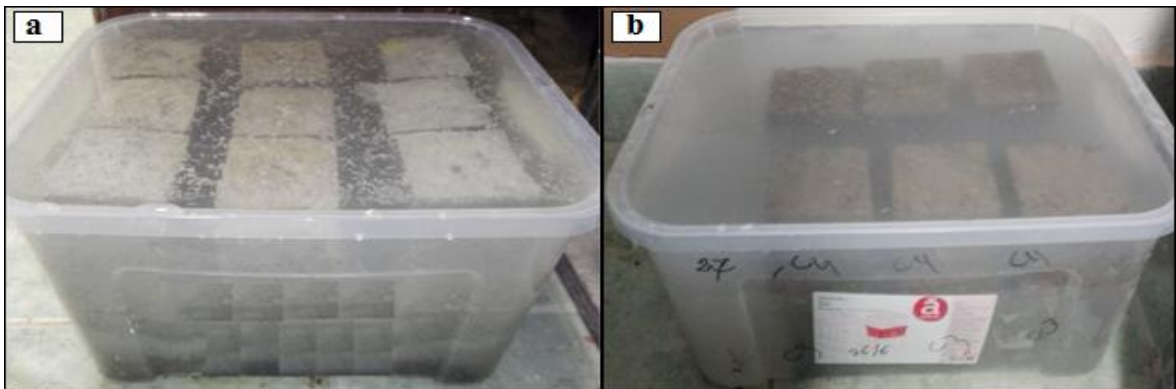
Figure 6.10 Curing of compressive strength specimens in tap water a) samples with green inhibitor, b) with calcium nitrate

Figure 6.11 Specimens of half-cell corrosion potential test and linear polarization resistance test immersed partially and specimens of chloride ion ingress test completely immersed in 3.5% NaCl solution a) samples with green inhibitor, b) with calcium nitrate

6.4 Concrete Testing

6.4.1 Chemical Composition Analysis of the Admixtures and steel rebar

Make detection of active compounds in the admixtures in Institute of Ceramics and Polymer Engineering for orange peels (green inhibitor). To detection the active compounds in the calcium nitrate (inorganic inhibitor) and to detection the composition of superplasticizer admixture was used also FTIR spectroscopy test but in BorsodChem company in Hungary. ICP-OES (Inductively Coupled Plasma-Optical Emission Spectroscopy) spectrometer manufactured by Varian Inc. (720 ES) and EDS (Energy dispersive X-ray spectroscopy) analytical techniques were used to determine the major chemical elementary components of water-resisting admixture in Institute of Chemistry at Faculty of Materials Science and Engineering. Chemical composition of steel rebar was used analyzed by ICP-OES spectrometer also.

6.4.2 Compressive Strength Test

The concrete compressive strength was measured with 70mm*70mm cube by using the machine of compressive strength test (KISPESTI VAS ÉS FÉM (KTSZ)) in the workshop of Institute of Ceramics and Polymers Engineering at Faculty of Materials Science and Engineering (as shown in Fig. 6.12). The cubes were removed from the curing water at age of 28 days after that tested by compressive strength machine as shown in Fig. 6.13. The reported values are the average of three specimens for each mix.

Figure 6.12 Machine of compressive strength during test the samples

Figure 6.13 Specimens before and after compressive strength test a) samples with green inhibitor, b) with calcium nitrate

6.4.3 Porosity

Pores are voids which filled with liquid or air, pores can be open and close. Between crystals in the solid material or gas bubbles in the hydration phase the cavities are formed [96]. The porosity of concrete samples was determined by vacuum saturation as recommended by Hall [97].

6.4.3.1 Vacuum saturation porosity

Vacuum saturation is a method which is used to assess the total porosity of the material. Concrete samples as a small cube with dimensions 4x4 cm was used to measure the

porosity of concrete after drying the samples in an air oven at 100 °C ± 5 °C according to ISO1920-5 until the mass became stable for 24 h [98]. The dried specimen was allowed to cool and placed in small container filled with water to cover the specimen and then this container placed in a chamber which was connected to a vacuum system. The sample was left to soak for a further 50 min as shown in Fig. 6.14 after the chamber was returned to atmospheric pressure [18]. The porosity was calculated from:

Porosity % = (volume of pores/ volume of sample) x 100   (6.1)

volume of pores = $(W_{sat} - W_{dry})$/density of water   (6.2)

density of water = 1 g/cm^3, W_{sat} :weight of saturated sample, W_{dry}: weight of dry sample

Figure 6.14 Porosity by vacuum saturation

6.4.4 Chloride Concentration (Cl⁻ ions)

The concrete sample cubes (7cm*7cm) had been immersed and kept in 3.5% NaCl solution, then the chloride tests, according to EN 13396 [99], were commenced after 1 days, 3 months and 6 months immersion periods by cutting the cubes into three parts at depths of 1.75 cm, and 5.25 cm as shown in Fig 6.15. With this method one can determine the chloride contents at different depths of the sample cubes in the function of exposure (i.e. immersion) times.

Reference samples with the same initial composition were immersed and kept in tap water to compare with samples immersed in 3.5% NaCl solution. Before chloride testing every sample cube was cut to 3 pieces (Side 1 with width of 1.75 cm, Middle part with width of 3.5 cm, and Side 2 with width again of 1.75 cm as shown in Fig. 6.15), then these pieces were ground to fine powder. Cutting and grinding were done in labs of Institute of Mining

and Geotechnical Engineering in Faculty of Earth Science and Engineering at University of Miskolc. The chloride chemical analysis was done at the BorsodChem company, Hungary. For this latter test, according to Standard BIS - IS 3025: Part 32 [100], at first about 1.5g portions from the powdered concrete pieces were taken/sampled, then mixed with 200 ml deionized water (to dissolve the chlorides in water). The water dissolved chloride was measured by argent metric titration using a semi-automatic titration apparatus (in the BorsodChem laboratory, Fig. 6.16). For the analysis 5ml $AgNO_3$ solution (0.02M), 1ml NaCl solution (0.01M) and 2 drops of K_2CrO_4 indicator were used. The apparatus was so calibrated that it gave the Cl^- ion concentrations automatically.

The critical chloride threshold limits, as described in Table 6.5, can characterize the effect of chloride ions on the corrosion risks in reinforced concrete.
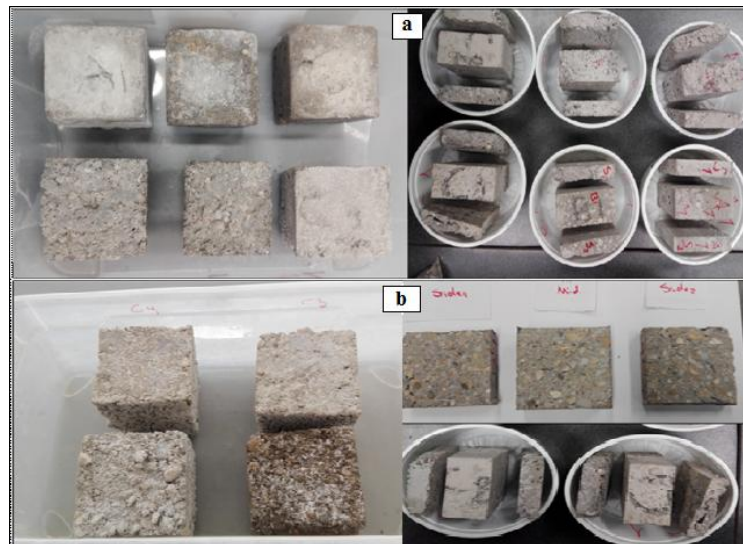

Figure 6.15 Samples of chloride ions concentration test before cutting and after cutting for a) samples with green inhibitor, b) with calcium nitrate
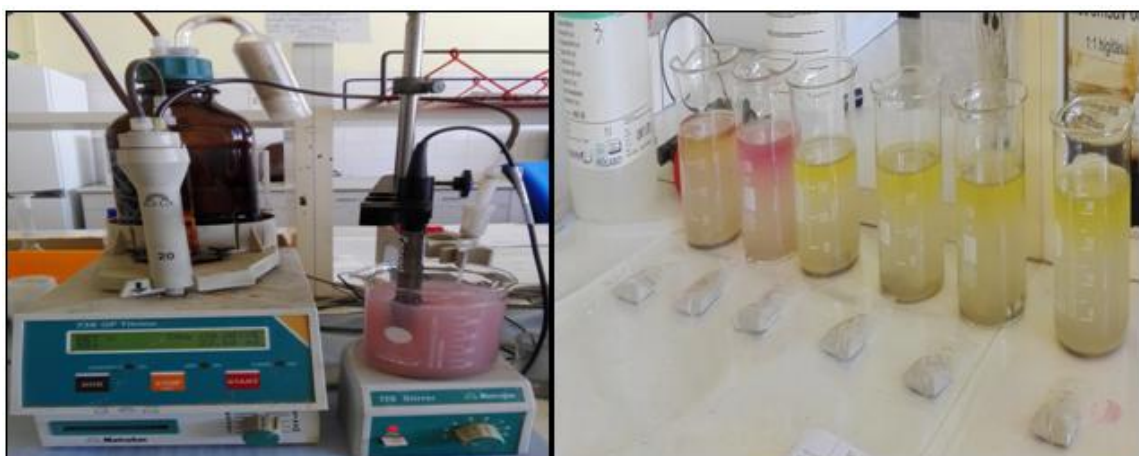
Figure 6.16 Test Cl^- ions concentration process

Table 6.5 Critical Chloride Thresholds [101]

Total Chloride by Mass of Cement	Concrete Society [102]
< 0.4%	Low risk
0.4-1.0%	Medium risk
1.0-2.0%	High risk (for > 1.0%)
> 2.0%	Certain risk

6.4.5 Electrical Resistivity Measurement

Electrical resistivity is a property widely used to monitor concrete structures because it is a nondestructive method and allows for external monitoring by means of embedded electrodes. This property is fundamentally related to fluid permeability and to ion diffusivity through concrete pores [103]. ($150 \times 150 \times 150$ mm^3) concrete cube reinforced with three (8 mm diameter) longitudinal wires. The three bars of reinforced concrete samples are arranged as equal leg triangular with 8 cm leg length as shown in Fig. 6.17.

Figure 6.17 Details of reinforced concrete specimen for electrical resistivity test

The electrical resistance of the reinforced concrete specimens was measured with an Ohmmeter (MTX 3250) digital multimeter by measuring the electrical resistance between each two wires [104] as shown in Fig. 6.18. The average of three readings was recorded and the readings are in KΩ units.
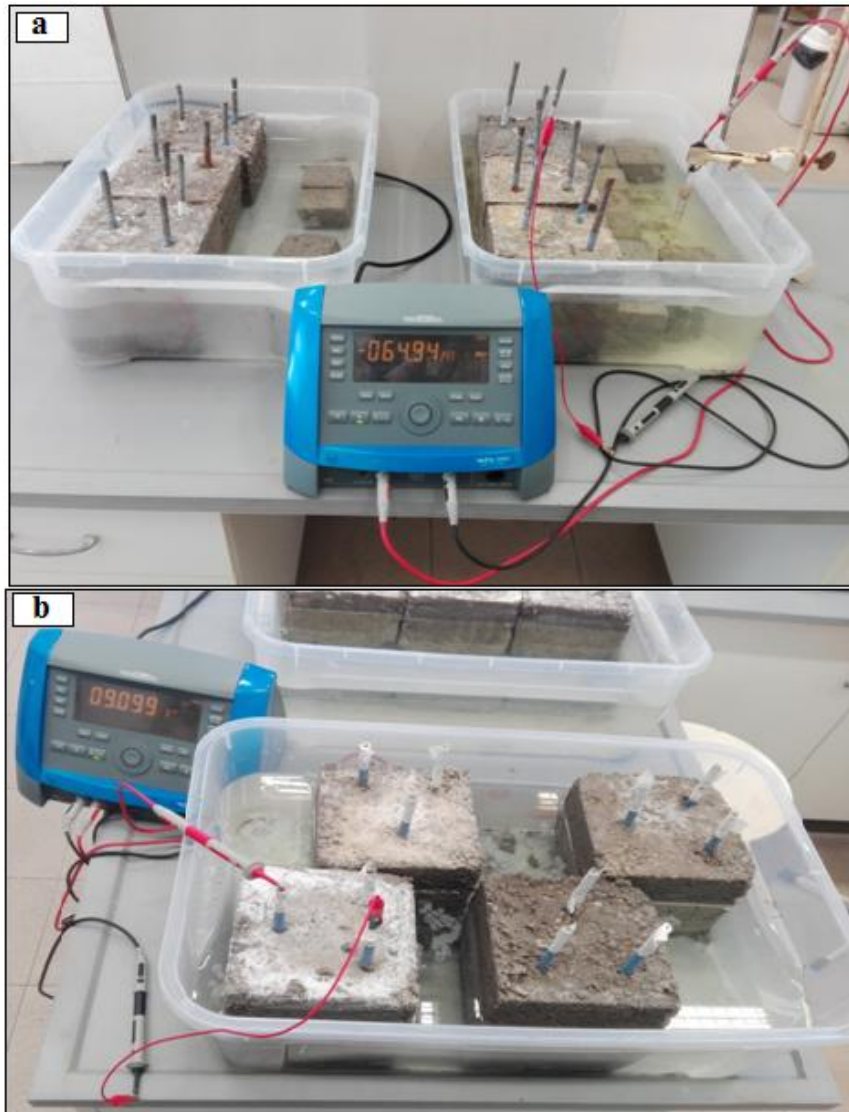
Figure 6.18 Electrical resistance test setup with the specimens and the ohmmeter a) samples with green inhibitor, b) with calcium nitrate
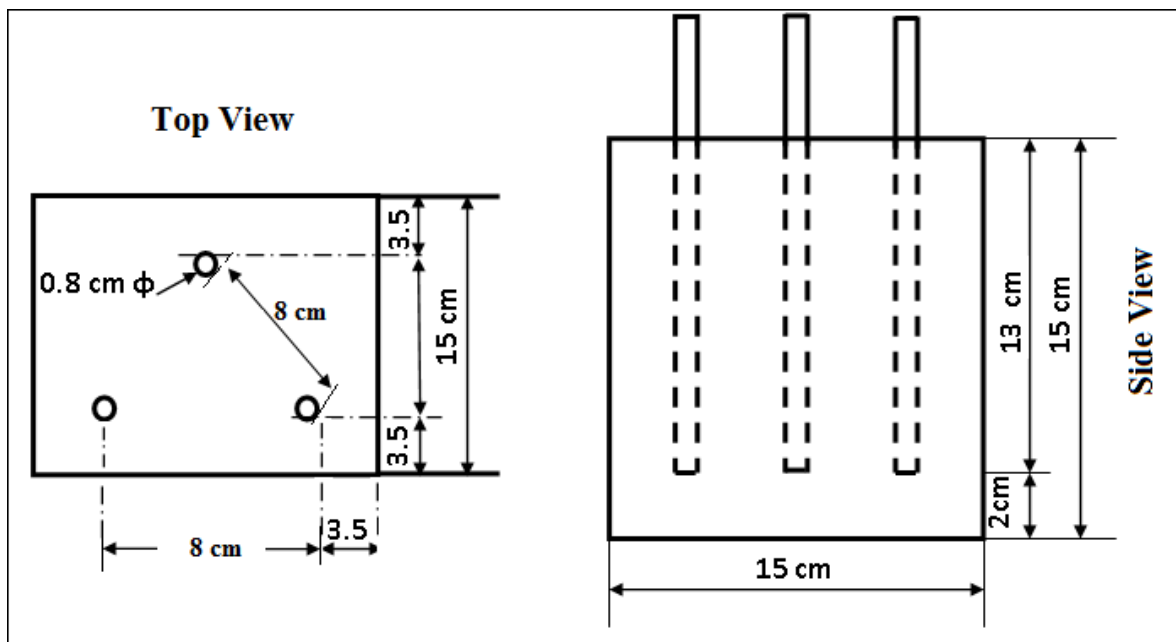
6.4.6 Half-Cell Corrosion Potential

The half-cell potential test is described by BS EN 1504 [105]; it is an electrochemical testing method that indicates active corrosion, which would probably occur in the reinforcing steel bar. This method uses a copper-copper sulfate (Cu-$CuSO_4$) reference electrode and a standard voltmeter to measure the potential difference between the reinforcing steel and reference electrode. The steel reinforcement was connected to the positive end of the voltmeter and the reference electrode was connected to the negative end. The potential difference provides an indication of the presence or lack of active corrosion of the reinforcing steel as described in Table 6.6. The copper – copper sulfate electrode consists of a plastic tube, having a height of 150 mm and an inside diameter of 50mm. Low permeability ceramic filter material of a porous plug is made for the bottom

end of tube, while the upper end of the tube is a plastic bushing having a central hole of 6mm diameter to allow a copper rod to pass through the tube.

The electrochemical potential of steel of concrete specimens was measured through comparing it to a reference electrode (copper – copper sulfate electrode). The concrete specimens were reinforced by one steel rebar (8 mm). For each bar, three readings (one in the first part, one in the middle, and one in the end part of sample) were taken to calculate their average as the recorded potential. This test was conducted periodically, and during the period of testing the area was wetted a little bit by 3.5% sodium chloride solution as show in Fig. 6.19. The samples were tested in the surface treatment labs of Institute of Metallurgy at Faculty of Materials Science and Engineering.

Table 6.6 Probability of corrosion related with half-cell potential measurements with Cu/CuSO$_4$electrode [106]

Half – cell potential (mV)	Interpretation
> -200	Low probability (10%) of corrosion
-200 to -350	Corrosion activity (50%)
< -350	High probability (90%) of corrosion
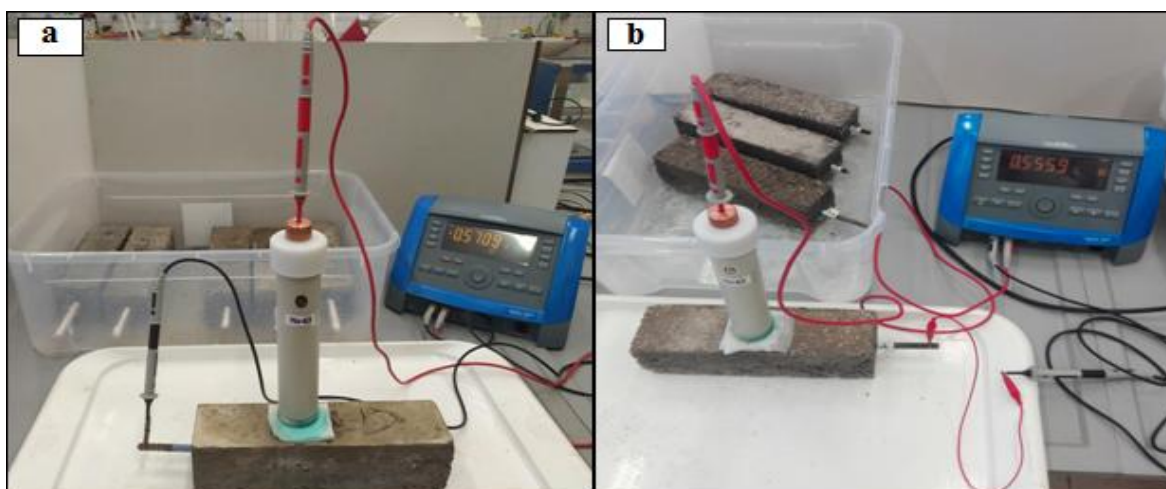
Figure 6.19 Half-cell potential test setup with the specimen and the measuring circuit with the reference Cu/CuSO$_4$ electrode and the voltmeter a) samples with green inhibitor, b) with calcium nitrate

6.4.7 Linear Polarization Resistance (Corrosion Current)

Corrosion current was determined through Tafel plot using programmer polarizing device. Our electrochemical polarization (Corrosion Current) experiments have already been commenced in collaboration with the Department of Surface Technology, Engineering Division in Budapest at the Bay Zoltán Nonprofit Ltd. for Applied.

The examination was implemented upon the steel bars embedded in concrete specimens, exposed to 3.5% NaCl solution, in addition to specimens that were subjected to accelerated corrosion program. For this purpose, the three electrode of the device were used differently. The calomel electrode used as reference electrode, the platinum electrode as auxiliary electrode, and the steel bars that were embedded in concrete were used as working electrode. The device was programmed to polarize the potential of the steel up to ±120 mV from/to the value of open circuit potential in both directions (cathodic and anodic). Afterwards, the program would draw a relationship between the potential and current through semi-logarithmic scale. Accordingly, the corrosion current intensity can be calculated then through dividing the corrosion current (I_{corr}) by the surface area of the rebar, which was embedded in concrete that was exposed to the solution. Fig. 6.20 shows the way of connecting the electrodes to measure corrosion current of reinforcing steel.
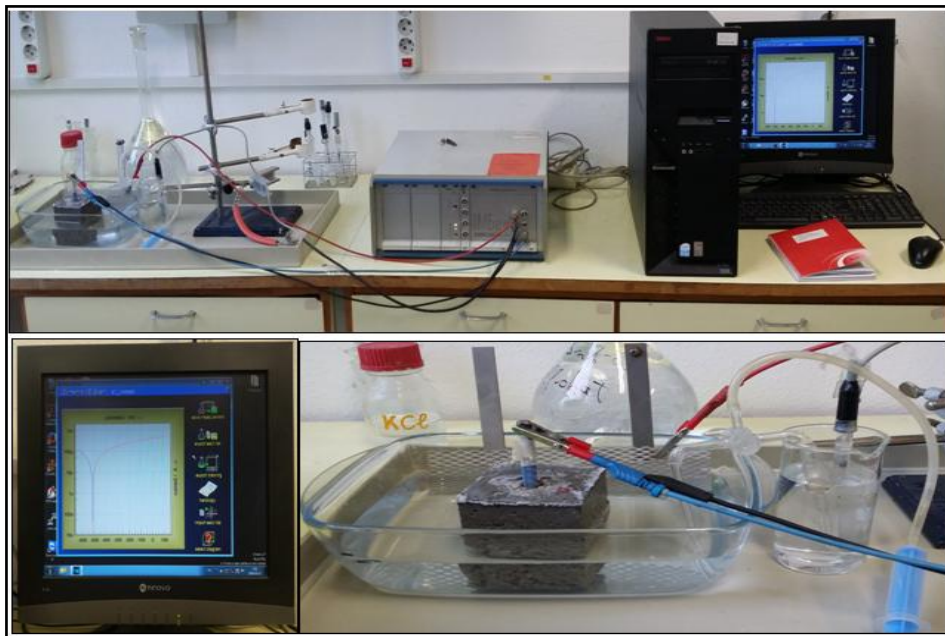
Figure 6.20 Linear polarization resistance test setup with the specimen and the measuring circuit

6.4.8 Studying Corrosion Products at the Steel-concrete Interface of the Samples

The concrete samples with two types inhibitors had been immersed and kept in 3.5% NaCl solution for 18 months, then the samples were removed from the 3.5% NaCl solution as shown in Fig. 6.21.
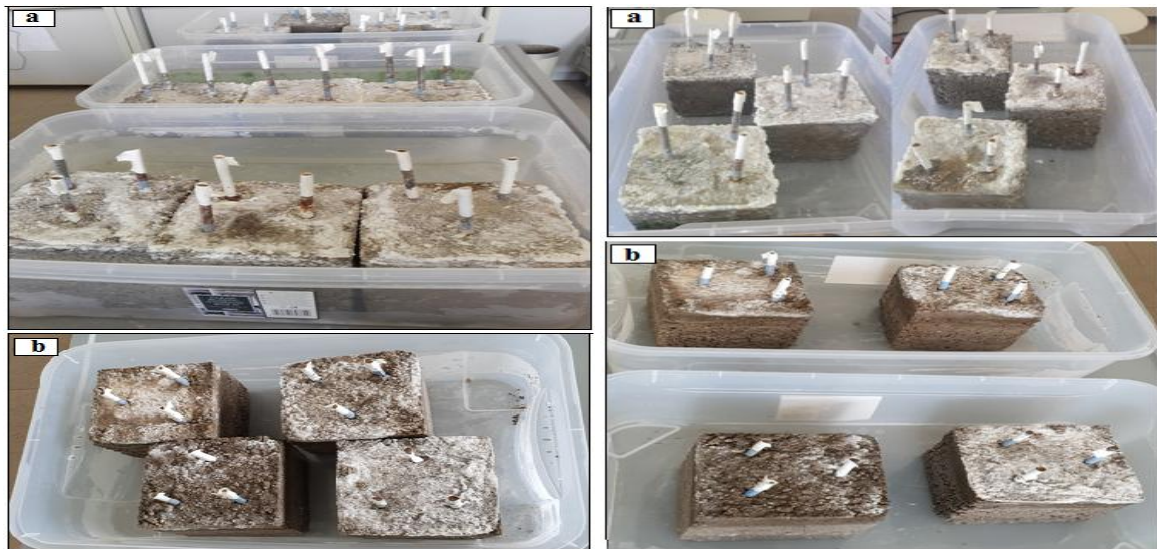
Figure 6.21 Reinforced concrete samples, from the left: were immersed in 3.5% NaCl solution for 18 months, from the right: removed after 18 months immersion in 3.5% NaCl solution; a) samples with green inhibitor, b) with calcium nitrate

After drying the samples, the concrete cubes (15cm*15cm) was selected to cutting into three parts as shown in Fig. 6.22, after that the steel rebar was took out from the cubes. Cutting processes were done in labs of Institute of Mining and Geotechnical Engineering in Faculty of Earth Science and Engineering at University of Miskolc.

Figure 6.22 Reinforced concrete samples after cutting a) samples with green inhibitor, b) with calcium nitrate

6.4.8.1 SEM Observation

It is well-known that not all corrosion products participate in concrete cracking as some of them fill in the voids around the rebars and some of them migrate from the steel/concrete interface to the pores in concrete. Scanning electron microscopy (SEM) imaging and EDS elemental mapping were employed on the surface of the steel rebars after detaching them from the concrete blocks in order to assess spatial distribution of corrosion products at the steel/concrete interface. Measurements were done on Zeiss EVO/MA10, using accelerating voltage of 15 kV.

6.4.8.2 Optical Microscopy

Thin sections (thickness 1cm) were also cut from each sample to examine with light optical microscopy. The cut sections were dried in air, impregnated with epoxy resin under vacuum, and finally grounded and polished by silicon carbide papers of up to 1200 grit; then diamond spray and finally, 0.05-mm Al_2O_3 suspension, etched (in 3% Nital, for approximately 10 s). In this study, light optical microscopy was especially used to detect the extent and spatial distribution of rust, capillary porosity and secondary precipitated phases in voids and cracks at the steel-concrete interface of the samples.

6.4.8.3 XRD Analysis

To clarify the rust compositions and diffusion of water and chloride ions, small concrete parts were sampled from the concrete in direct contact with the steel bars as shown in Fig. 6.23. These parts were then ground and analyzed by X-ray powder diffraction (XRD). The powder samples (size <5 µm) were analyzed by the XRD technique using CuKα-radiation at angles from $2\theta = 2º$ to $70º$ ($0.007º2\theta/24$ sec counting time) on a Bruker D8 Advance instrument, in parallel beam geometry obtained with Göbel mirror, equipped with Vantec-1 position sensitive detector (1° opening).
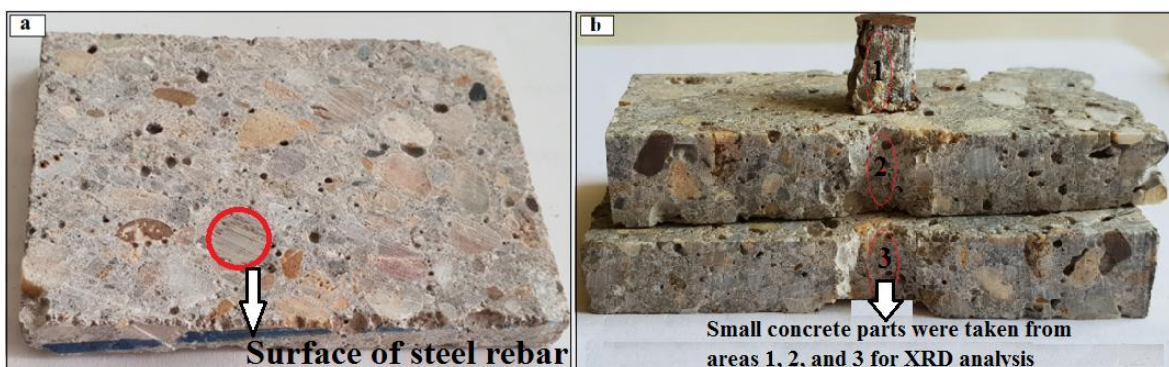

Figure 6.23 Sliced concrete blocks showing the embedded and cut steel rebar (a), and the three small areas /1,2,3/ in (b) from where materials were sampled for the XRD analysis

Chapter Seven: Results and Discussion

In this chapter, the results of the tests described in Chapter six are presented and discussed. Tests were carried out in laboratory conditions. To summarize the data, only the average values are provided in the tables and figures below.

7.1 Analysis of the Chemical Composition

7.1.1 Inhibitors and Admixtures

The chemical structure of the green inhibitor (orange peels extract) was determined by FTIR technique (as shown in Fig.7.1).

Figure 7.1 Fourier transform infrared spectrum (FTIR) depicting its IR absorbance peaks in the function of wave number with the most significant values indicated above the peaks for dry orange peels powder

In the high energy region the peak at $(3280.93)cm^{-1}$ is due to a large amount of OH groups of the carbohydrates and those of lignin. Also at $(1045)cm^{-1}$ this peak corresponds to the link C–O–H or C–O–R (alcohols or esters) while the distinctive band at $(2925)cm^{-1}$ is related to the presence of C–H stretching vibration together with bending vibrations around $(1428)cm^{-1}$ of aliphatic chains ($-CH_2-$ and $-CH-$) forming the basic structure of this lignocellulosic materials. All of these compounds can form double bounds, triple ties and aromatic rings linkages with the surface of steel rebar causing the formation of a protective layer around it. Some researchers explain the corrosion reduction after adding green inhibitor to the fresh reinforced concrete due to the increase in the alkalinity near the

region of the steel reinforcement, which favors the reestablishment of the passivating film, in addition to the high concentrations of aluminates, which hinder the diffusion of chlorides [107]. The chemical structure of calcium nitrate was determined by FTIR technique (as shown in Fig.7.2).
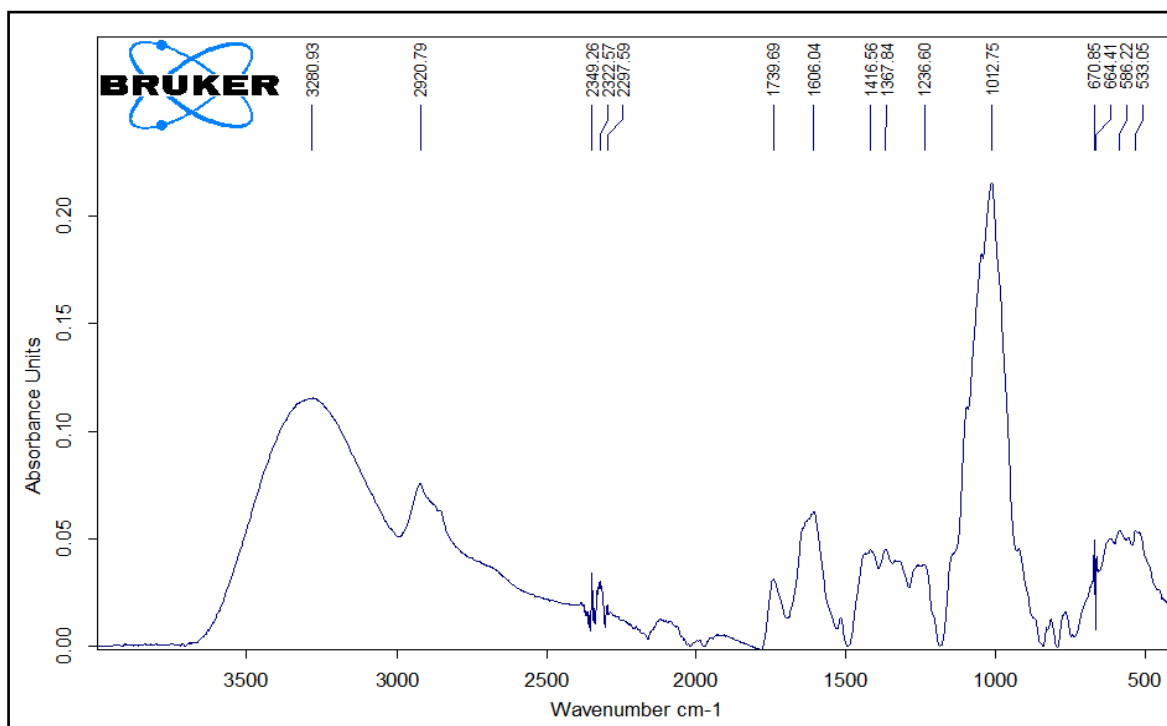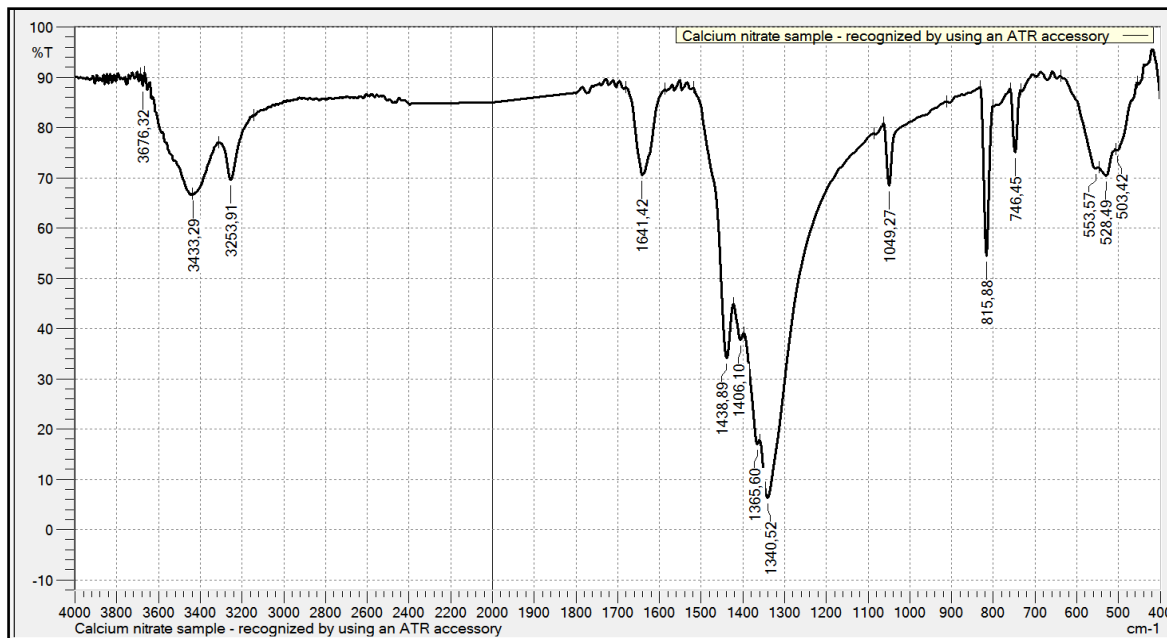

Figure 7.2 Fourier transform infrared spectrum (FTIR) depicting its IR absorbance peaks in the function of wave number with the most significant values indicated above the peaks for calcium nitrate inhibitor

The relatively strong absorption band at ~3642 cm^{-1} corresponded to the OH stretching mode. The OH stretching absorption band was not so sharp. Similarly, the broad band from ~3253 to 3433 cm^{-1} also corresponded to the OH stretching modes. The peak at ~1641 cm^{-1} was due to the NO$_2$ symmetric stretching. The broad band centered at ~1438 to 1406 cm^{-1} refers to the deformation of C-H group. The peak at ~1365 cm^{-1} was due to the NO$_3^-$ stretching. The peak at ~1340 cm^{-1} was due to the symmetric stretching mode of the N=O. The sharp peak at ~815 cm^{-1} corresponded to the wagging and twisting of NH$_2$ group. The peak at ~746 cm^{-1} was due to the vibration. All of these compounds can form double bounds, triple ties and aromatic rings linkages with the surface of steel rebar causing the formation of a protective layer around it. A somewhat similar approach was considered and taken by M. Esthaku Peter, P. Ramasam [108] when they studied structural, growth and characterizations of triglycinium calcium nitrate.

From Fig.7.3 it appears that the main component of the liquid superplasticizer admixture is a low molecular weight polyethylene glycol together with a smaller portion of a lower ester.
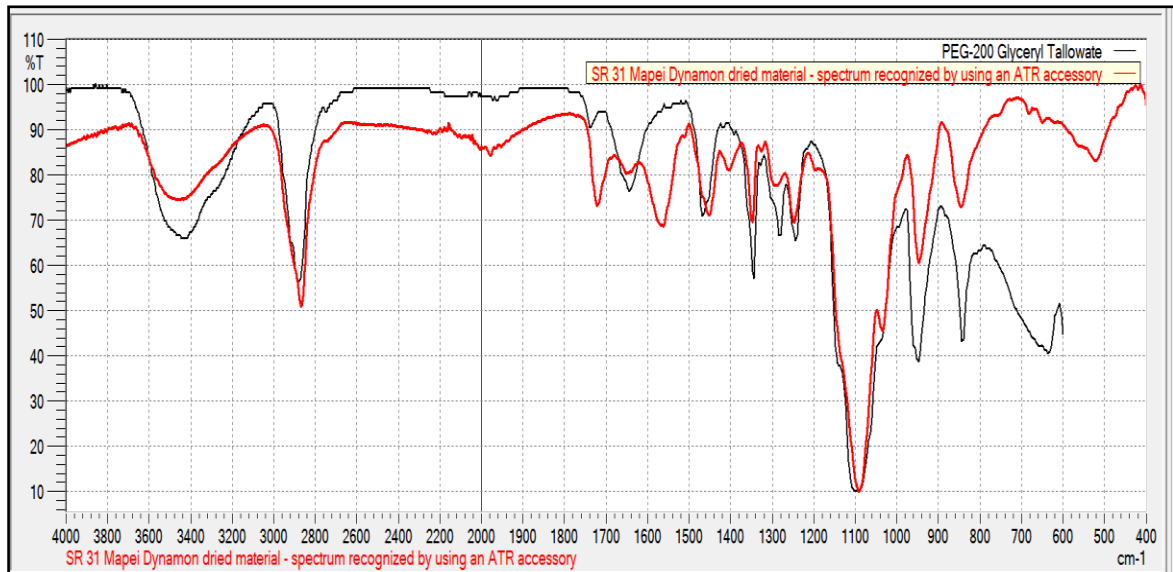
Figure 7.3 Fourier transform infrared spectrum (FTIR) depicting its IR absorbance peaks in the function of wave number with the most significant values indicated above the peaks for: Dynamon SR31

ICP-OES and EDS analytical techniques were used to determine the major chemical elementary components of water-resisting admixture as given in Table 7.1. The water-resisting admixture should consist of some mineral components such as calcium oxide, silicates and aluminates, so these components should also play important roles during the hydration of the freshly prepared concrete.

Table 7.1 The approximate chemical composition of water-resisting admixture (expressed as oxides) derived from two different chemical elementary analytical techniques

Components (as oxides)	Composition in wt% and in at% (approximatevalues)		
	by EDS (using SEM) method, in wt%	by EDS (using SEM) method, in at%	by ICP-OES method, in wt%
CaO	61.8	57.2	58.0
SiO$_2$	27.3	27.1	21.4
Al$_2$O$_3$	2.59	4.4	4.47
MgO	2.11	1.4	1.20
Na$_2$O	0.83	0.85	0.31
K$_2$O	0.91	1.4	0.78
Fe$_2$O$_3$	1.31	3.5	2.67
SO$_3$	3.18	4.2	2.50
TiO$_2$	-	-	0.27
ZnO	-	-	0.14
SrO	-	-	0.09
Mn$_2$O$_3$	-	-	0.05
Cr$_2$O$_3$	-	-	0.006

7.1.2 Steel Rebar

The chemical composition (in% by mass) of steel rebar was determined by analytical analysis using ICP-OES technique and the result was presented in Table 7.2.

Table 7.2 The approximate chemical composition of steel rebar (concentration in wt%)

C	Mn	Si	P	S	Cr	Ni	Cu	Mo	Fe (calculated)
0.19	0.78	0.24	0.027	0.035	0.11	0.11	0.27	0.02	98.22

7.2 Compressive Strength Test

Fig.7.4 shows the results of compressive strength test at age 28 days for samples with green inhibitor (orange peels extract).
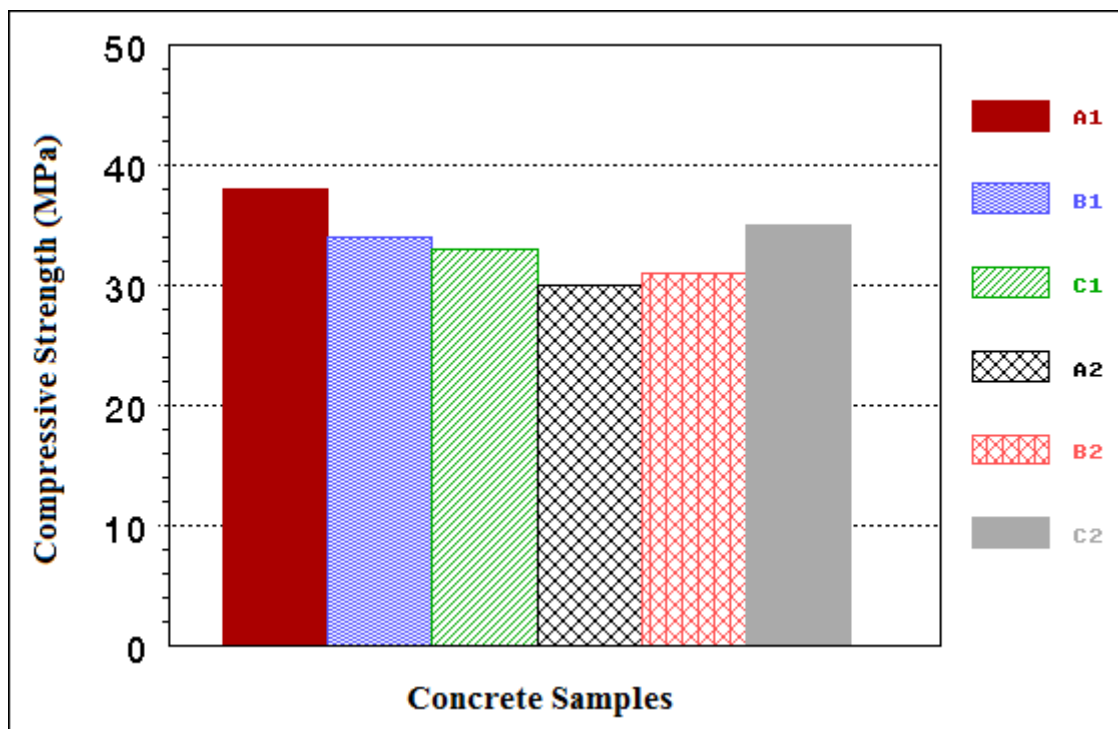

Figure 7.4 Compressive strength of concrete samples with green inhibitor after immersion in tap water for 28 days

The results showed that:

1) For superplasticizer admixture in concrete there was not much reduction observed in the compressive strength. By using the orange peels extract as corrosion inhibitor in conc. 1% and 3% by weight of cement, it reduced the compressive strength considerably by 10.5% for 1% addition and 13% for 3% addition, respectively.

2) For water-resisting admixture with concrete causes reduction in compressive strength more than superplasticizer admixture in sample without green inhibitor. After using green inhibitor with 1% and 3% by weight of cement affect compressive strength with an increase 3.3% for 1% addition and 16.6% for 3% addition respectively. That's may be due

to this inhibitor works as a retarder, it retards the action or effect of tricalcium silicate (C_3S) or tricalcium aluminate (C_3A) and these action modifies the compressive strength at the early ages of the concrete. The increase in compressive strength after addition green inhibitor because adding inhibitor mean decreasing the amount of cement (inhibitor adding to concrete by weight of cement%), so with increasing the concentration of inhibitor leads to decreasing the cement (decreasing the hydration components because it depend on water and cement) and already causing increasing the compressive strength.

The hydration reaction of ordinary Portland cement (OPC) involves four major types of hydration components, i.e. tricalcium silicate (C_3S), belite (C_2S), tricalcium aluminate (C_3A), and ferrite or brownmillerite (C_4AF). These compounds begin to react with water within a few minutes and absorb the water then do not generate much strength, but can stiffen the mix and reduce workability.

After adding calcium nitrate as a corrosion inhibitor, the results of compressive strength (as shown in Fig. 7.5) showed that:

(1) For superplasticizer admixture in concrete (without inhibitor) there was not much reduction observed in the compressive strength. By using calcium nitrate as corrosion inhibitor in conc. 1% and 3% by weight of cement, it increased the compressive strength considerably by 8% for 1% addition and 21% for 3% addition, respectively.
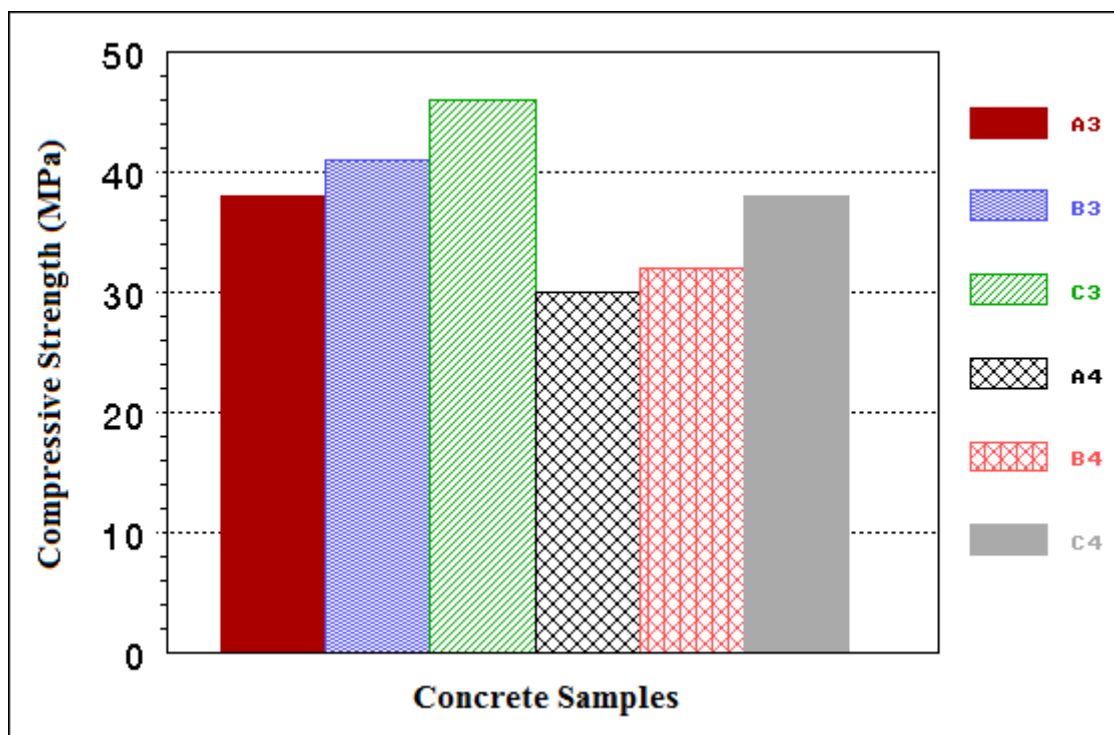

Figure 7.5 Compressive strength of concrete samples with calcium nitrate inhibitor after immersion in tap water for 28 days

(2) For water-resisting admixture with concrete causes reduction in compressive strength more than superplasticizer admixture in sample without inhibitor. After using calcium nitrate inhibitor with 1% and 3% by weight of cement, affect compressive strength with an increase 7% for 1% addition and 27% for 3% addition respectively.

The increasing in compressive strength after added calcium nitrate because this admixture provides a shortening of setting time or an increase in development of early strength (calcium nitrate is a multifunctional admixture for concrete, can work as setting accelerator for hydration process and as corrosion inhibitor). Calcium nitrate accelerate hydration process because that have Ca^{2+} cation like cement minerals C_3S and C_2S. In such a case crystallization processes are going intensively. Compressive strength at 3% calcium nitrate higher than 1 wt.% due to changes in composition of the amorphous calcium silicate hydrate binder (CSH-gel), (CSH-gel precipitated around the cement grains). An increased calcium concentration in the pore water when calcium nitrate is applied may stabilize a CSH-gel with a higher Ca/Si and thus a shorter average length of the polysilicate anions. The replacement of cement by CSF (Condensed Silica Fume), on the other hand, will lead to a CSH-gel with a lower Ca/Si ratio and longer length of the polysilicate anions, in addition to the formation of more gel due to the pozzolanic reaction. Another contributing factor may be a change in morphology of calcium hydroxide due to a lower solubility caused by a higher Ca^{2+} concentration in the pore water, this agree with several of researchers [109-113]

7.3 Porosity Measurement

Porosity is the sum of the entrained air pores and voids within the paste. By increasing the concentration of green inhibitor, porosity decreased as shown in Fig. 7.6.

The lowest porosity was obtained for the concrete with 3 wt.% green inhibitor and water-resisting admixture (sample C2). The maximum porosity of the samples tested was found with samples without inhibitor (A1, A2) but with high value in the sample with water-resisting admixture (A2). Comparing the effect of the superplasticizer admixture, it was observed that during the hardening of concrete, the superplasticizer (in A3) caused a decrease in water greater than water-resisting admixture (in A4) and this decreasing in water causes a decrease in porosity as a result of a sequence of chemical reactions (called hydration) of cement with water to form the binding material.
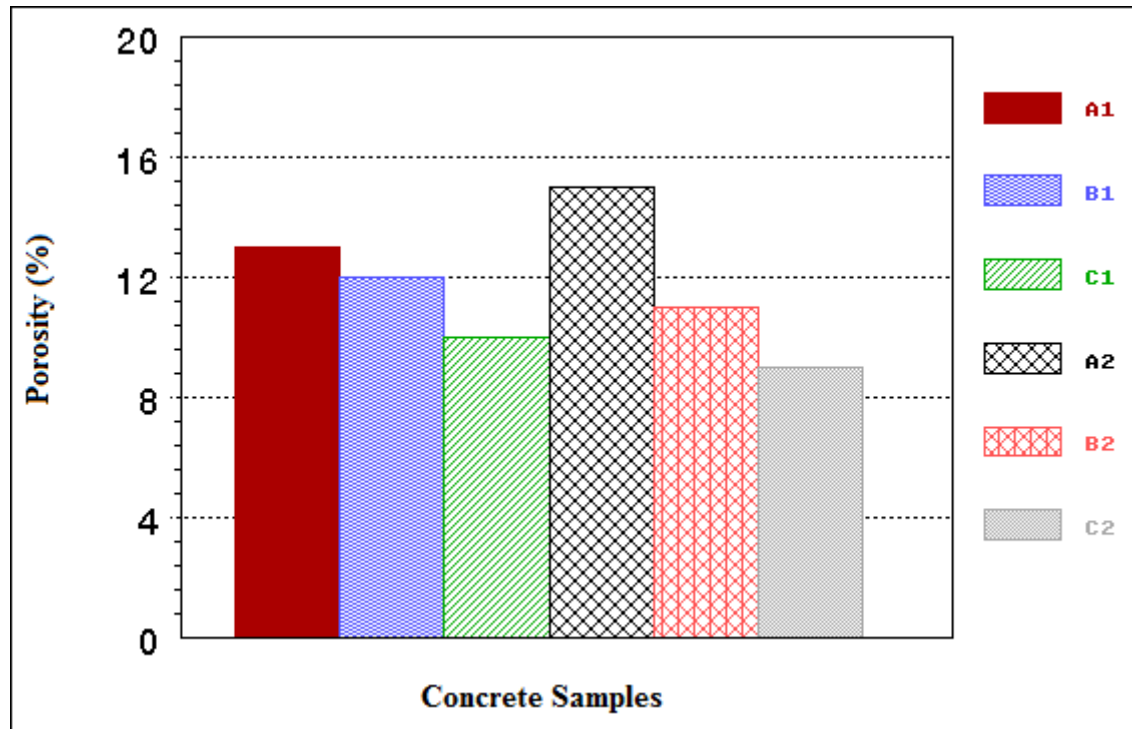
Figure 7.6 Variation in porosity for concrete samples with green inhibitor

Porosity did not change with 1 wt.% of the calcium nitrate inhibitor (particularly with superplasticizer admixture) but decreased with 3 wt.% of the same inhibitor as shown in Fig.7.7 for concrete samples.
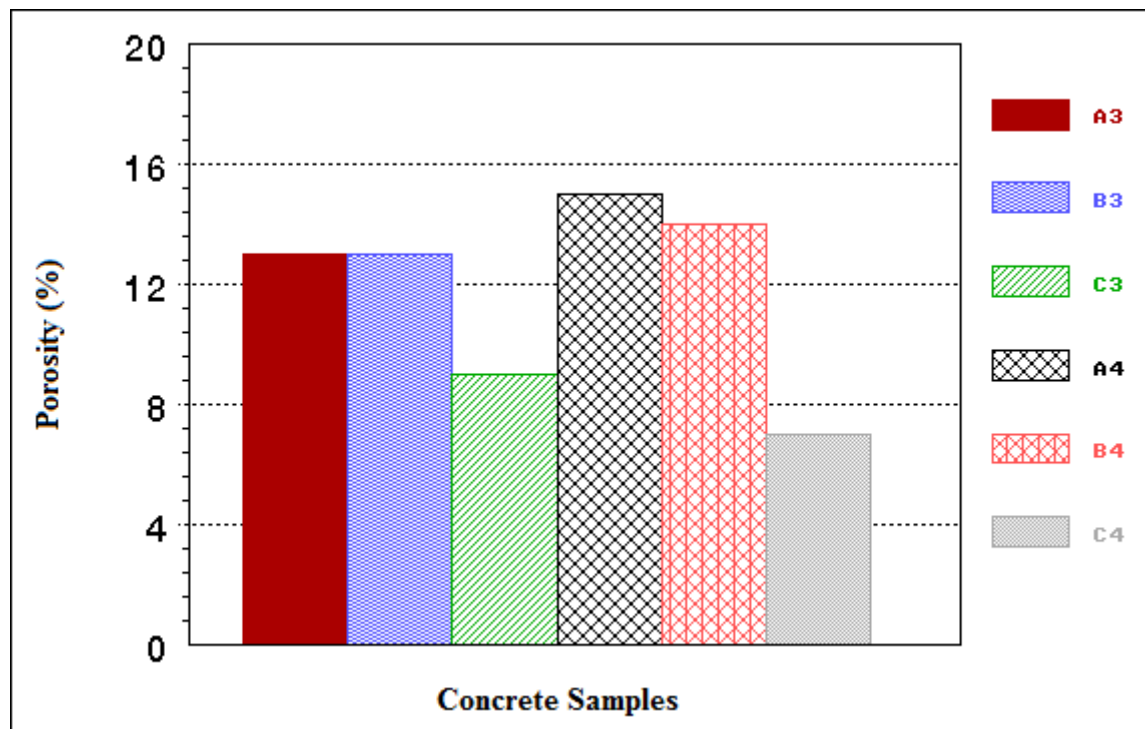

Figure 7.7 Variation in porosity for concrete samples with calcium nitrate inhibitor

For concrete with a 3 wt.% calcium nitrate inhibitor and water-resisting admixture (sample C4), the lowest porosity was obtained. The maximum porosity of the samples tested was found in samples without inhibitor (A3, A4), particularly in the water-resisting admixture sample (A4) and in high porosity samples with a 1 wt.% inhibitor.

7.4 Chloride Concentration (Cl⁻ ions) Test

The baseline chloride content was taken from three separate specimens (from the same sample with different depths (As I mentioned in the previous 6.4.4 part) from the concrete surface) prior to accelerated corrosion exposure. Figs.7.8 and 7.9 show the results of the chloride ions concentrations in concrete samples determined at the end of the different immersion periods of 1, 3, and 6 months, in 3.5% NaCl solution. The cut side and middle sections of the samples were analyzed in the laboratory of the BorsodChem company.

As the Cl⁻ ions testing apparatus, shown in Fig.6.16, provides the chloride ions concentrations in ppm units, to be able to compare them with any given standard values, I must convert them to the mass of cement or bwoc (the chloride content is most commonly expressed as a concentration of chlorides in the binder, and is usually expressed as a percentage by weight of the cement, or "% bwoc") according to the Technical Notes [114] given in eq. (7.1):

$$\frac{cement\ content\ \left[\frac{kg}{m^3}\right]}{concrete\ density\ \left[\frac{kg}{m^3}\right]} \cdot 100\% \qquad (7.1)$$

In this work was the cement content is 400 kg/m³ and the density of the concrete is 2400 kg/m³, so the cement content will be:

$$\frac{400\frac{kg}{m^3}}{2400\frac{kg}{m^3}} \cdot 100\% = 0.167 \cdot 100\% = 16.7\%$$

To convert an analytical result for the chloride content of ppm_{conc} to % bwoc, it must be divided first by the cement content as a percentage, then divided again by 100.

For example, if the analytical result for the chloride ions content is 1000 ppm_{conc}, and if the cement content is 16.7%:

$$from\ 1000\ ppm_{conc}\ \rightarrow\ \frac{1000}{16.7\cdot100} = 0.6\%\ \text{bwoc}$$

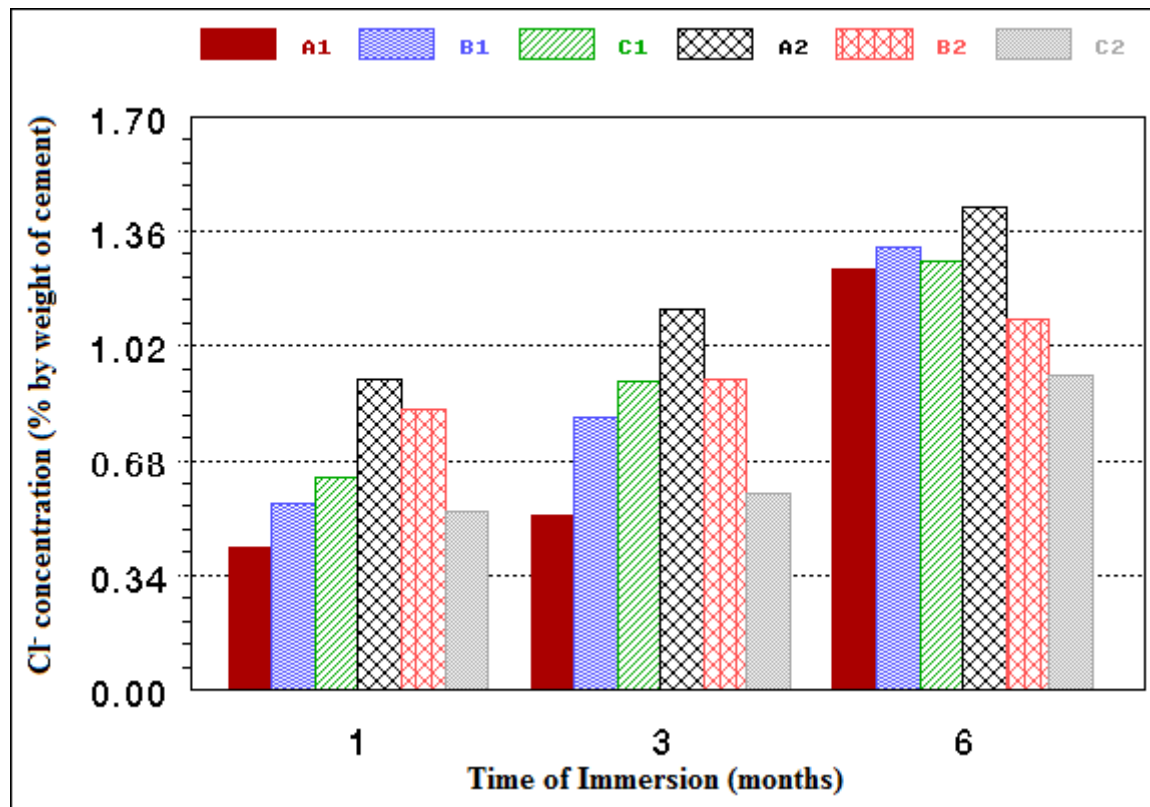So in this way I have converted all the results of Cl⁻ ions concentration to the mass of cement [bwoc].

Figure 7.8 Cl⁻ ions concentrations in the middle (from depths 1.75 to 3.5cm) of concrete samples with green inhibitor after immersion in 3.5%NaCl solution for different months
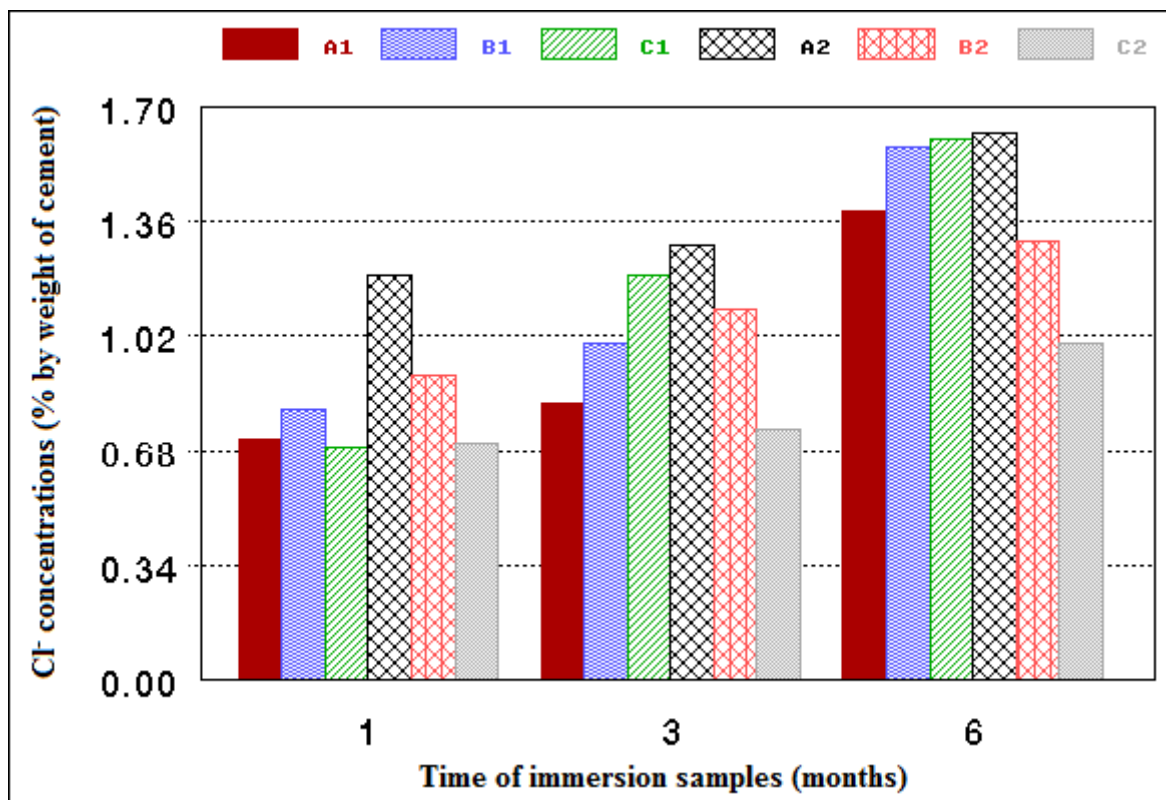

Figure 7.9 Cl⁻ ions concentrations in the outer sides (from depths 0 to 1.75cm) of concrete samples with green inhibitor after immersion in 3.5%NaCl solution for different months

From the results of Cl⁻ concentrations given in Figs. 7.8 and 7.9 for the samples immersed in 3.5%NaCl, it appear that all the samples after 6 months (only samples C1 it shows low value from the Cl⁻ concentrations) show high risk of corrosion because the Cl⁻ concentrations are higher than 1% by weight of the cement.

The sample C2 (both in the outer sides and the middle part) has the lowest concentrations of chloride ions after 6 months immersion in 3.5%NaCl. This sample had about 3 wt.% green inhibitor together with water-resisting admixture, hence, its many active groups and strong bonding ability must have reduced the porosity the most and reduced effectively the diffusion of chloride in the sample. Moreover, the wide particle distribution of the green inhibitor can also help provide better particle packing, and it can be speculated that this shifts the pore size distribution towards the micropores, constricting pathways from diffusing chloride ions even when total porosity may be similar between different mixes of having the same water-cement ratio.

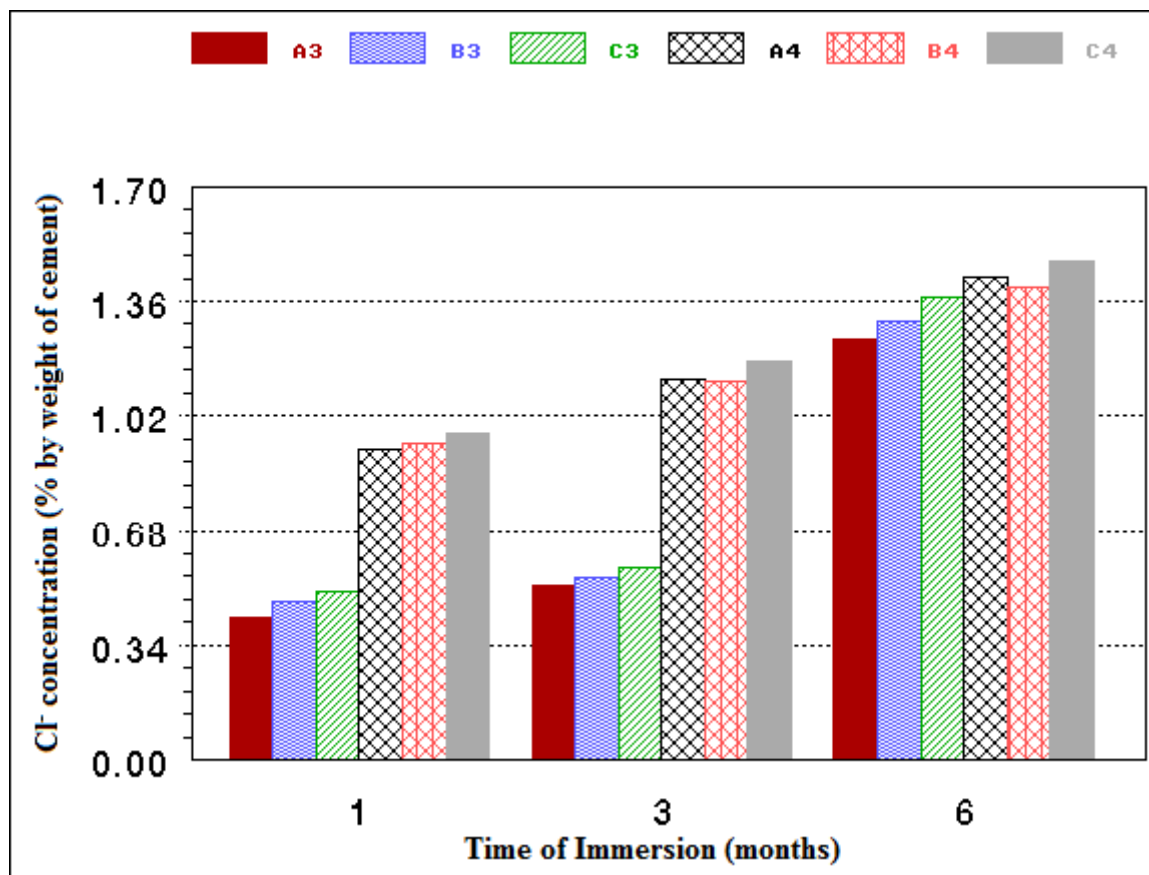After added calcium nitrate inhibitor the results of Cl⁻ ions concentrations shown in Figs. 7.10 and 7.11.

Figure 7.10 Cl⁻ ions concentrations in the middle(from depths 1.75 to 3.5cm) of concrete samples with calcium nitrate after immersion in 3.5%NaCl solution for different months
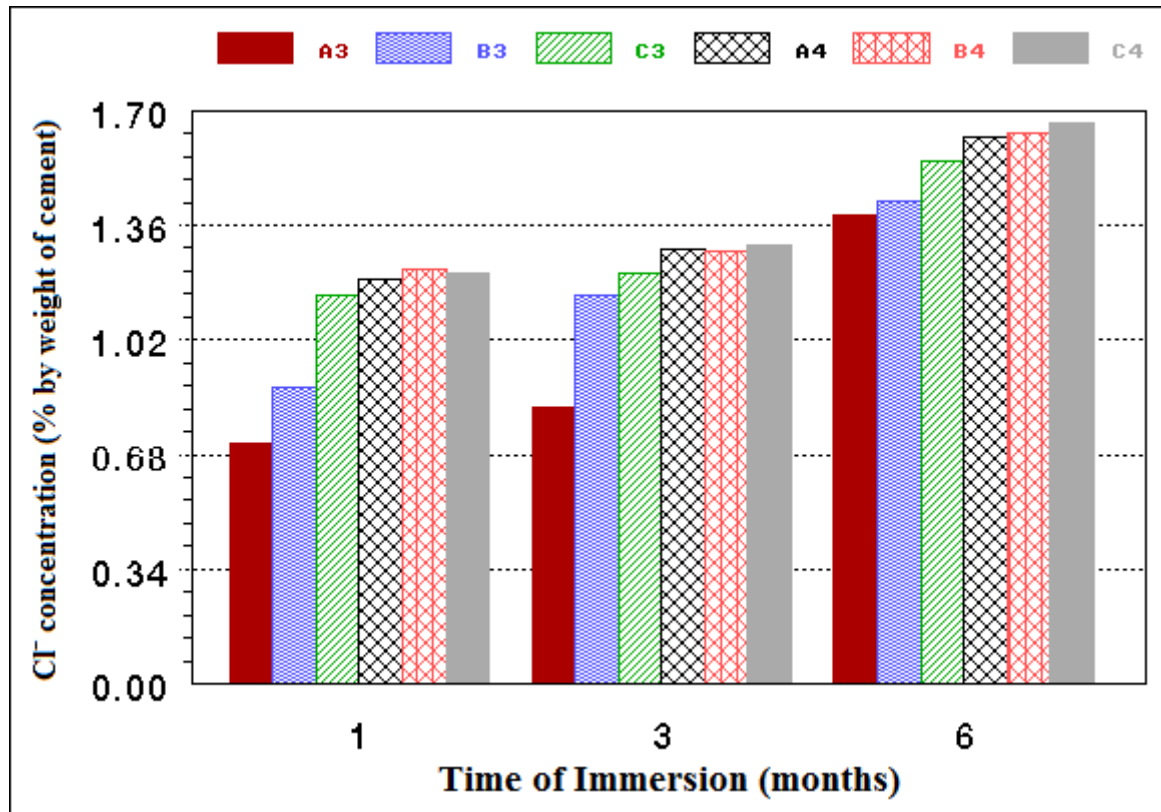
Figure 7.11 Cl⁻ ions concentrations in the out sides (from depths 0 to 1.75cm) of concrete samples with calcium nitrate after immersion in 3.5%NaCl solution for different months

The results of Cl⁻ concentrations in Figs. 7.10 and 7.11 for the samples immersed in 3.5%NaCl, it appeared all the samples after 6 months have high risk for corrosion because the Cl⁻ concentration more than 1% by weight of the cement. Normally Cl⁻ ions concentration in depths from 1.75 to 3.5cm (in the middle of the sample) less than in the depths from 0 to 1.75cm. The Cl⁻ ions concentration increasing with increase the concentration of calcium nitrate, so the concrete samples with 3 wt.% calcium nitrate have the highest ratio from Cl⁻ ions comparing with other samples and thereby slightly increases the risk of depassivation of the protective oxide layer on the embedded steel. However, this is not due to a decrease in chemical bound chloride as Friedels salt (Friedel's salt is an anion exchanger mineral belonging to the family of the layered double hydroxides, well-known as a synthetic phase in cement mineralogy. It has affinity for anions as chloride and iodide and is capable to retain them to a certain extent in its crystallographical structure, the formula of it: $[Ca_2Al(OH)_6 (Cl, OH) \cdot 2H_2O]$. The reason for the increased Cl⁻ ions is a slight reduction in the OH⁻ concentration by increasing the Ca^{2+} concentration, which is due to the low solubility of calcium hydroxide;

$$Ca(OH)_2 \text{ (s)} \leftrightarrow Ca^{2+} + 2OH^- \qquad\qquad (7.2)$$

This also approved by the researchers H. Justnes and E.C. Nygaard [113].

7.5 Electrical Resistivity Measurement

When the concrete is produced with a good quality, its electrical resistance will be high. The micro cracks in concrete mass that open a way for water and salts to go through increase the conductivity and decrease the electrical resistance for concrete. Chloride ions, if found, increase the conductivity of the pores solution and carbonation decreases it, therefore, an increase in electrical resistance of concrete is accompanied by a reduced corrosion rate. Hence, in our investigation as well, the electrical resistance changes and/or trends of our concrete samples can be correlated with the probable corrosion rate changes in the function of testing time periods.

The results of our electrical resistance test for reinforced concrete samples with green inhibitor (in KΩ) are shown in Fig. 7.12.
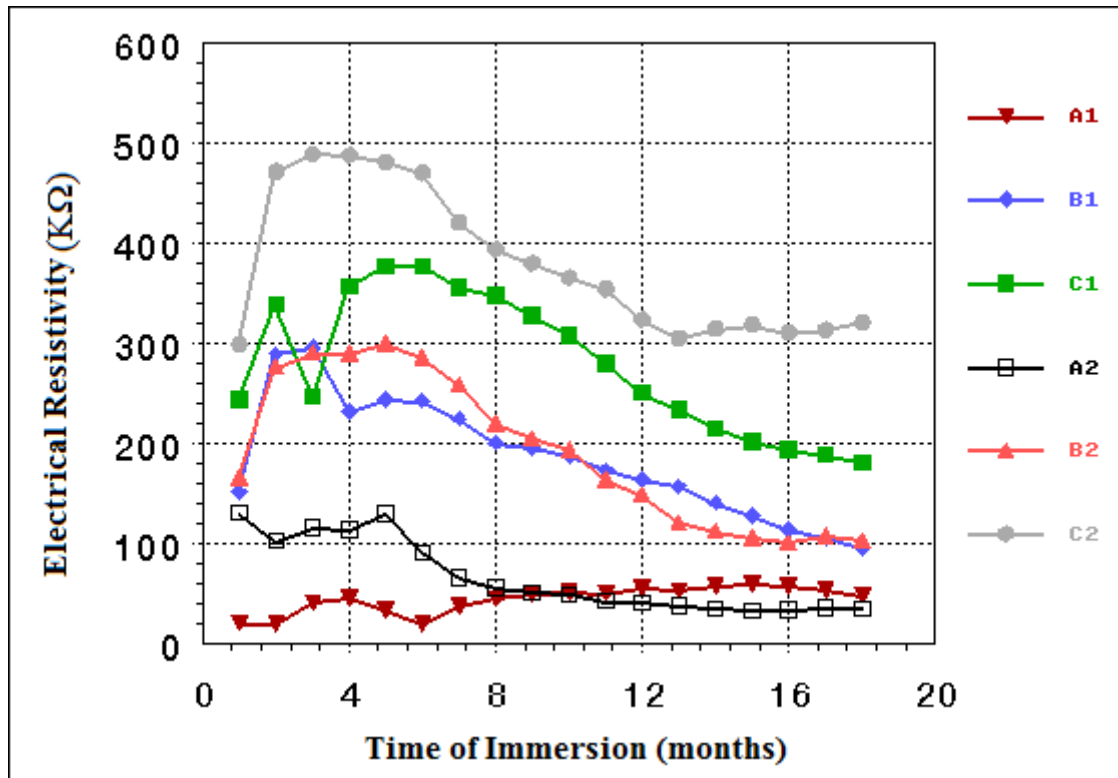

Figure 7.12 Electrical resistivity of concrete samples (with green inhibitor) with different time of immersion

Figure 7.12 sum up the electrical resistivity measured regularly during 18 months, at the first six month testing period it is apparent that all the samples with green inhibitor (B1, B2, C1 and C2) show increased electrical resistivity due most probably to the fine particle of the green inhibitor with the capacity of filling in most of the micropores of the samples during hardening. And, such a chloride ingress mitigation effect will reduce the mobile ions (first of all the chloride ions) concentration in the concrete pores and is making them less conductive.

65

During 18 months, and in this respect, the best sample showing the highest electrical resistivity was C2, first, because the chemical composition of the water-resisting admixture (with more active groups and forming stronger bounds), and second, together with C2 was containing the greatest admixing amount of green inhibitor (3 wt.%) could fill in well the pores and microcracks, and so increase considerably also the electrical resistivity in this sample. Otherwise, this interpretation agrees well with the findings of several authors [115-118], who showed that electrical resistivity is related to the microstructural characteristics of the cement matrix, such as porosity, pore size distribution, pore connectivity, and the conductivity of the aqueous solution in the matrix. The results of our electrical resistance test for reinforced concrete samples with calcium nitrate inhibitor (in KΩ) are shown in Fig. 7.13.
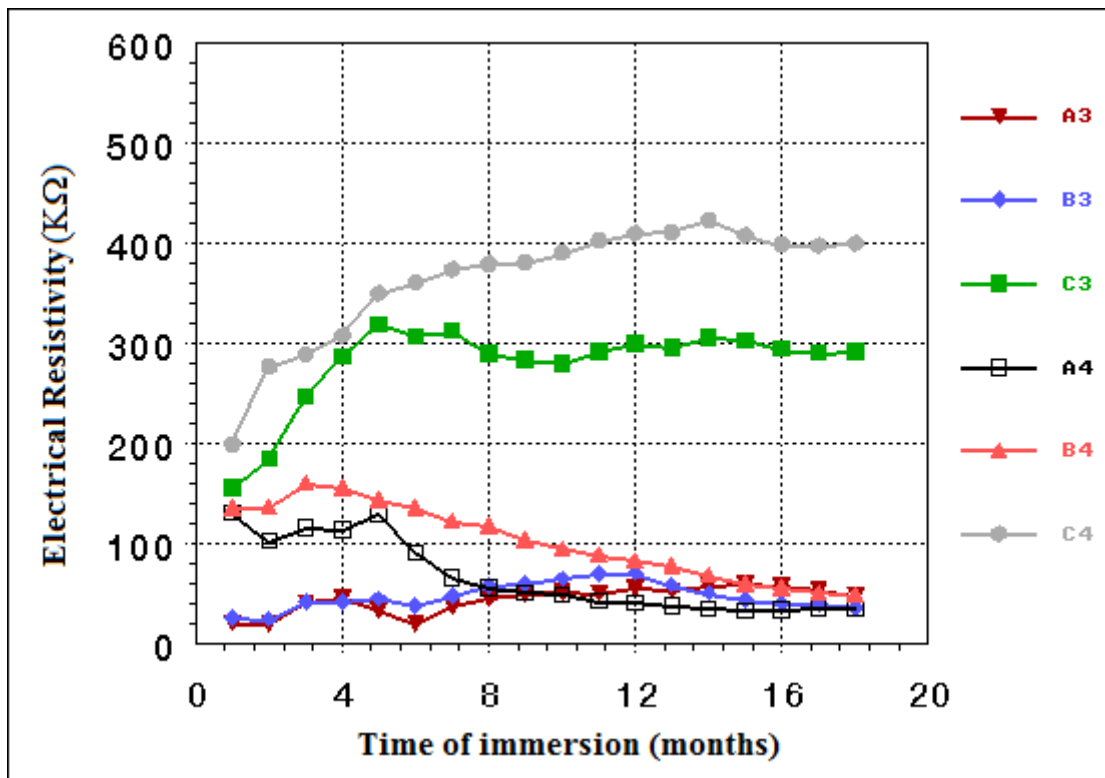

Figure 7.13 Electrical resistivity of concrete samples (with calcium nitrate) with different time of immersion

The average results of the electrical resistivity of the samples were indicated in Fig. 7.13, the samples with 3 wt.% calcium nitrate inhibitor showed increased electrical resistivity and it high values comparing with reference samples (A3, A4) but the electrical resistivity increased a little bit in the samples with 1 wt.% inhibitor because between 2 – 4% calcium nitrate of cement weight seems sufficient to protect the rebar against chloride-induced corrosion.

Calcium nitrate in the samples C3 and C4 successfully stopped most of the chloride-induced because calcium nitrate's corrosion inhibition is associated with the stabilization of the passivation film, which tends to be disrupted when chloride ions are present at the steel level. The destabilization of the passivation film by chlorides is largely due to interference with the process of converting the ferrous oxide to the more stable ferric oxide. Electrical resistivity in the samples B3 and B4 showed not low resist to corrosion because it have only 1 wt.% calcium nitrate (less than 2%) so the chloride ion transport is driven by permeation through the pores since the samples and these chlorides have broken into the passive film on the steel rebar because the inhibitor can't make this passive film as a stable. These behaviors similar with some researchers [119,120].

Samples with water-resisting admixture have high resistance comparing with samples have superplasticizer admixture because the pozzolanic behaviour of water-resisting admixture which reduces the porosity of the cement stone.

7.6 Half-Cell Corrosion Potential

Exemplary results of the half-cell potential measurements for samples with green inhibitor are shown in Fig. 7.14, on each sample, three half-cell readings were taken every test after that took the average for these reading.
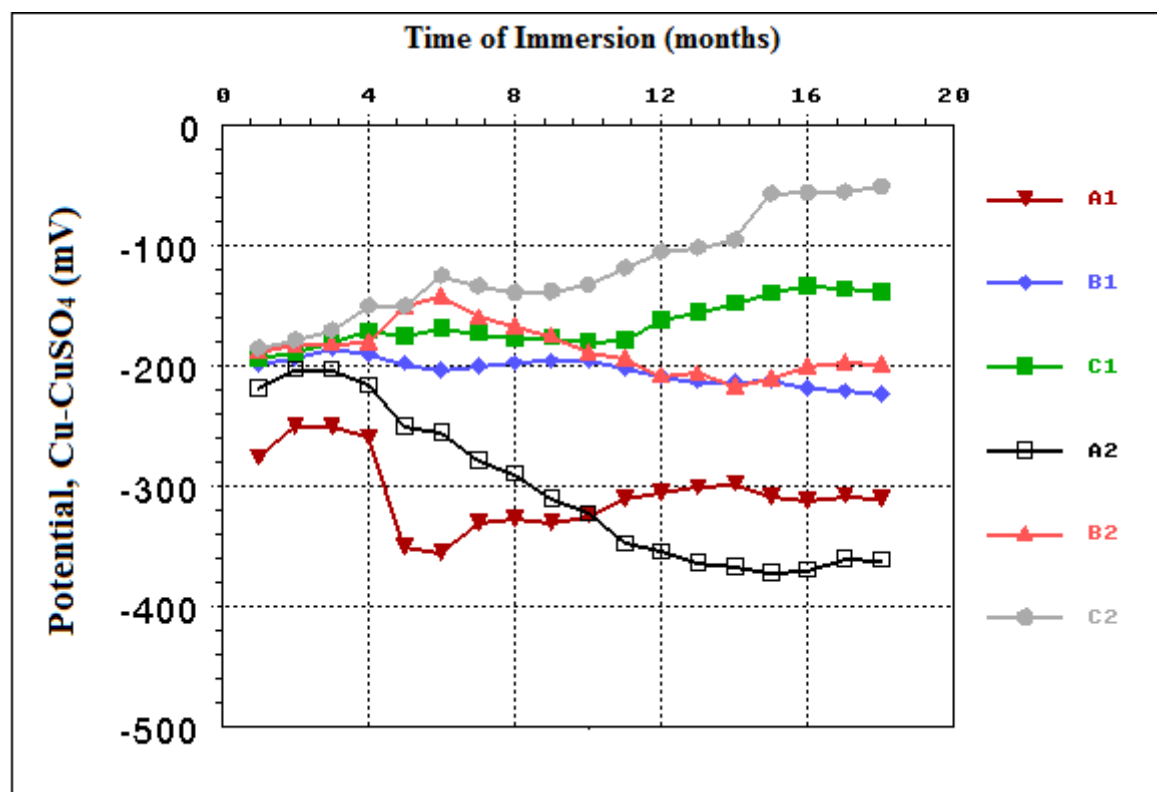

Figure 7.14 Corrosion potentials versus time for concrete samples with green inhibitor

It is clearly seen from Fig. 7.14 that the half-cell potential readings for all samples with green inhibitor (B1, B2, C1, and C2) are less negative (indicating greater resistance to corrosion) than samples without green inhibitor. In contradistinction to that the potential results obtained for samples A1 and A2 were more negative (between -200 to -350mV) after 5-6 months immersion in 3.5%NaCl, which corresponds to a 50% probability that corrosion was occurring.

Half-cell potential measurements became consistently less negative with increasing age for all six specimens. This course of change in potentials may be attributable to reductions in concrete permeability due to both the loss of moisture and the continuing formation of hydration products in the concrete bodies. Although it is falling a bit outside of the scope of the current project, long-term analysis of concrete slabs may provide further insight into the mechanisms associated with this observation. Previous research conducted on bridge decks having ages between 2 and 21 years indicated [121] that the relationship between age and half-cell potential was in fact not significant after so much longer ages than just during the first few months as it was studied in our present experiments [121].

In this research, however, during the 18 months period observed half-cell potential changes for the samples A1 and A2 are consistent with the measured increasing ingress chloride concentrations reflecting the role of chlorides in the corrosion process.

According to Naish et al. [122], half-cell potentials are very sensitive to the ambient environment, especially the oxygen concentration at the interface between the reinforcing steel and the concrete. In fact, the most challenging aspect of on-site measurement of outside concrete structures is the fact that the corrosion current is weather-dependent and, therefore, its actual value will depend on the particular climatic conditions around the structure [123]. In many cases, the corrosion states predicted using the standard guidelines are quite different from the actual corrosion conditions. For example, in many bridges major discrepancies occur between the assessment of the corrosion state using the ASTM guidelines and the actual deterioration that have been observed at the time of repair [124]. For instance, the potential often shifts to more negative values when the concrete cover is saturated by rainfall. Studies of bridge decks in Europe, where waterproofing membranes are used, or where de-icing salts are applied less frequently, have resulted in a different set of interpretive guidelines [125]. Usually, a decrease in oxygen (O_2) can also drive the half-cell potential significantly towards more negative values. Completely water saturated concrete can lead to oxygen starvation, resulting in potential values more negative by up to

200 mV [121]. A test carried out on carbon steel in an electrochemical cell at the National Research Council of Canada's Institute for Research in Construction showed that a significant shift of potential towards more negative values by 350 mV could be observed when oxygen was purged from the electrolyte by bubbling nitrogen gas into the cell [126]. All in all, the above cited examples also underscore the rather complex nature of the corrosion process of steel rebars embedded in concretes and being or occasionally becoming in contact with aqueous solutions, which most often are containing chloride salts as well in different concentrations.

Measurements of half-cell potential for samples with calcium nitrate after immersion in 3.5%NaCl for 18 months were shown in Fig. 7.15.
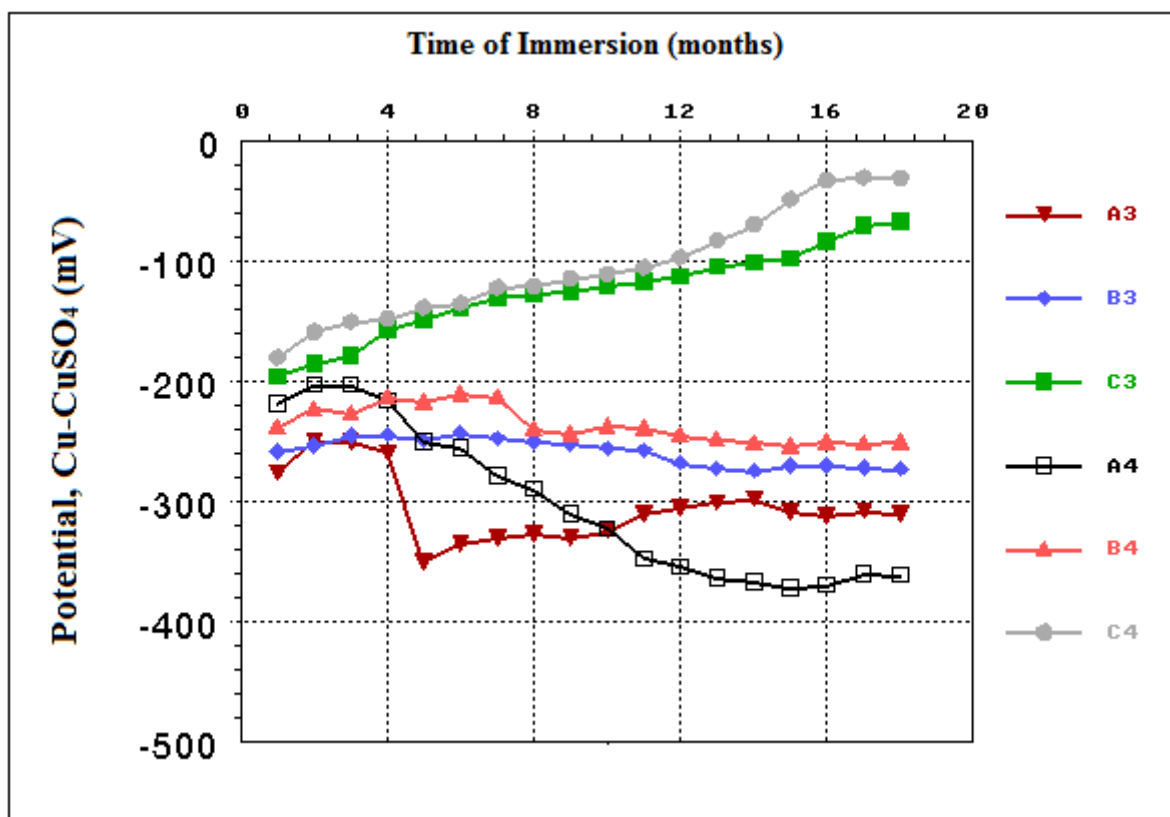

Figure 7.15 Corrosion potentials versus time for concrete samples with calcium nitrate

Fig. 7.15 showing that the half-cell readings for samples with 3 wt.% calcium nitrate inhibitor less negative (more resistance to corrosion) than samples with 1 wt.% and samples without calcium nitrate inhibitor. The potential results obtained for samples A3 and A4 were more negative (between -200 to -350 mV) during 18 months (especially after 5 months) from immersion in 3.5%NaCl, which corresponds to a 50 % probability that corrosion was occurring (see Table 6.6 in part 6.4.6).

Calcium nitrate disrupts the corrosion process by enhancing the formation of the passivating layer on the surface of the reinforcing steel. The nitrate ions compete with any chloride ions present to react with the free iron ions. So in the samples C3 and C4 (3% calcium nitrate) the ratio of nitrate to chloride ions at the level of the steel is greater than about one and this will cause a reaction between nitrate and iron to bind the iron into an oxide, which reinforces the passive layer on the steel. In samples B3 and B4 (1 wt.% calcium nitrate) the ratio is less than one (that is, there's more chloride than nitrate present) and this ratio will lead the chloride ions to react with the iron to begin the corrosion process. During the chemical reaction between the nitrate and iron, the supply of nitrate ions is depleted.

## 7.7 Linear Polarization Resistance

7.7.1 Concrete Samples with Green Inhibitor

The electrochemical polarization curves of reinforcing steel samples imbedded in samples of concrete blocks (without and with orange peels extract inhibitor) and kept immersed in 3.5% NaCl solution were determined and are graphically represented in Fig. 7.16. The corrosion current densities obtained from the electrochemical polarization measurements on the concrete samples are given in Fig. 7.17.
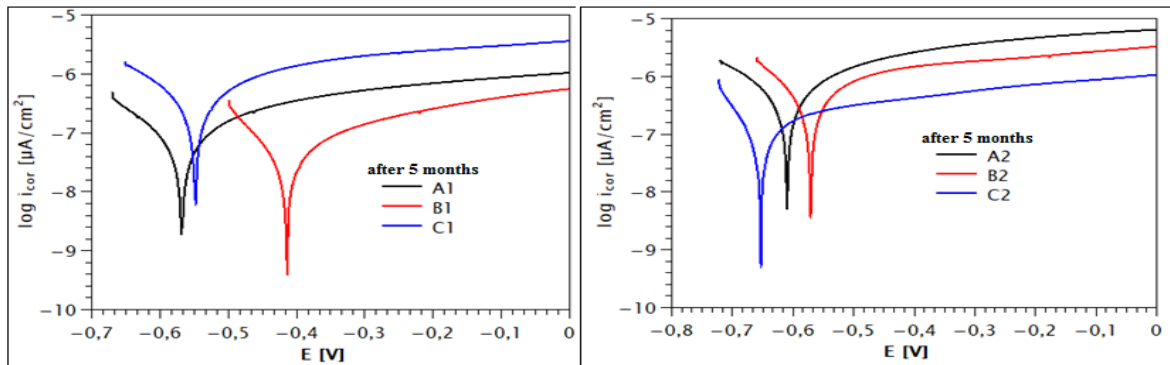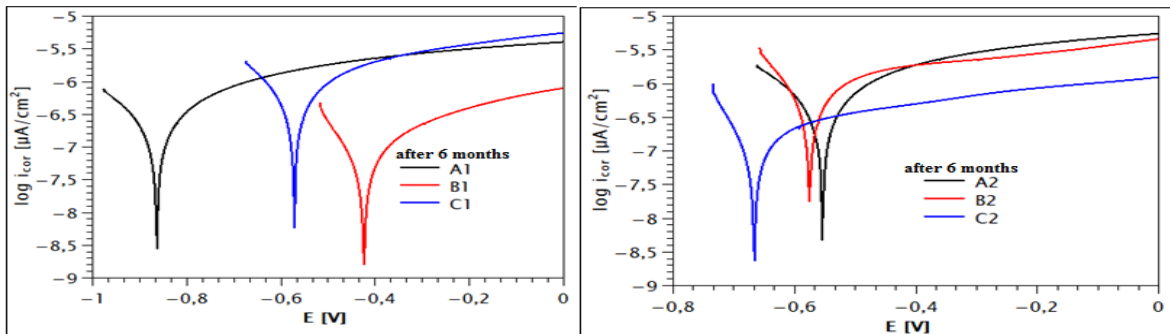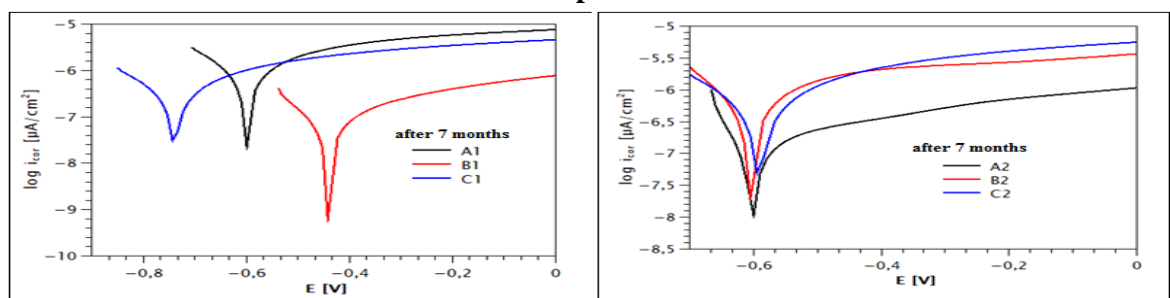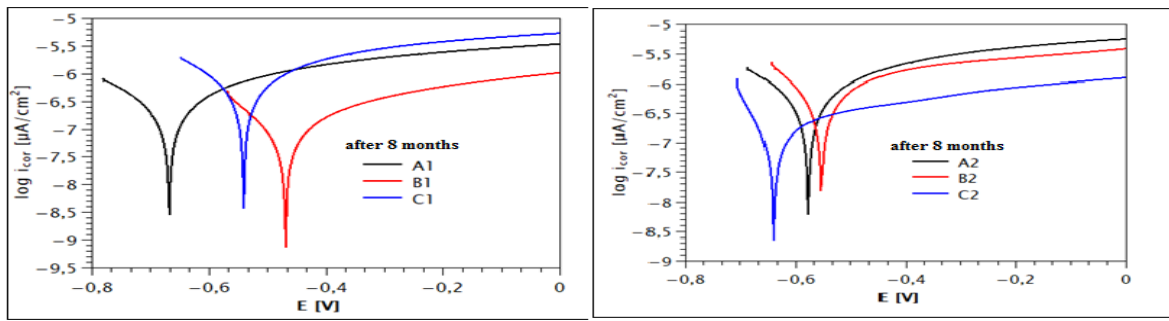

a-

b-

c-

d-

e-

f-

g-

h-

i-

j-

k-

l-

m-

n-

o-

p-

q-

r-
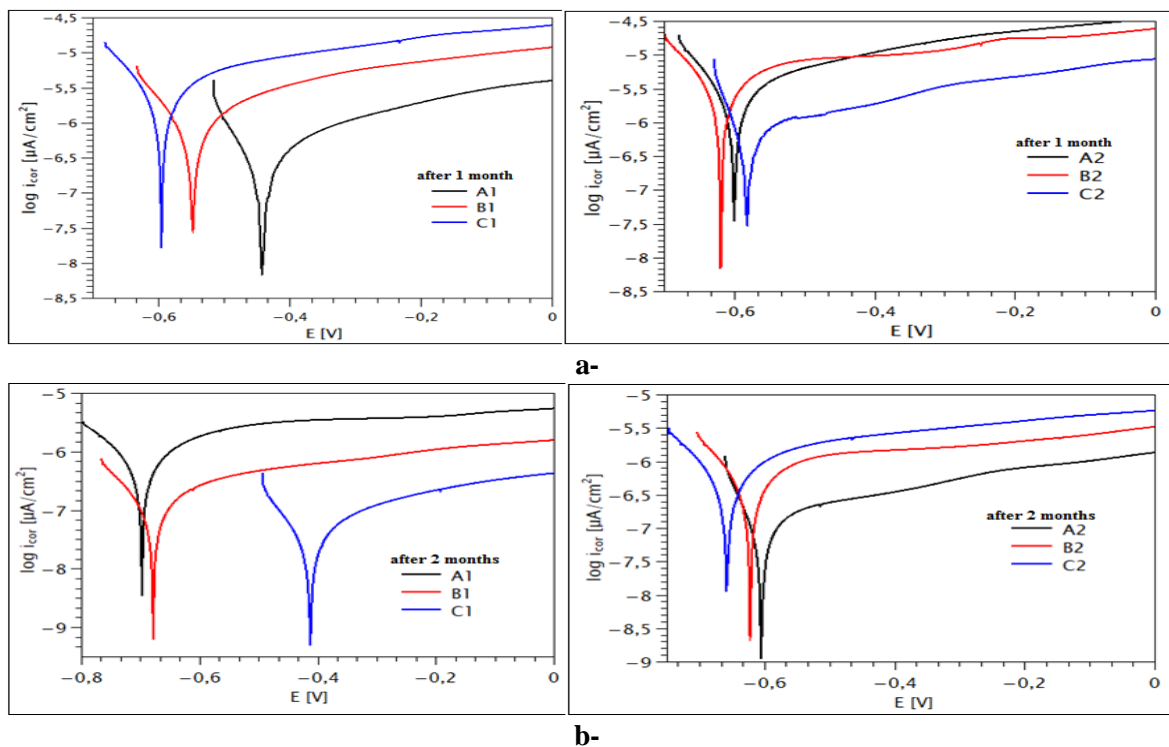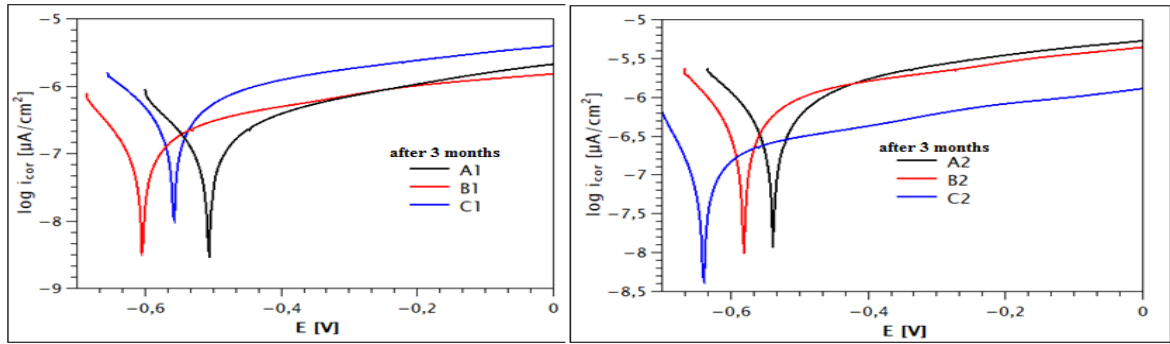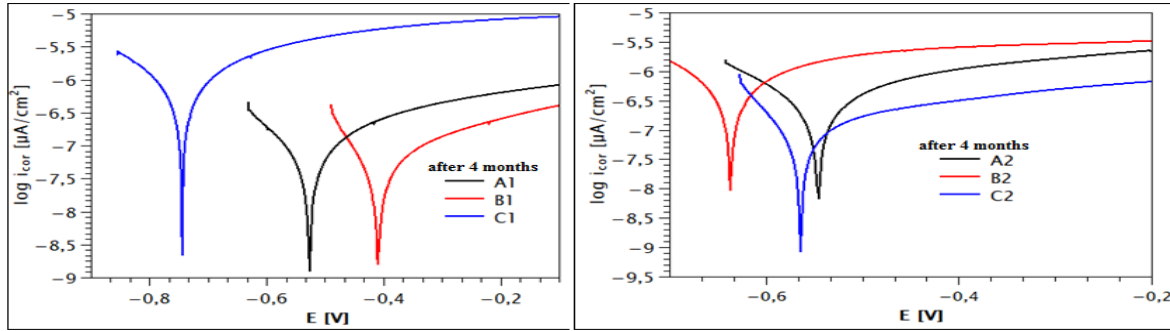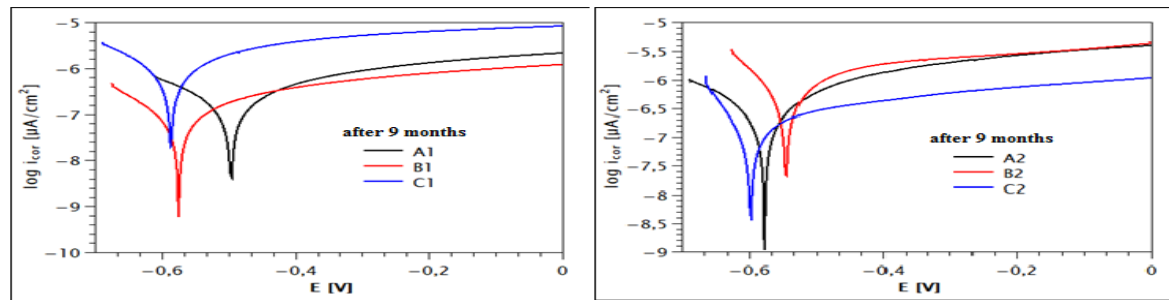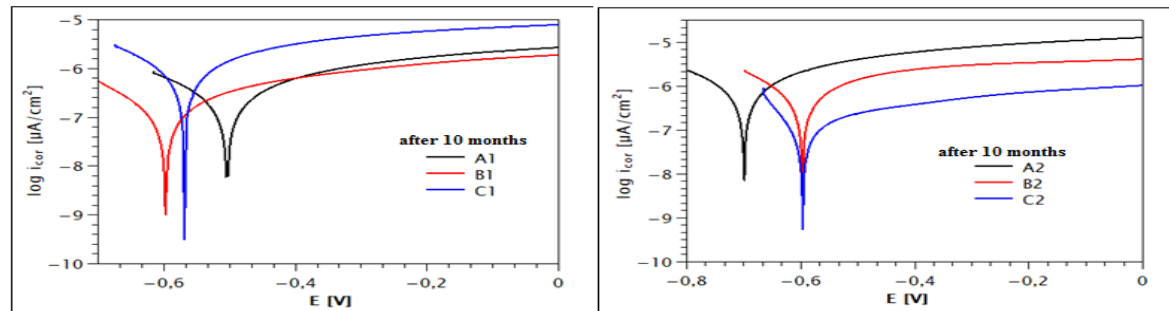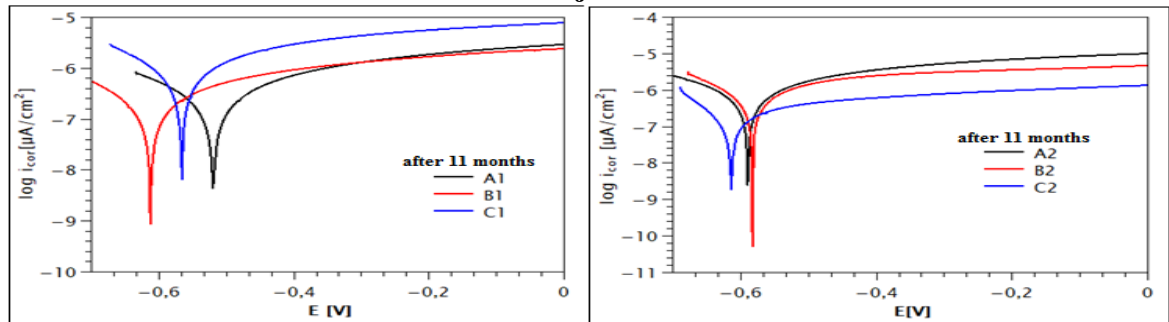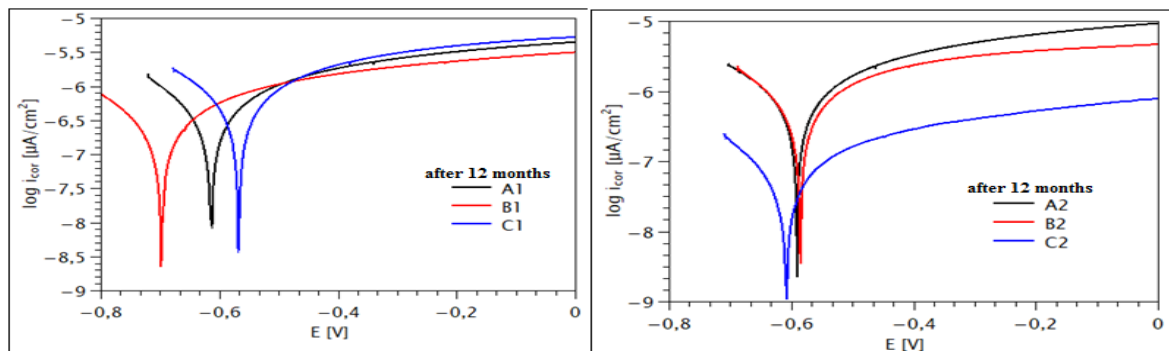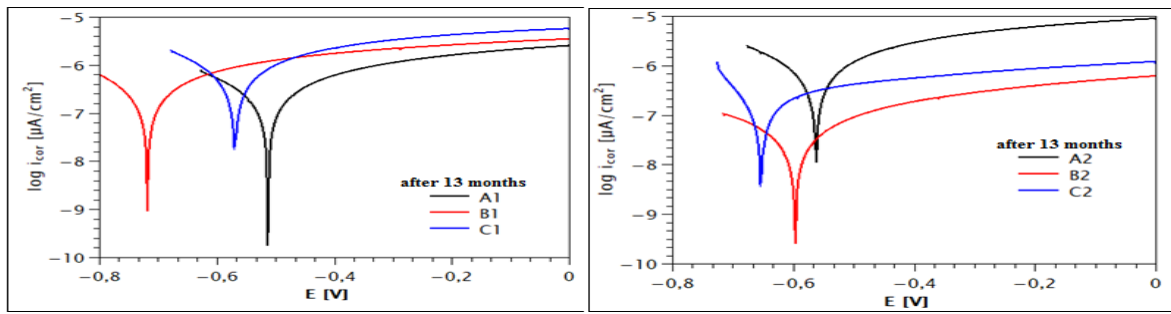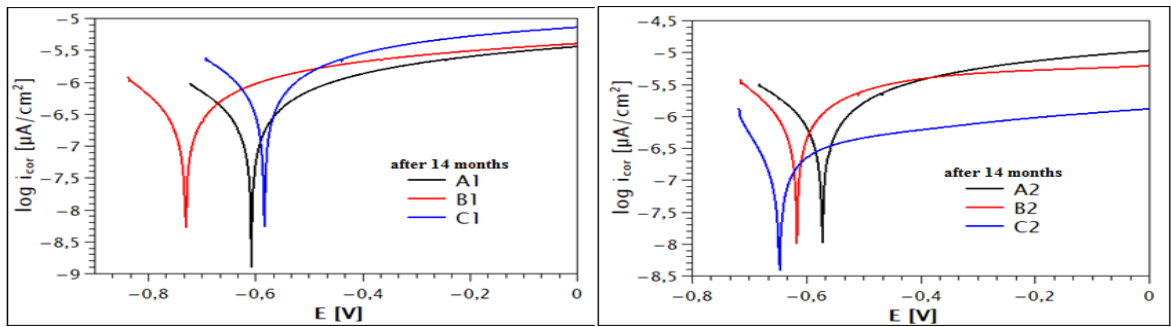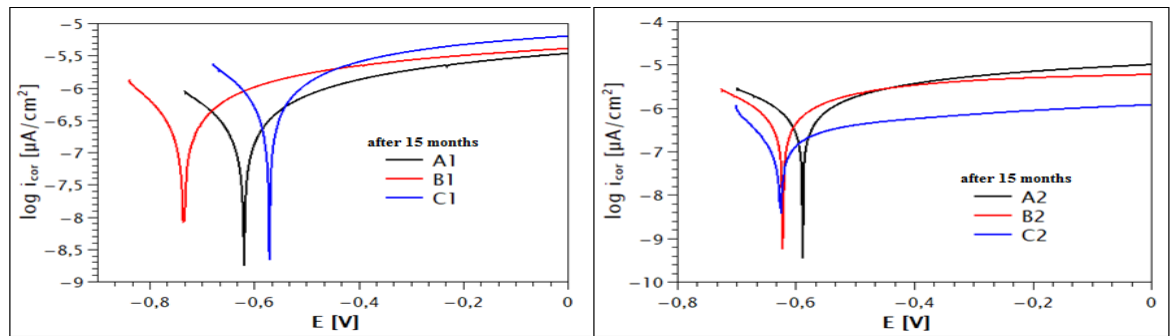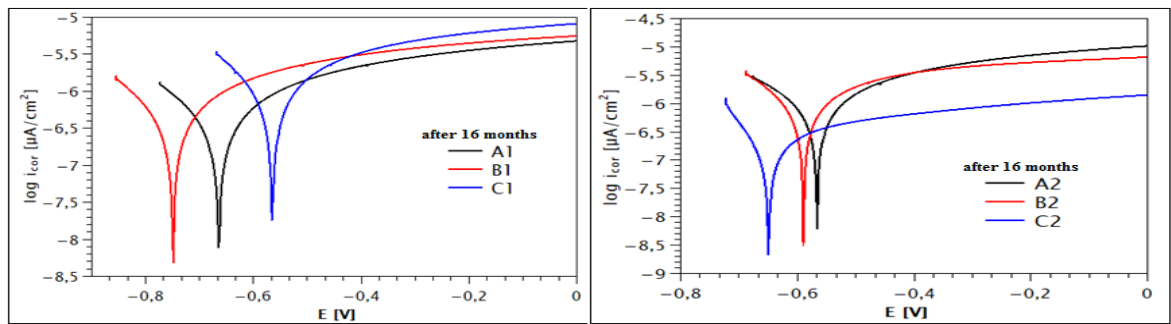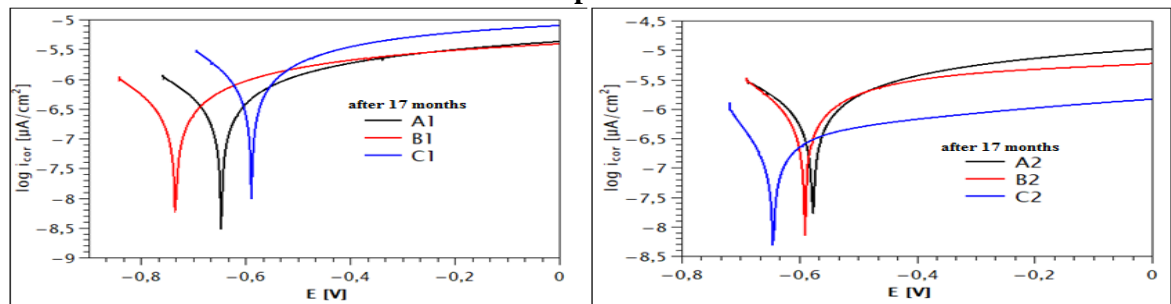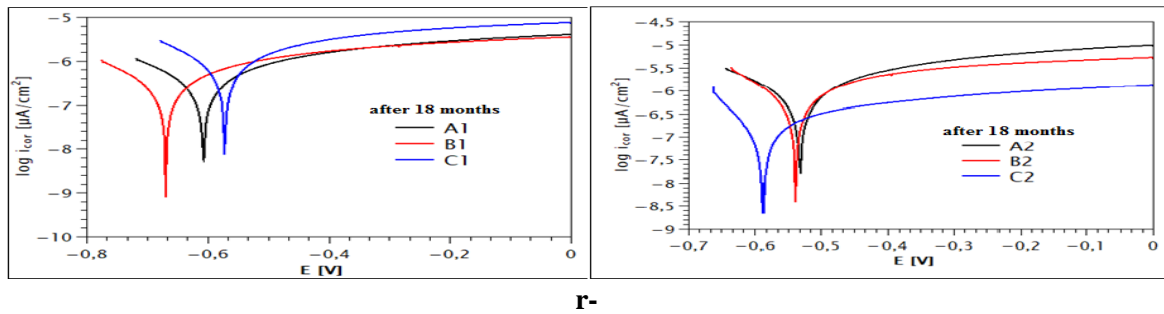
Figure 7.16 Polarisation curves recorded from a to r for A1, B1, C1, A2, B2, C2 concrete samples with green inhibitor after immersion concrete samples in 3.5% NaCl solution for 18 month
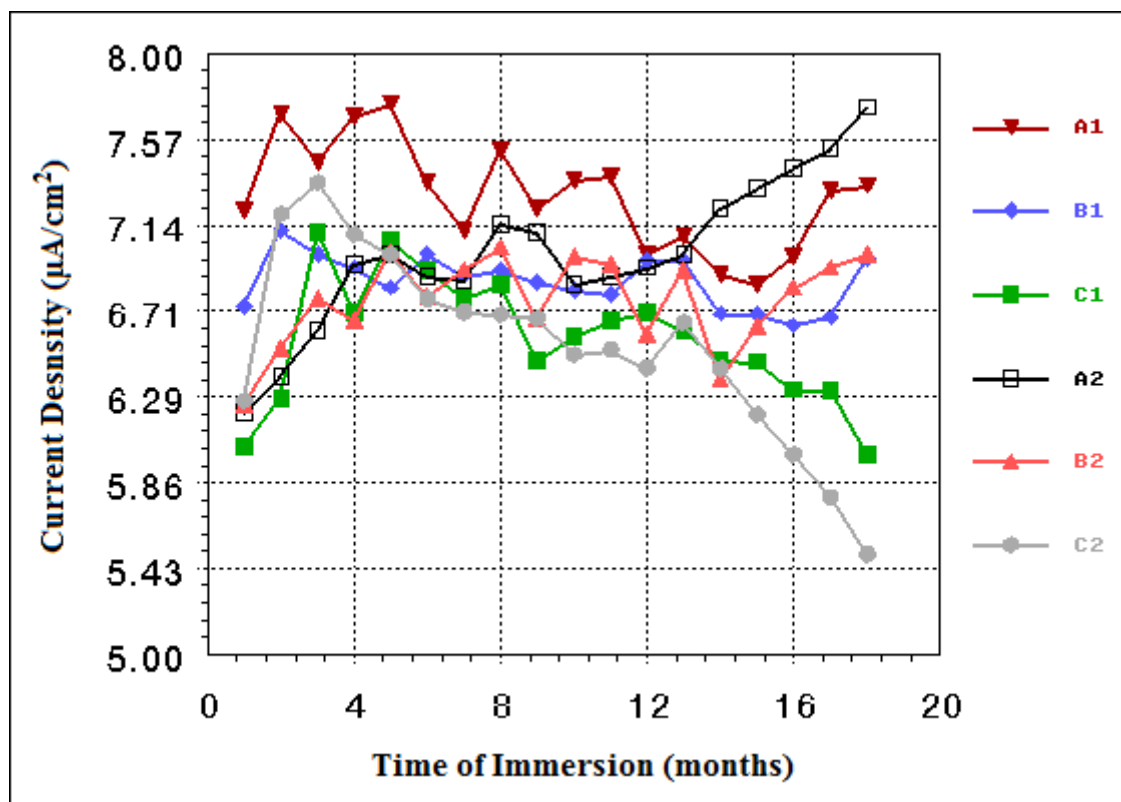
Figure 7.17 Current density obtained from the measured polarisation curves of concrete samples with and without green inhibitor in 3.5% NaCl during 18 months

The observed electrochemical polarisation features (presented in Fig. 7.16) and the calculated corrosion current densities (Fig. 7.17) indicate the effects of the changing bulk and boundary materials properties, like the porosity and pore solution, as well as alterations at the metal/solution interfaces inside the concrete samples being immersed upto 6 months in 3.5% NaCl solution. In this respect our observations are in harmony with those of some other researchers [107, 127] having dealt with somewhat similar systems

and explained the observed phenomena by the formation of porous corrosion products modifying the charge transfer resistance at the steel/solution interface.

The corrosion current densities of all the samples decrease with increase of concentration of the green inhibitor, which phenomenon can, with high probability, attributed to the formation of a protective layer around the surface of steel in contact with the inhibitor containing aqueous medium. Samples of A2, B2, and C2 indicate a remarkable changing trend of the corrosion current densities, which are of smaller values than for the samples of A1, B1, C1). It should be the consequence of an unfolding physico-chemical protection developing due to pozzolanic reactions and associated chemical passivation (i.e. higher resistance against corrosion) of the embedded steel rebars in the concrete blocks (A2, B2, C2 samples) prepared with the water-resisting admixture. The corrosion current densities for all samples increase a little bit after two months due to the chloride attack. After three months of immersion time of the concrete samples kept in chloride solution; the corrosion current density for all samples continues increasing. Samples with green inhibitor (B1, B2, C1, and C2) show smaller values than the samples without inhibitor (A1, A2), from which trends it is also clearly seen that samples with water-resisting admixture (A2, B2, and C2) resist corrosion better than samples with superplasticizer admixture (A1, B1, and C1); the corrosion current density for all samples increased except samples B2, C2 (started to resist corrosion). After five months immersion time of the concrete samples the corrosion current density was increased with decrease in the electrochemical corrosion potential. Same tendency was found with the results extracted from the Tafel-plot type experiments, that is the effect of 3 wt.% green inhibitor together with water-resisting admixture present in the C2 sample showed further decrease in the corrosion current density. Finally, during 18 months immersion the sample C2 which appeared the best sample with green inhibitor can resist corrosion.

The increases in the corrosion current density can mainly be related to the structural consequences of the hydration processes (so-called hardening) of the concrete bodies, that is the liberation of calcium hydroxide, $Ca(OH)_2$, and/or the formation of the well known cementitious compounds C_3S or C_3A, etc. The tested two admixtures (water-resisting admixture and superplasticizer admixture) added to the fresh concrete during the preparation step of the samples gave rise to reducing the water/cement ratio during the concrete blocks hardening, therefore there was not enough time for the formation of $Ca(OH)_2$ and/or C_3S and/or C_3A, .. etc. (which compounds cause greater capillary porosity in concrete and weakens the properties). While discussing the topic of the so-called

nanocement admixtures as well, Yakub et al. [128] described some relevant details of the so-called pozzolanic reaction of vitreous silica with calcium hydroxide (Ca(OH)$_2$ also abbreviated as (C-H). During this hydration reaction of the Ordinary Portland Cement (OPC) this binder is producing additional calcium silicate hydrate (CSH) that resembles tobermorite or jennite structure, which is the main constituent for providing the strength and density in the hardening binder paste. The pozzolanic activity includes two parameters; the amount of lime (Ca(OH)$_2$) that pozzolan can react with it and the rate of reaction. The rate of the pozzolanic activity is related to the surface area of pozzolan particles where higher surface area of pozzolan particle (or finer particle) gives more pozzolanic reactivity. And, due to the very high specific surface area and the spherical particle shape of the synthetic nanosilica admixture, it can potentially enhance the performance of binder mainly due to its reaction with C-H to develop more of the strength-carrying compound in binder structure: CSH [128]. Hence, just by analogy, it can be stated with high probability, that the water-resisting admixture should also behave in a somewhat similar fashion to that of the nanosilica admixture.

7.7.2 Concrete Samples with Calcium Nitrate Inhibitor

The electrochemical polarization curves of reinforcing steel samples imbedded in samples of concrete blocks (without and with calcium nitrate inhibitor) and kept immersed in 3.5%NaCl solution were determined and are graphically represented in Fig. 7.18. The corrosion current densities obtained from the electrochemical polarization measurements on the concrete samples are given in Fig. 7.19.

Fig. 7.18a represents the variation in polarization curves of reinforced concrete samples after immersion for one month in 3.5%NaCl. The corrosion current densities of the samples with inhibitor decrease with increase of concentration of calcium nitrate inhibitor, which phenomenon can, with high probability, attributed to the formation of a protective layer around the surface of steel in contact with the inhibitor containing aqueous medium.
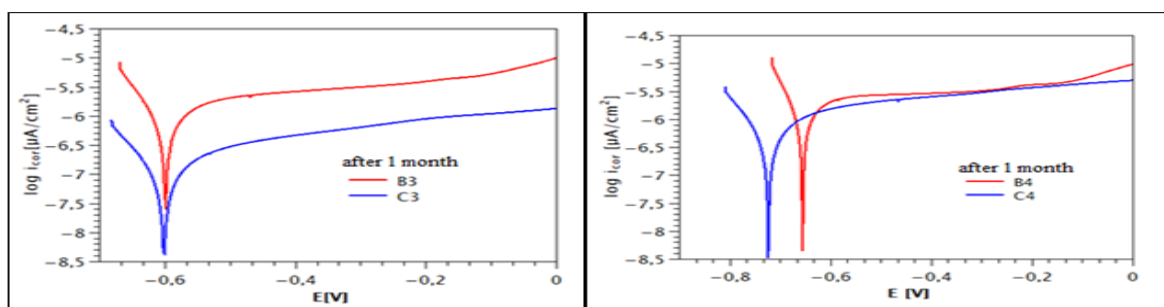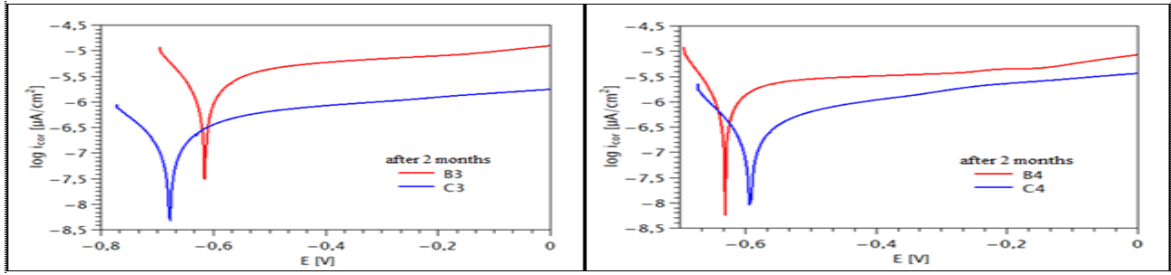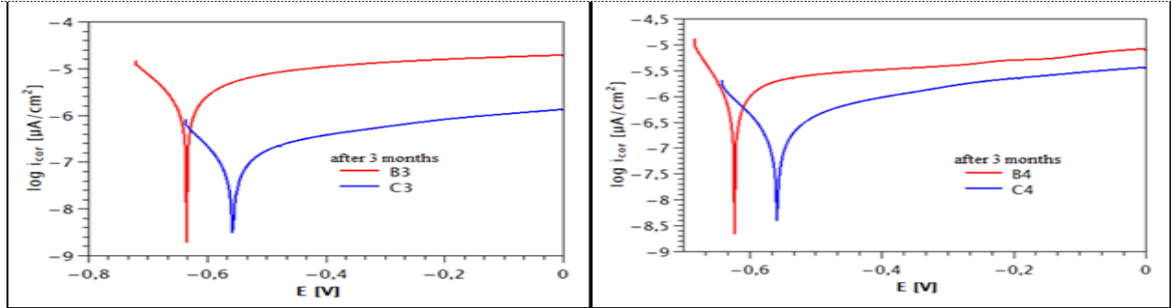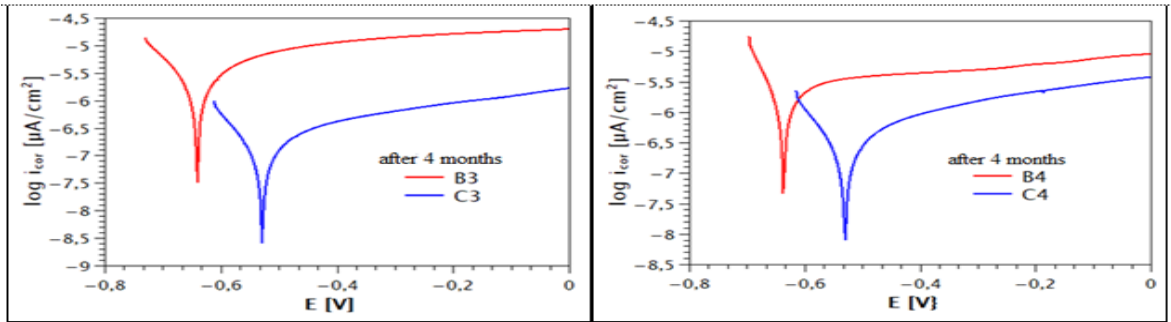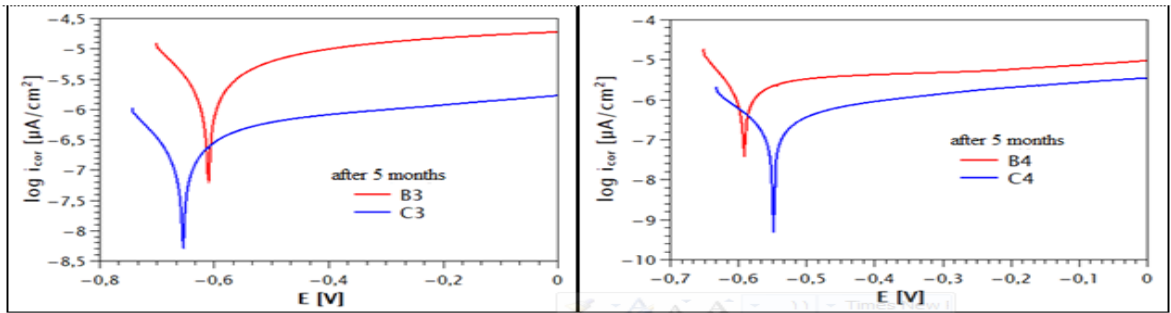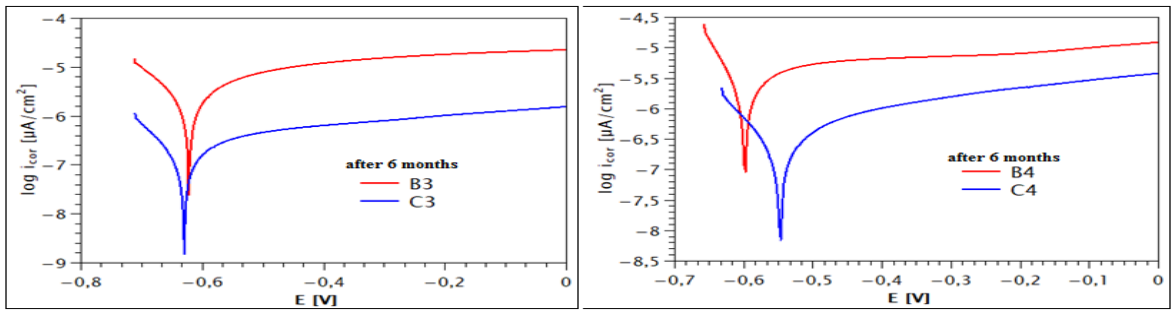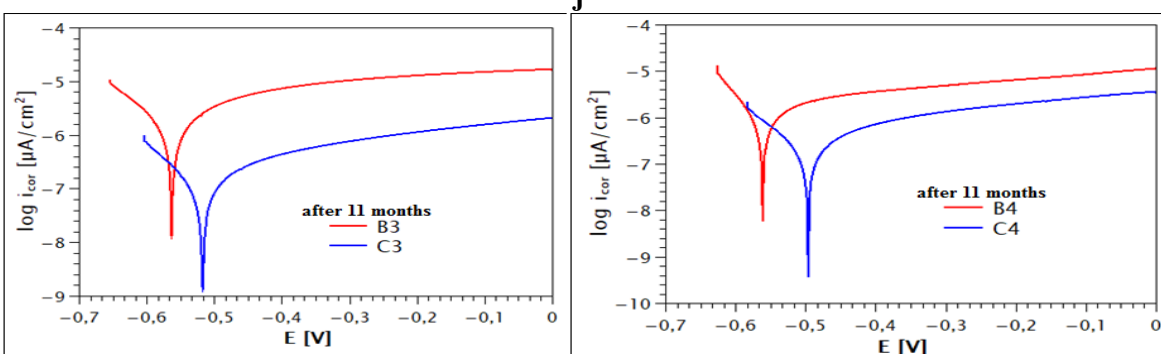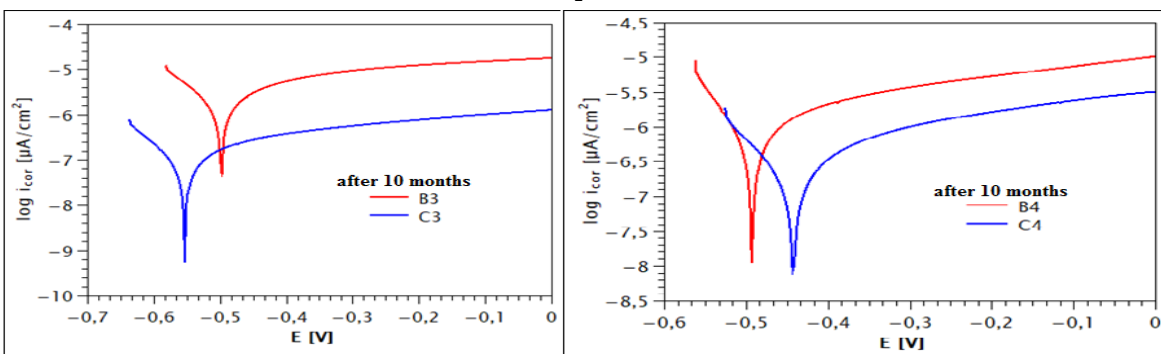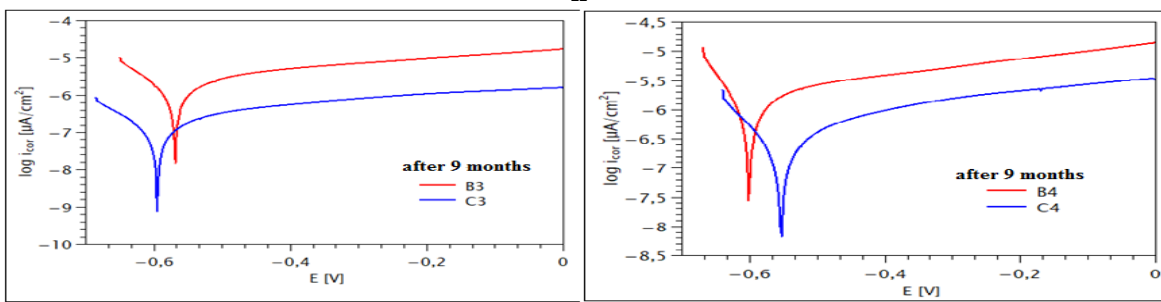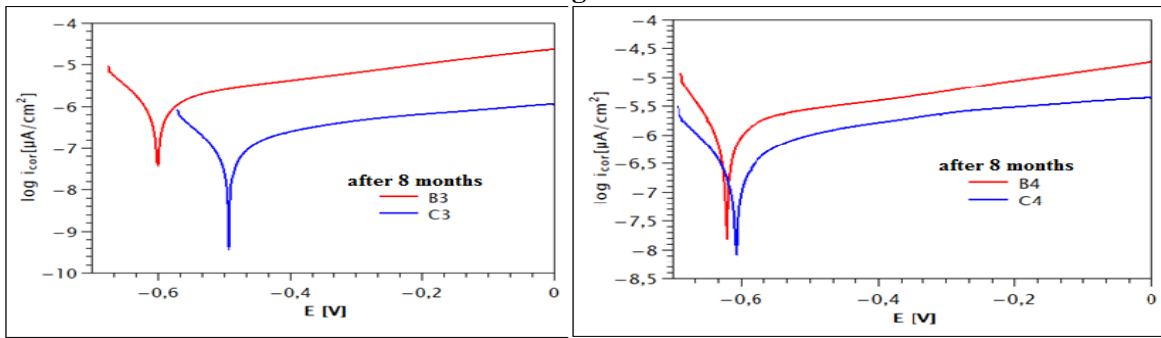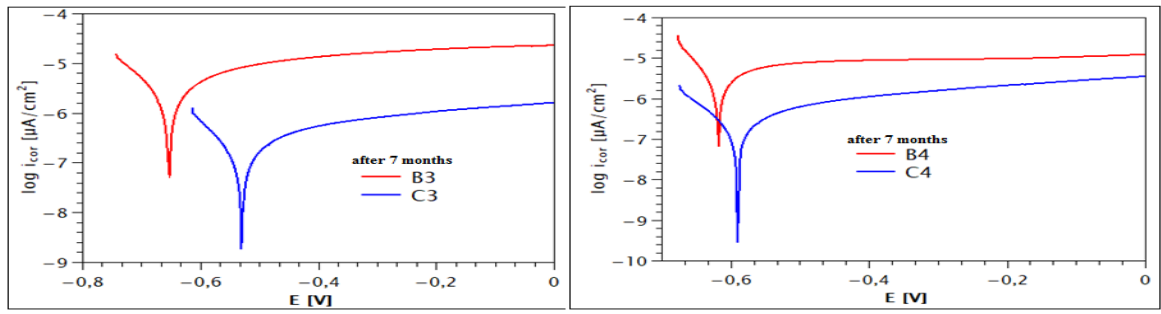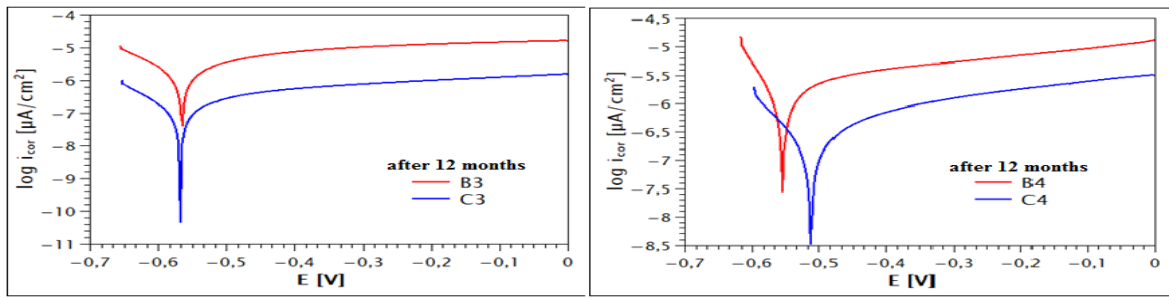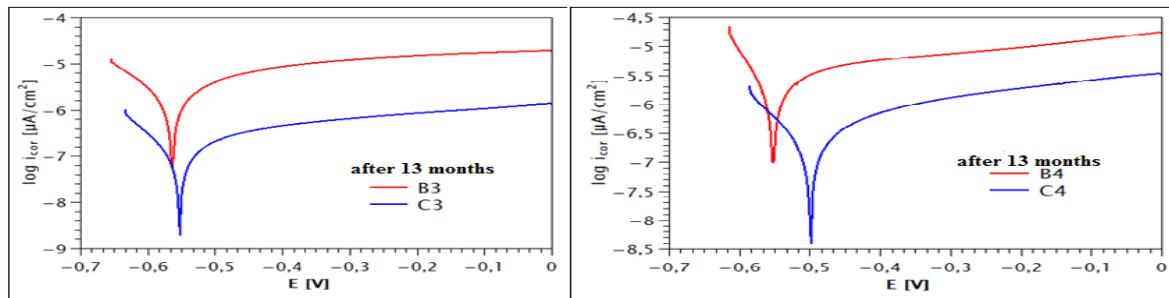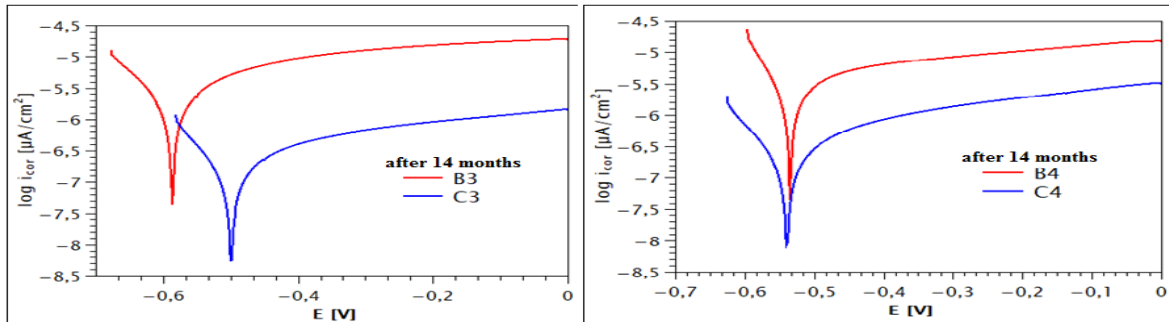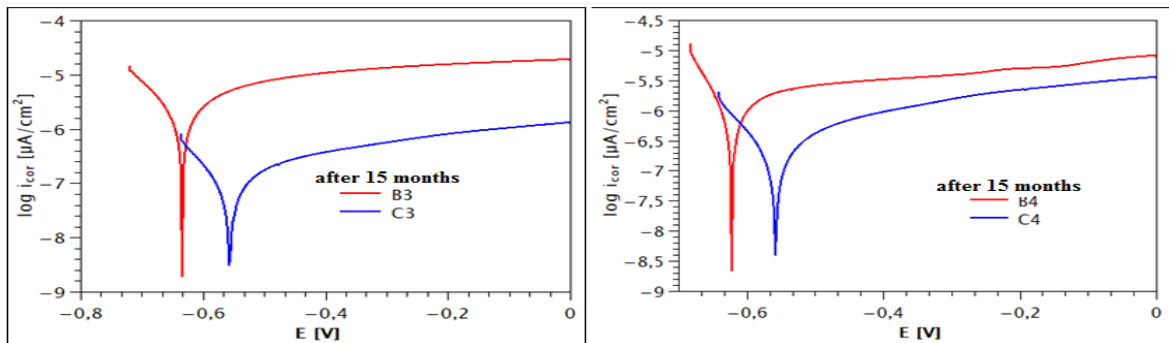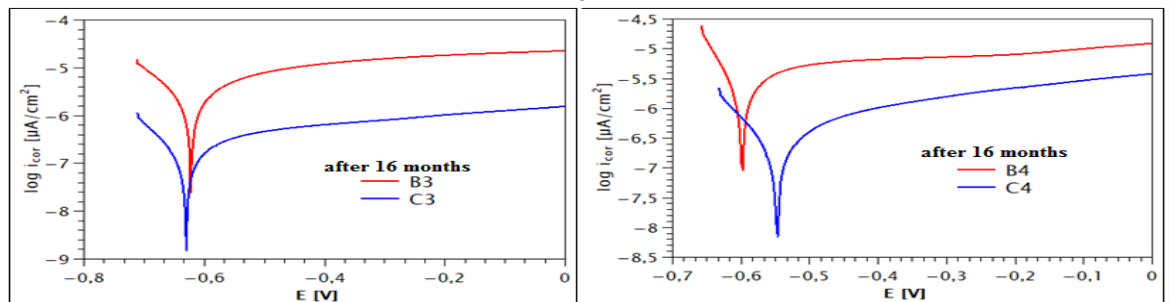
a-

b-

c-

d-

e-

f-

g-

h-

i-

j-

k-

l-

m-

n-

o-

p-
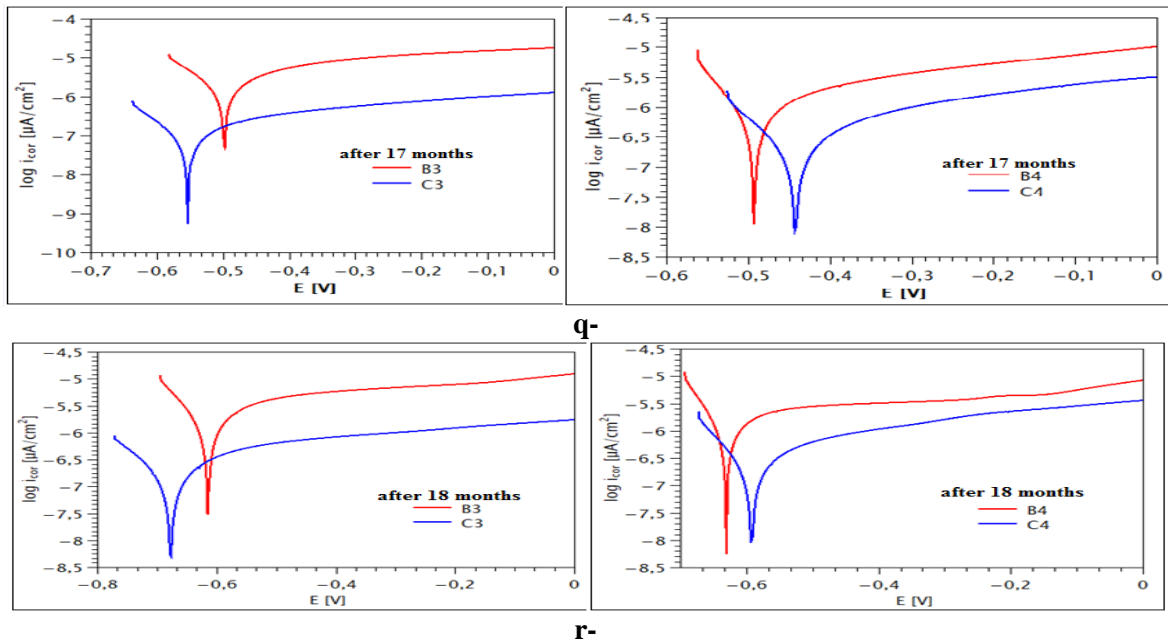
Figure 7.18 Polarisation curves recorded from a to r for B3, C3, B4, C4 concrete samples with calcium nitrate inhibitor after immersion concrete samples in 3.5% NaCl solution for 18 months
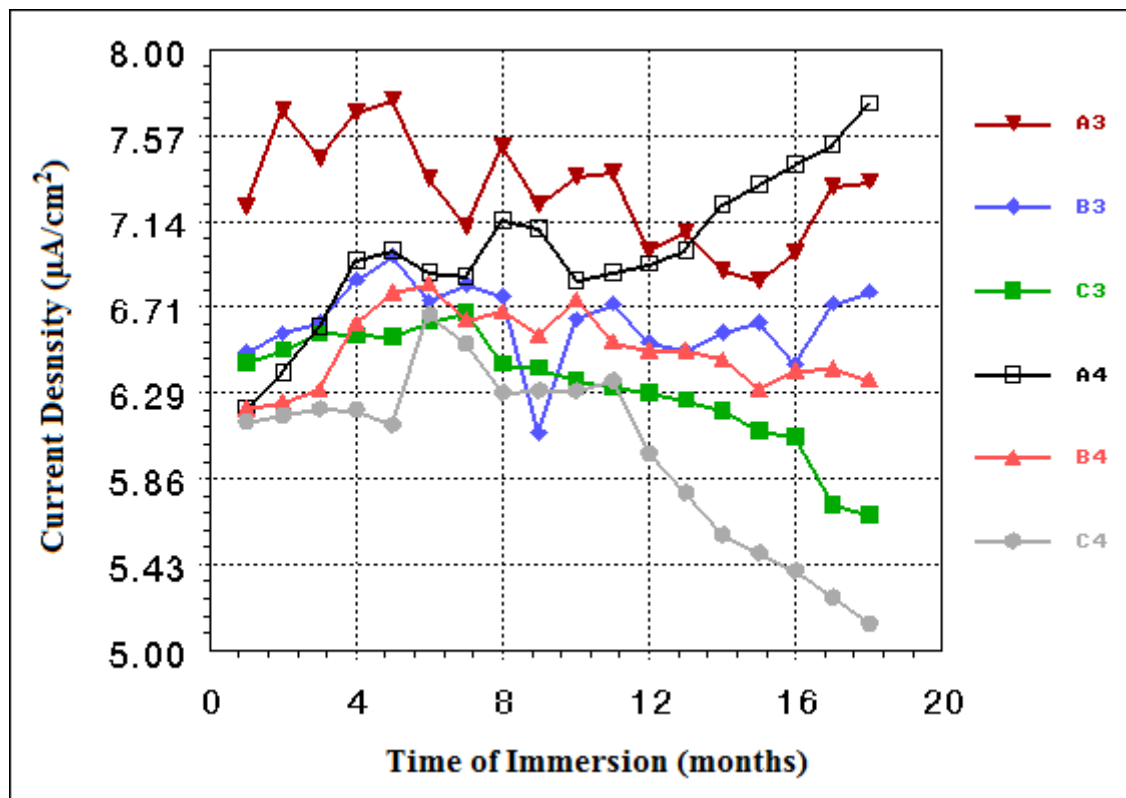
Figure 7.19 Current density obtained from the measured polarisation curves of concrete samples with and without calcium nitrate inhibitor in 3.5% NaCl during 18 months

Fig. 7.18b shows that the corrosion current densities for all samples increase a little bit after two months due to the chloride attack. After three months of immersion time of the

concrete samples kept in chloride solution (as it is seen in Fig. 7.18c) the corrosion current density for all samples continues increasing.

Samples with calcium nitrate inhibitor (B3, B4, C3, and C4) show smaller values increasing than the samples without inhibitor (A3, A4), from which trends it is also clearly seen that samples with water-resisting admixture (A4, B4, and C4) resist corrosion better than samples with superplasticizer admixture (A3, B3, and C3).

The values of corrosion current density for all samples after 4 months increased except samples C3, C4 (started to resist corrosion) as shown in Fig. 7.18d.

After 18 months immersion time of the concrete samples the corrosion current density was increased with decrease in the electrochemical corrosion potential. Same tendency was found with the results extracted from the Tafel-plot type experiments. Samples with 3 wt.% calcium nitrate inhibitor (C3, C4) showed lower corrosion current density and this is an indication there's a stable protective layer was formed around surface of steel rebar by this inhibitor.

Samples of A4, B4, and C4 indicate a remarkable changing trend of the corrosion current densities, which are of smaller values than for the samples of A3, B3, and C3). It should be the consequence of an unfolding physico-chemical protection developing due to pozzolanic reactions and associated chemical passivation (i.e. higher resistance against corrosion) of the embedded steel rebars in the concrete blocks (A4, B4, and C4 samples) prepared with the water-resisting admixture.

Calcium nitrate inhibitor at 3 wt.% worked a good protector for steel rebar from attack chloride ions by formation a stabilization passive layer, but at 1 wt.% there's less resist to corrosion and after 3 months chloride ions can arrive to the metallic surface of the steel.

The inhibiting mechanism of calcium nitrate for the corrosion of steel in concrete was suggested firstly by Justnes [129]. He assumed that the oxidation action of nitrate is the consequence to its easy reduction to nitrite. The two half-reactions illustrate the mechanism:

$$\text{Reduction: } 2NO_3^- + 2H_2O + 4e^- \rightarrow 2NO_2^- + 4OH^- \quad\quad (7.3)$$

$$\text{Oxidation: } 4Fe(OH)_2 + 4OH^- \rightarrow 4Fe(OH)_3 + 4e^- \quad\quad (7.4)$$

They are combined to give the total reaction:

$$2Fe(OH)_2 + NO_3^- + H_2O \rightarrow 2Fe(OH)_3 + NO_2^- \quad\quad (7.5)$$
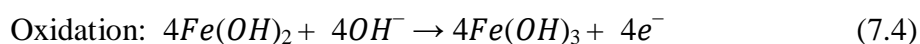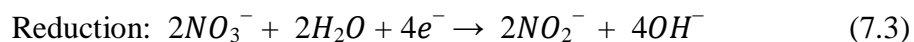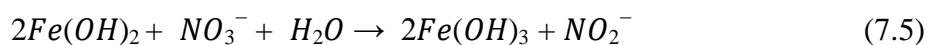
However, in contrast to Justnes, the authors P. Saura, E. Zornoza, C. Andrade, and P. Garcés [130] considered a different ferrous oxide compound creation: $\gamma\text{-}Fe_2O_3$. The two half equations describe the mechanism:

$$\text{Reduction: } NO_3^- + H_2O + 2e^- \rightarrow NO_2^- + 2OH^- \quad\quad (7.6)$$

$$\text{Oxidation: } 2Fe^{2+} + 3OH^- \rightarrow \gamma\text{-}Fe_2O_3 + 2e^- + 3H^+ \quad\quad (7.7)$$

They are combined to give the total reaction:

$$2Fe^{2+} + NO_3^- + H_2O + OH^- \rightarrow \gamma\text{-}Fe_2O_3 + NO_2^- + 3H^+ \quad\quad (7.8)$$
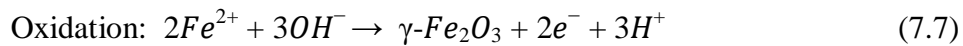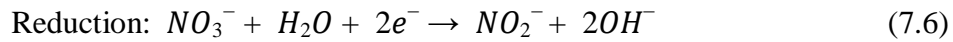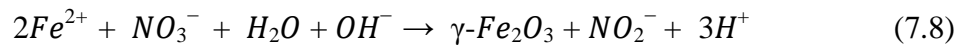
The above mechanism was assessed in simulating concrete pore solution and the $\gamma\text{-}Fe_2O_3$ formed layer was proved to be stable in alkaline environments, inducing a strong protective effect on the steel surface [131].

7.8 Corrosion Rate

The corrosion rate (Cr.Rate) or corrosion velocity, V, represents the volumetric loss of metal by unit of area and unit of time. In the present recommendation it is expressed in mm/year, although other units may also be used. Cr. Rate expressed in mm/year is obtained from the corrosion current, (either i_{corr} or I_{corr}) in $\mu A/cm^2$ through Faraday's law and the density of the metal. For the steel, 1 $\mu A/cm^2$ is equivalent to a corrosion rate of 0.0116 mm/year for uniform attack [132].

$$\text{Cr. Rate } (mm/y) = 0.0116\, i_{corr}\, (\mu A/cm^2) \quad \text{................}(7.9)$$

In our case a computer controlled (ZAHNER type potentiostat was used to record the current – potential data which were then converted to corrosion rates according to standard procedures.
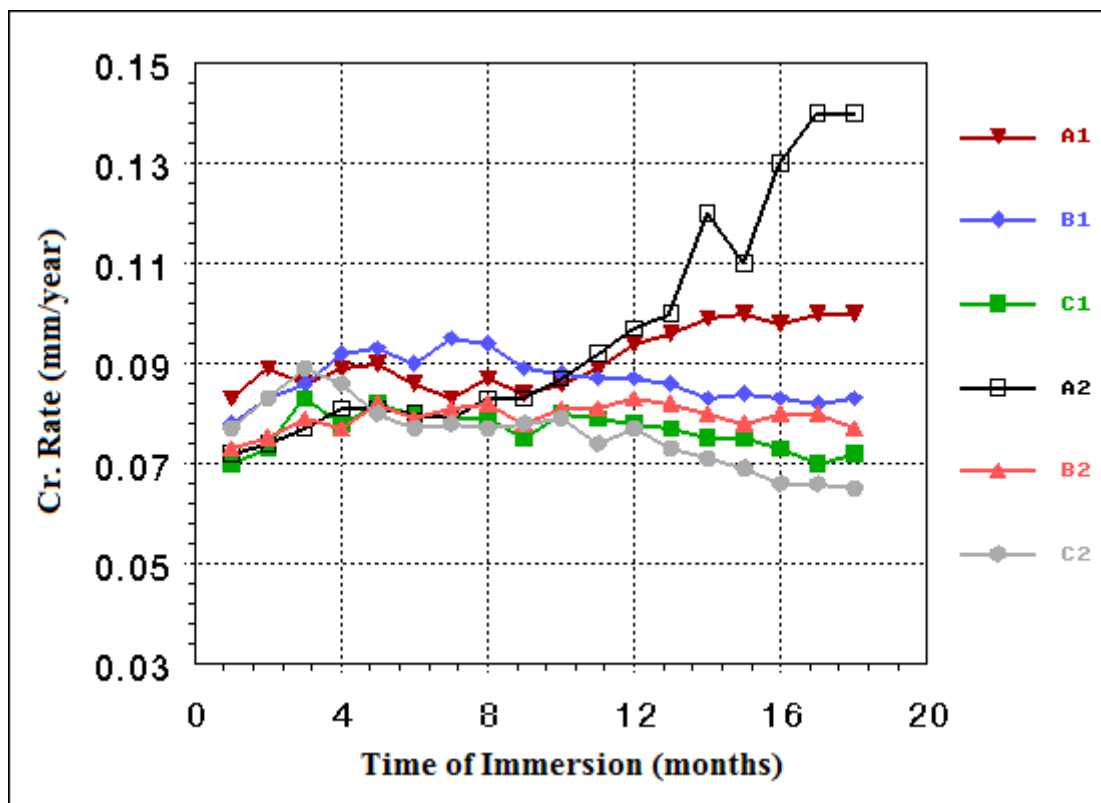
Figure 7.20 Corrosion rate for concrete samples with green inhibitor after immersion for 18 months in 3.5%NaCl solution

From Fig. 7.20 corrosion rates is increasing with time of immersion during the tested period of 18 months, and the rates are always somewhat lower in cases when the concrete samples contained the extract of the orange peel inhibitor with water-resisting admixture. After six months the increase in the corrosion rate of the samples (with water-resisting admixture) was lower compared with the increase of corrosion rate in samples (with superplasticizer admixture as in A1 and B1 samples). It means that the inhibitive effect of the chosen and so tested green inhibitor is really plausible and promising especially together with water-resisting admixture.

The results of the corrosion rate for concrete samples with calcium nitrate were indicated in Fig. 7.21
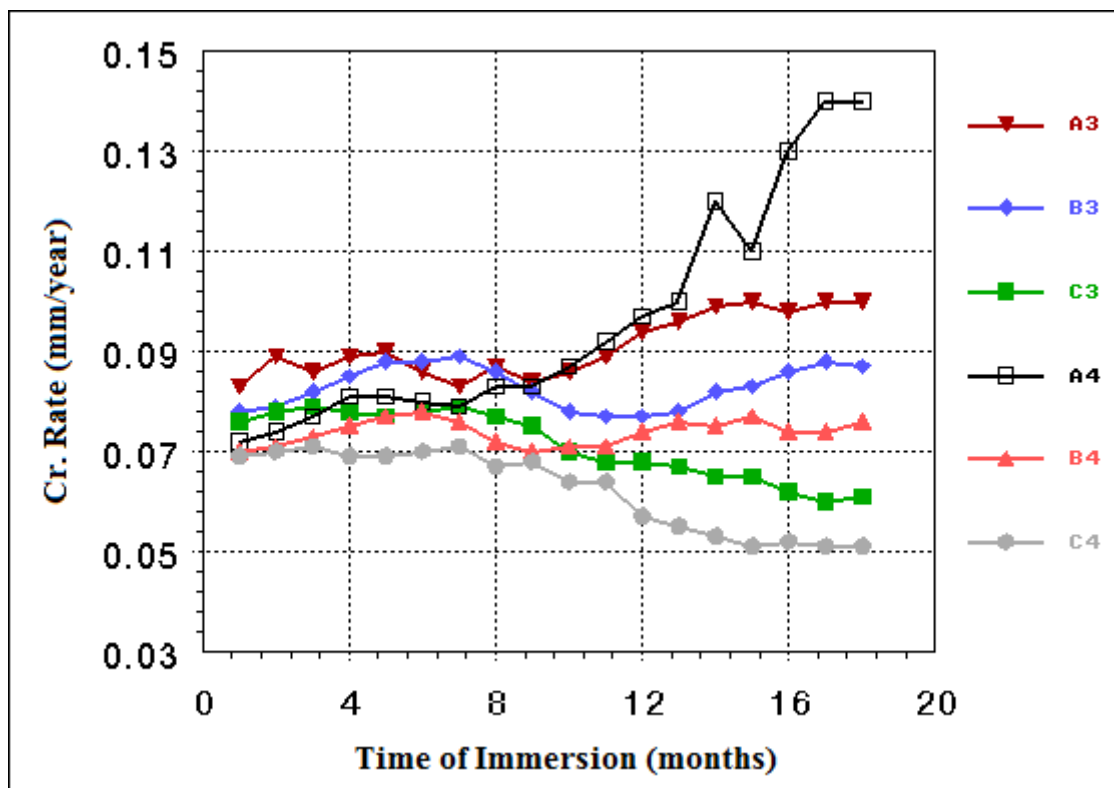
Figure 7.21 Corrosion rate for concrete samples with calcium nitrate after immersion for 18 months in 3.5%NaCl solution

As it is seen in Fig. 7.21, the tendency of the corrosion rates is increasing with time of immersion during the tested period of 18 months, and the rates are always somewhat lower in cases when the samples have calcium nitrate inhibitor at 3 wt.% and samples with water-resisting admixture. During 18 months the corrosion rate in samples C3 and C4 started decreasing with increasing the time of immersion but the samples with 1 wt.% inhibitor during 18 months have high increasing in corrosion rate because calcium nitrate have

effective inhibition mechanism on chloride-induce corrosion of calcium nitrate at concentrations higher than 1% by weight of cement [133].

7.9 SEM-EDS Microstructural and Composition Analysis of the Steel Rebar Surface

For the microstructural SEM investigations the steel rebar specimens/rods first had to be removed from the concrete blocks which had previously been kept immersed in 3.5% NaCl solution for 18 months. After that the SEM-EDS analysis could be commenced and the results are presented in Figs. 7.22 and 7.23. The chemical elemental compositions determined at some selected surface points on the steel rebars (as marked clearly in Figs. 7.22 ii and 7.23 ii) were obtained by the EDS method being coupled to the scanning electron microscope (SEM) and are given in wt% in Tables 7.3 and 7.4.

- **A1**

- **B1**
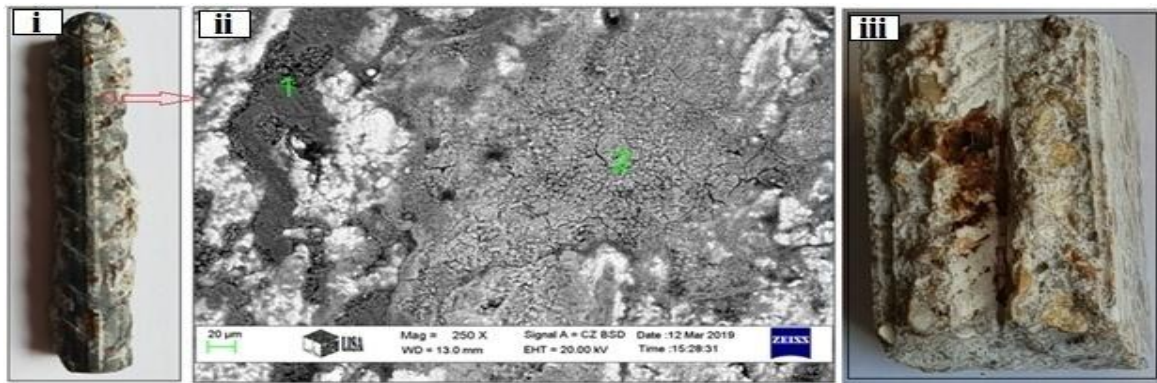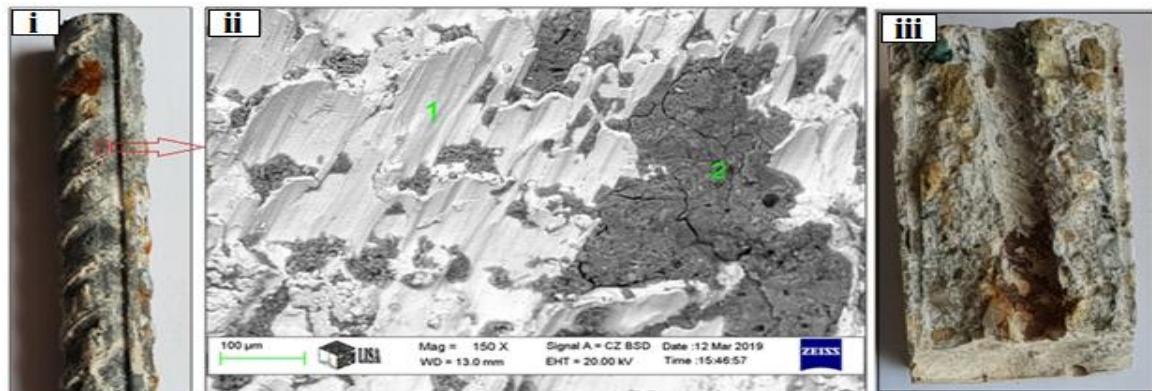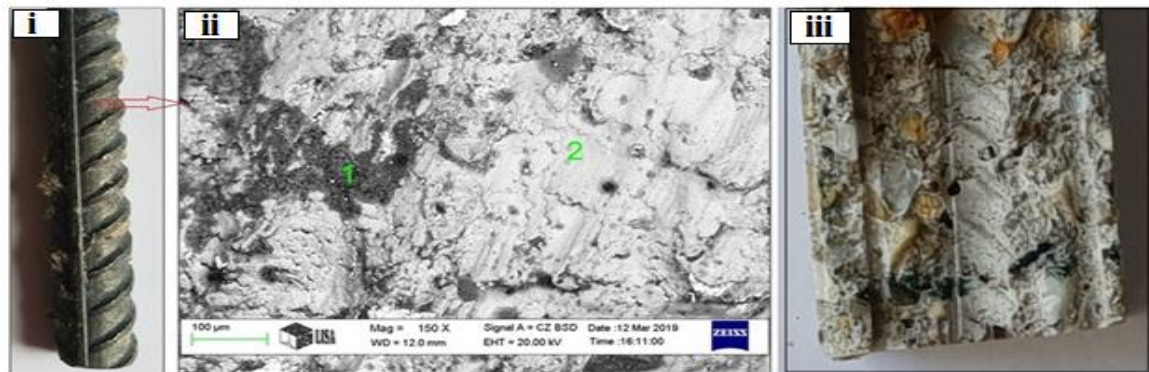
- **C1**

- **A2**

- **B2**

- **C2**

Figure 7.22 i) Close-up image of a steel rebar for samples after removal from the concrete, ii) SEM Micrograph of the section indicated in (i), iii) Representative image of a split concrete specimen with and without green inhibitor after removal of the steel rebar

Table 7.3 The approximate chemical composition (expressed as oxides) of some small selected surface areas (as indicated in Fig. 7.22i) of the steel rebars after removal from the concrete blocks by SEM-EDS

| Components (as Oxides) | Composition by EDAX (ZAF correction) given in wt%, not normalised | | | | | | | | | | | | |
| | A1 | | B1 | | C1 | | A2 | | B2 | | C2 | | |
	Point 1	Point 2	Point 1	Point 2	Point 1	Point 2	Point 1	Point 2	Point 1	Point 2	Point 1	Point 2	Point 3
Na_2O	0.13	0.46	3.61	1.38	2.36	1.40	0.14	0.35	13.6	6.01	3.61	6.45	0.61
MgO	0.00	0.30	1.42	4.13	2.29	2.26	1.16	0.25	3.13	2.31	3.15	0.50	4.28
Al_2O_3	0.19	0.95	1.21	10.9	5.62	1.22	1.26	0.59	2.35	1.32	2.39	0.57	2.77
SiO_2	1.38	2.01	3.41	17.6	24.7	10.7	0.59	1.07	10.6	7.80	10.6	3.11	16.7
SO_3	1.04	0.55	1.10	5.75	4.93	2.28	0.23	0.28	0.58	0.38	0.58	7.39	2.18
Cl_2O	3.51	0.23	1.83	0.68	3.98	0.31	5.10	2.06	0.24	0.11	0.20	1.90	0.91
K_2O	0.11	0.16	0.98	0.84	0.96	1.25	0.10	0.07	0.45	0.17	0.5	1.75	0.54
CaO	0.51	2.54	9.65	52.6	40.4	21.1	1.00	0.84	39.2	15.5	39.2	16.0	58.4
MnO	0.91	0.87	0.83	0.67	0.72	1.08	0.09	0.15	2.79	1.68	2.79	0.66	0.71
FeO	92.2	91.9	75.9	5.32	2.36	55.4	92.3	94.3	47.1	64.7	37.1	61.7	12.9

In Fig.7.22 the reinforcing steel specimen for sample A1 showed an oxidized surface state (small oxidized areas spread over most of the specimen surface) and its composition was found similar to that of pure FeO as it contained about 92.23 wt% FeO at point 1 and 91.93 wt% at point 2. It is seen from Table 7.3 at point 2 that at the steel surface of the same sample A1 also some compound-bound chlorine (expressed as Cl_2O of 3.51wt%) could be detected, which indicates that the chloride ions migrated inwards and could reach the surface of steel rebar. As this concrete sample did not contain any corrosion inhibitor (namely the orange peel extract), the chloride ions could diffuse easily and fast to the steel surface and even initiate and/or enhance its corrosion with the probable later formation of different iron-oxide-hydroxide (rust) compounds, although the marked and EDS tested two points may also be related to the original mill-scale coverage of the steel bars received directly from a reinforcing steel rod producer and studied also by us earlier [4, 5]. Anyhow, the presence of chlorine observed right at the steel/concrete interface is a strong indication of the chloride ion ingress reaching to the rebars surface also at some other samples (see in Table 7.3) after 18 months immersion in the given aqueous chloride salt solution.

The steel rebar specimen in sample B1 presents a little bit oxidized area on the surface but at the spot that was selected for testing and is marked as point 1 had FeO in 75.97 wt%, which means this point(s) were attacked by pitting corrosion due probably to the rather low

concentration of the green inhibitor (1 wt.%) that could not prevent the breakdown of the thin passive surface oxide layer. Hence, at some „weakest points" this protective layer could be „destroyed" (i.e. chemically modified and dissolved away) from the steel surface due primarily to the attack of chloride ions (given as Cl_2O of 1.83 wt%) which could reach the surface of steel as shown in Table 7.3 at point 1 of B1.

In Fig. 7.22 the surface of the reinforcing steel in sample C1 appears almost free of oxidation, but in the micro-structure analysis test made by EDS it showed FeO in ~ 55.4 wt%, and CaO ~21.1 wt% at point 2 and in the same point it also had some chlorine (expressed in Cl_2O of about 0.31 wt%), so these oxides must have formed in a surface reaction of rust with the concrete.

From Fig. 7.22 can note the effect of chloride on the surface of steel rebar in sample A2 because it has oxidized areas clearly seen and widespread on the surface (FeO ~ 92.33wt%, at point 1 and 94.34 wt%, at point 2). It seems that this sample did not have the ability to resist the corrosion attack of chloride ions that reached to the surface of steel. The measured high chlorine concentrations (expressed as Cl_2O ~ 5.10 wt% at point 1 and 2.06 wt% at point 2) should be considered as raising high risk of corrosion at these points.

The steel rebar in sample B2 did not show corroded parts viewed by naked eye, and had only very tiny oxidized spots indicated only by the EDS analysis (FeO ~ 64.74 wt% at point 2). Also the amount of chlorides in this sample was not high as shown in Table 7.3 at point 2. The reinforcing steel in sample C2 showed the least of corrosion attack and it did not appear on its surface. The very small amounts of corrosion products detected only by EDS, and compared with those at the other samples interfaces, it means that there is a very low probability and/or risk of corrosion in this sample.

The observed microstructure (observed by SEM imaging technique and presented in Fig. 7.22) and the EDS analysis for composition (Table 7.3) indicate the effects of the changing bulk and boundary materials properties, like the porosity and pore solution, as well as alterations at the metal/solution interfaces inside the concrete samples being immersed up to 18 months in 3.5%NaCl solution. In this respect our observations are in harmony with those of some other researchers [107, 127] having dealt with somewhat similar systems and explained the observed phenomena by the formation of porous corrosion products modifying the charge transfer resistance at the steel/solution interface.

The results of the samples with calcium nitrate shown in Fig. 7.23 and Table 7.4 as the following:
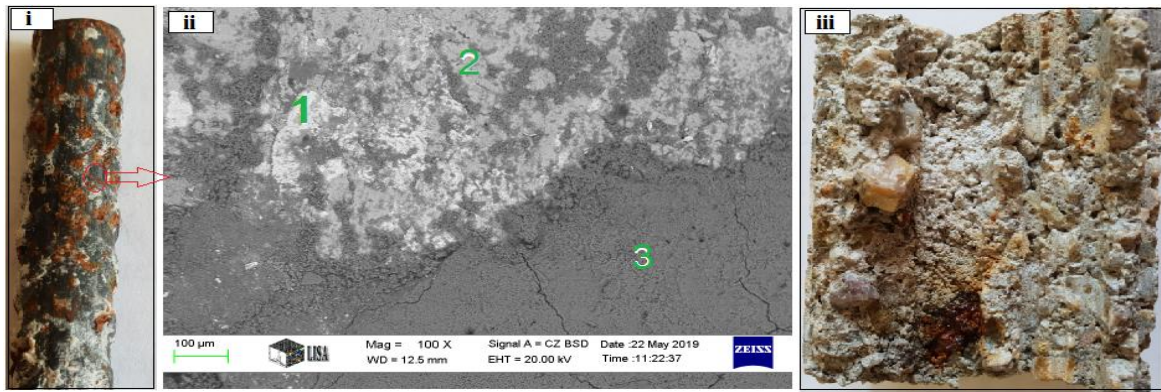
- **B3**
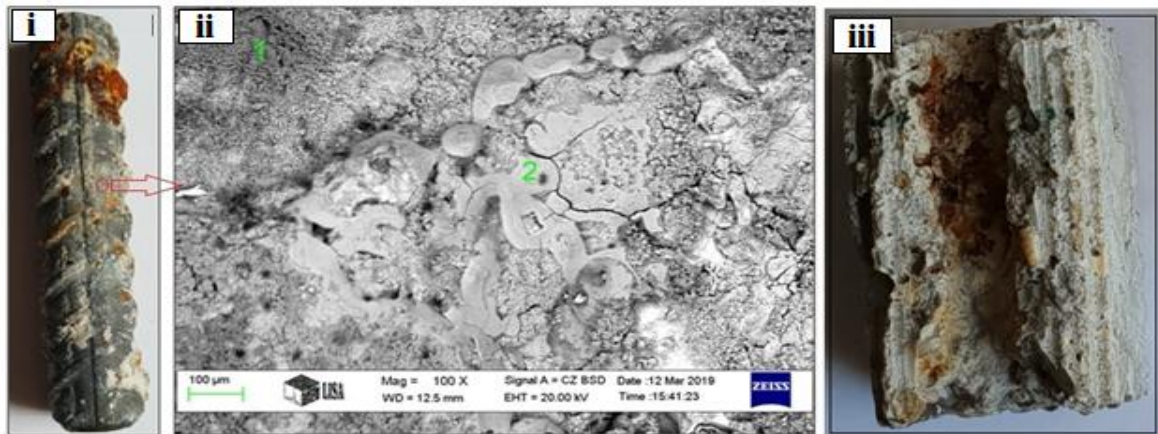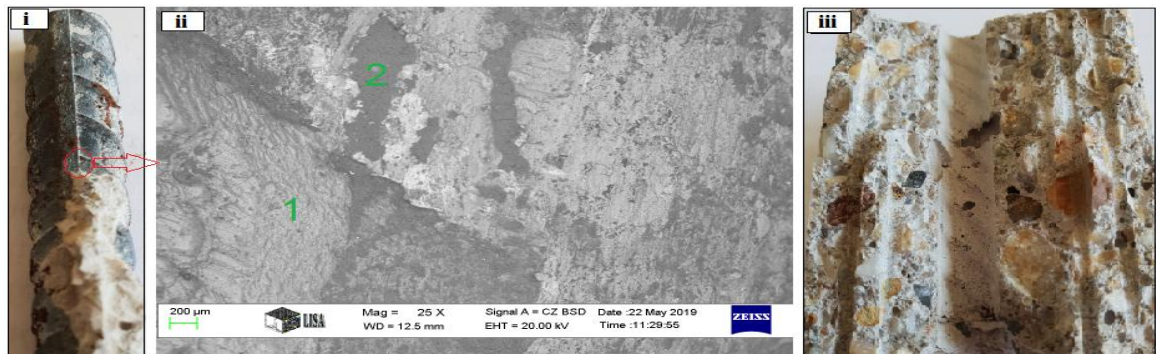

- **C3**
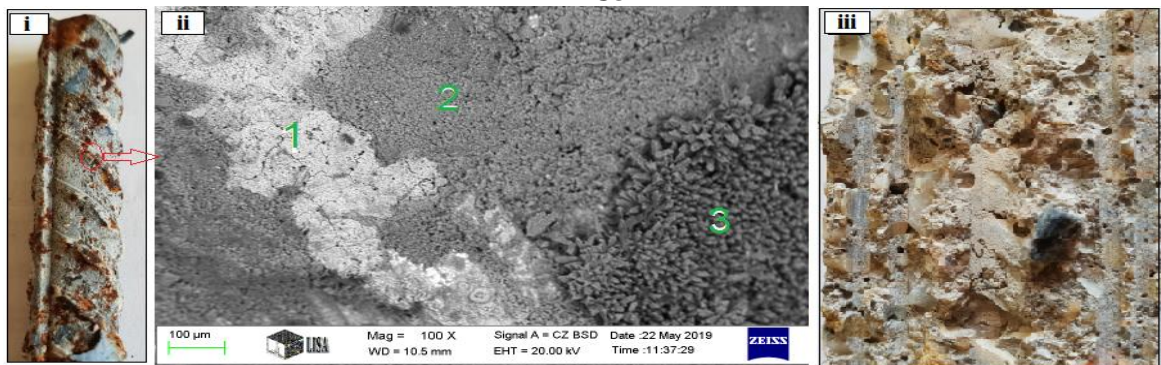
- **B4**
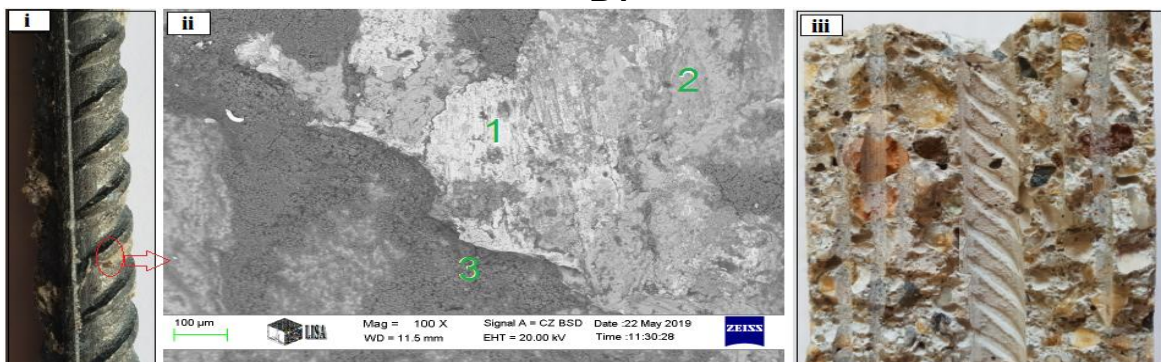
- **C4**
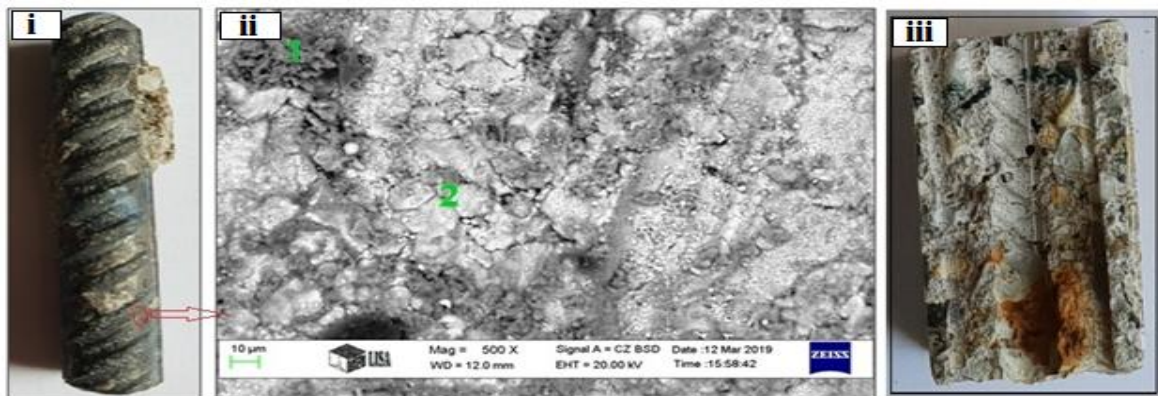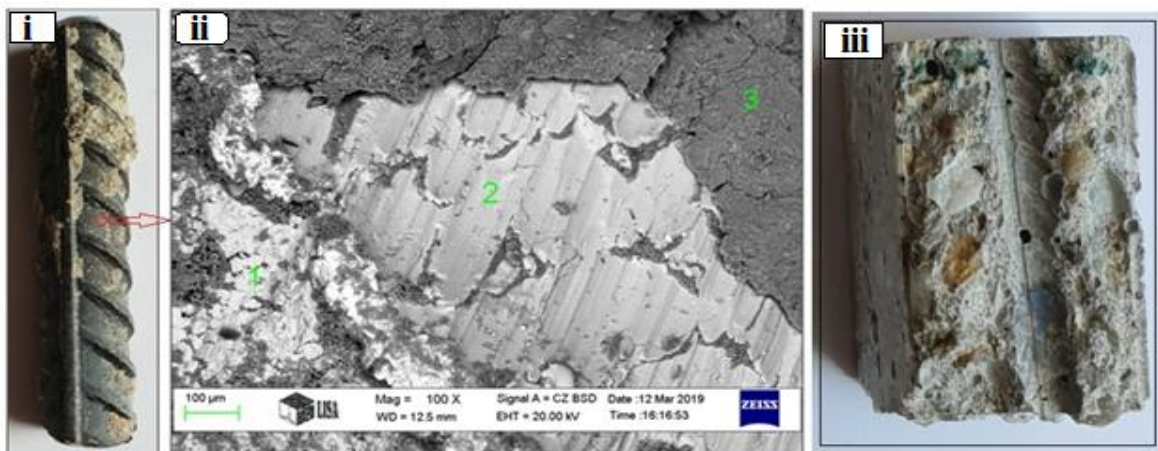
Figure 7.23 i) Close-up image of a steel rebar for samples after removal from the concrete, ii) SEM Micrograph of the section indicated in (i), iii) Representative image of a split concrete specimen with and without calcium nitrate inhibitor after removal of the steel rebar

Table 7.4 The approximate chemical composition (expressed as oxides) of some small selected surface areas (as indicated in Fig. 7.23i) of the steel rebars after removal from the concrete blocks by SEM-EDS

Components (as Oxides)	Composition by EDAX (ZAF correction) given in wt%, not normalised										
	B3			C3		B4			C4		
	Point 1	Point 2	Point 3	Point 1	Point 2	Point 1	Point 2	Point 3	Point 1	Point 2	Point 3
Na_2O	-	-	2.15	-	-	-	-	-	0.06	-	0.04
MgO	-	-	1.11	0.10	1.67	1.00	1.67	0.18	0.78	1.50	0.90
Al_2O_3	-	-	3.49	-	0.30	1.40	2.37	0.91	1.20	2.00	1.66
SiO_2	0.98	1.68	14.20	10.37	20.27	4.89	15.99	0.61	23.61	10.44	8.19
SO_3	-	-	-	3.36	0.29	-	-	-	2.45	3.50	2.57
Cl_2O	4.01	-	3.1	-	-	4.00	-	5.54	-	-	-
K_2O	-	-	1.61	-	-	-	-	-	-	-	0.78
CaO	2.23	5.81	72.29	9.65	31.54	2.10	76.65	1.71	30.56	35.65	76.5
MnO	0.14	1.49	0.00	0.83	1.20	0.49	0.74	1.28	3.15	3.80	1.86
FeO	92.7	91.02	2.56	75.9	46.29	86.13	2.58	90.77	38.39	43.91	8.32

From Fig.7.23 the effect of chloride on the surface of steel rebar in samples B3 and B4 can note because it has oxidized areas clearly seen and widespread on the surface (FeO ~ 92.66 wt%, at point 1 and 91.02 wt%, at point 2 in sample B3, FeO ~ 86.13 wt%, at point 1 and 90.77 wt%, at point 3 in sample B4). It seems that these samples did not have the ability to resist the corrosion attack of chloride ions that reached to the surface of steel. The measured high chlorine concentrations (expressed as Cl_2O ~ 4.01 wt% at point 1 and 3.1 wt% at point 3 in sample B3, Cl_2O ~ 4.00 wt% at point 1 and 5.54 wt% at point 3 in sample B4) should be considered as raising high risk of corrosion at these points.

The surface of the reinforcing steel in sample C3 appears almost free of oxidation, but there's a few oxidized spots on the surface of steel rebar and it also appeared in the micro-structure analysis test made by EDS it showed FeO in ~75.9 wt%, and CaO ~9.65 wt% at point 1, so these oxides must have formed in a surface reaction of rust with the concrete.

Sample C4 in Fig. 7.23 showed the least of corrosion attack in the steel rebar and it did not appear on its surface. The very small amounts of corrosion products detected only by EDS, and compared with those at the other samples interfaces, it means that there is a very low probability and/or risk of corrosion in this sample.

From Figs. 7.22, 7.23 the increases in the corrosion (by formation oxidized areas) can mainly be related to the structural consequences of the hydration processes (so-called

hardening) of the concrete bodies, that is the liberation of calcium hydroxide, $Ca(OH)_2$, and/or the formation of the well known cementitious compounds C_3S or C_3A, etc. The tested two admixtures (water-resisting admixture and superplasticizer admixture) added to the fresh concrete during the preparation step of the samples gave rise to reducing the water/cement ratio during the concrete blocks hardening, therefore there was not enough time for the formation of $Ca(OH)_2$ and/or C_3S and/or C_3A, .. etc. (which compounds cause greater capillary porosity in concrete and weaken the properties).

Usually, chloride ions cannot penetrate enough deep into the concrete within short time. However, after a long time in chloride ions containing environment chloride ions can arrive to and accumulate in a sufficiently high concentration at the metallic surface of the steel rebar in the concrete samples to initiate corrosion. This behavior is mainly due to distortion of passive layer (caused by the green inhibitor) on the surface of reinforced steel in agreement with the observations of the researchers Magdy A. et al. [134].

7.10 Optical Microscopy

Light optical micrographs for all concrete samples with and without green inhibitor are presented in Figs. 7.24.

- **A1**

- **B1**
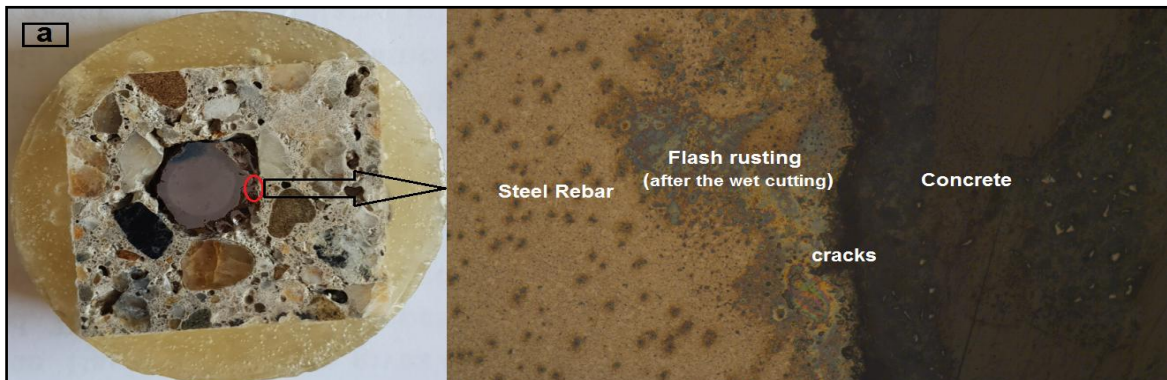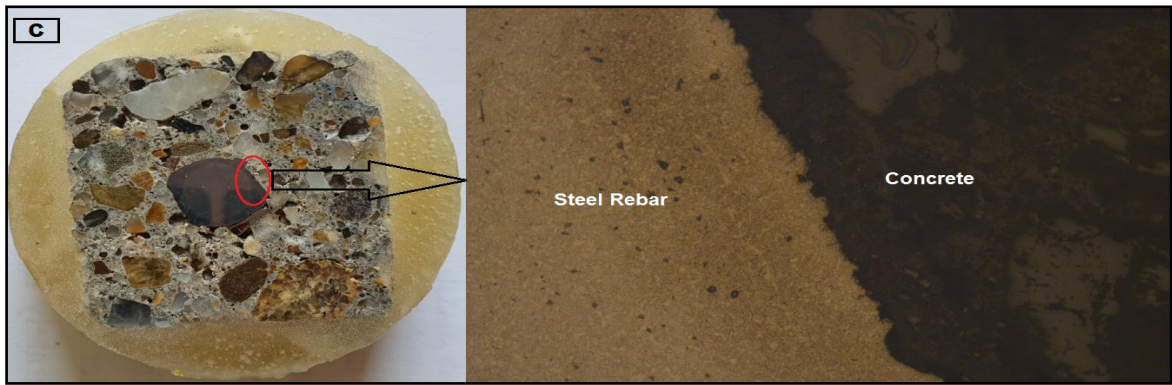
- **C1**
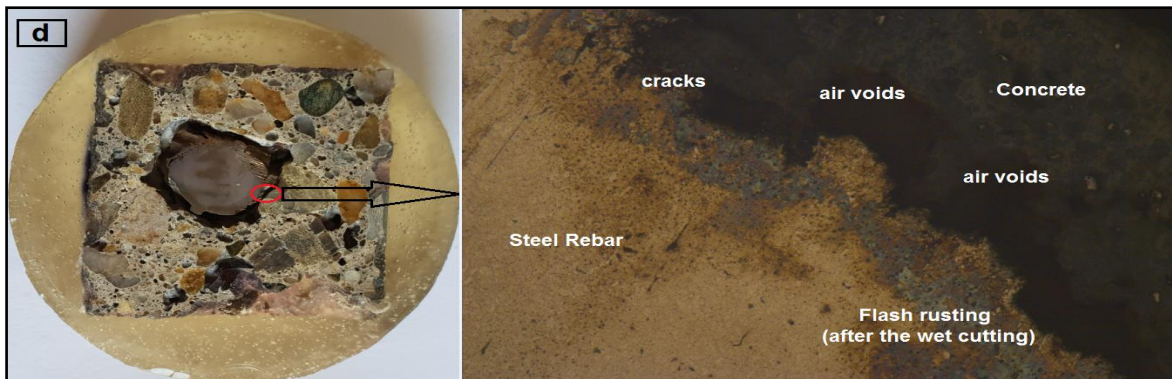
- **A2**
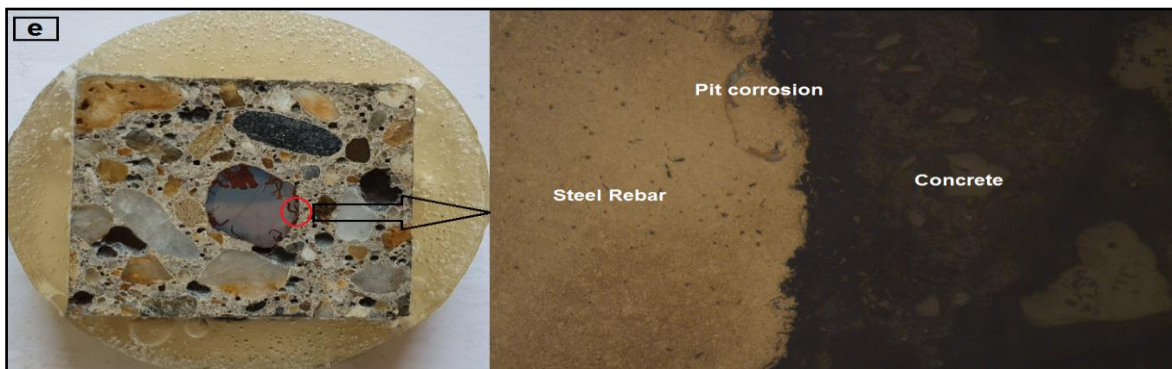
- **B2**
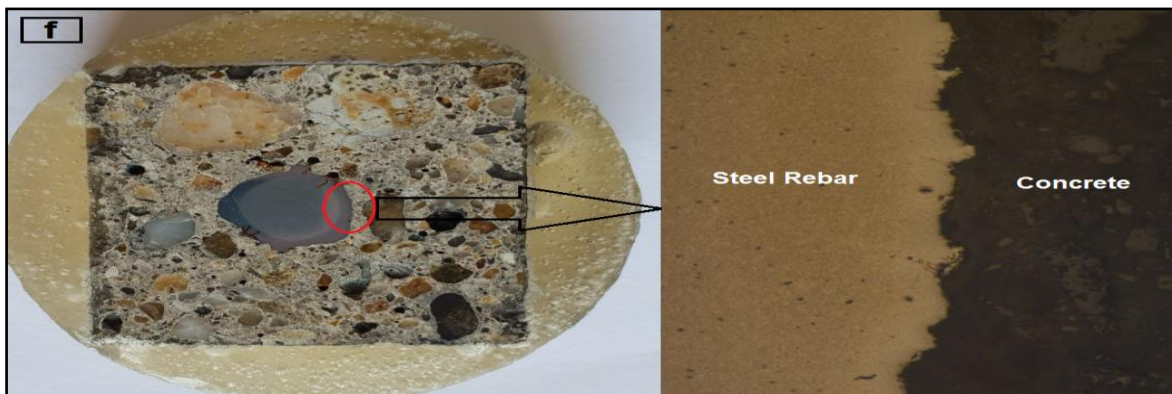
- **C2**

Figure 7.24 Light optical micrographs of the steel-concrete interface sections with magnification 50X of the concrete samples with and without green inhibitor showing the microstructure and the corrosion attack.

In Fig. 7.25 was shown the light optical micrographs of the steel-concrete interface sections for samples with calcium nitrate.
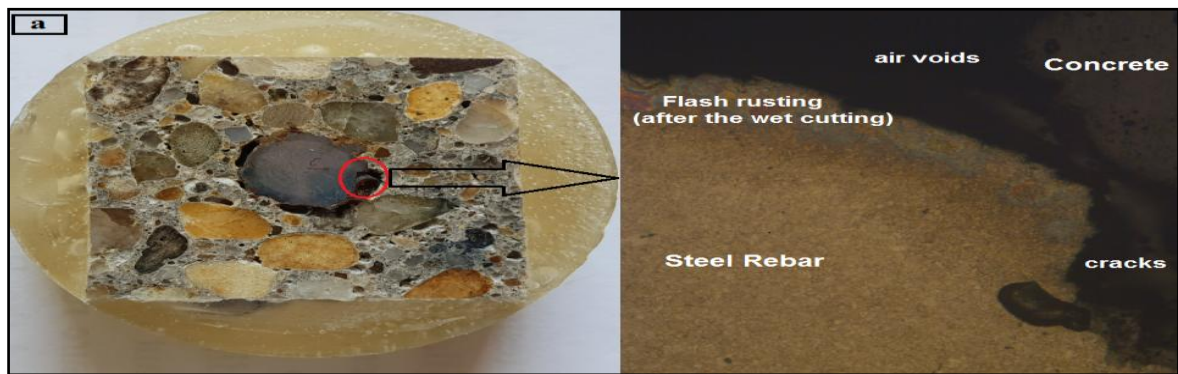
- **B3**
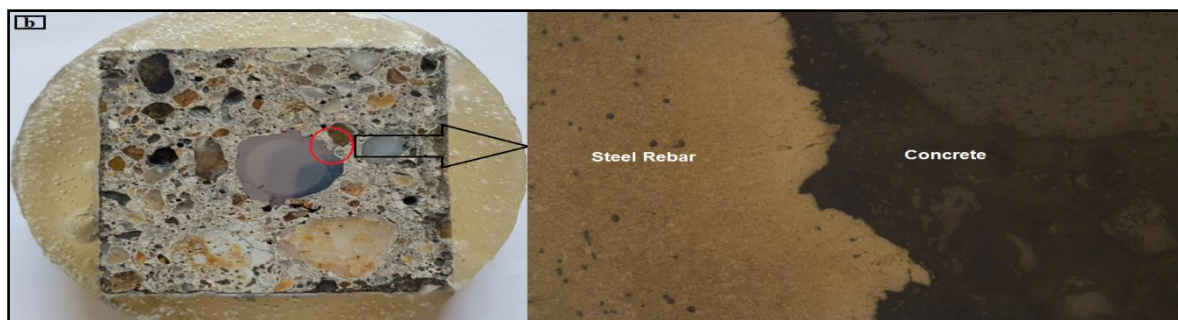
- **C3**
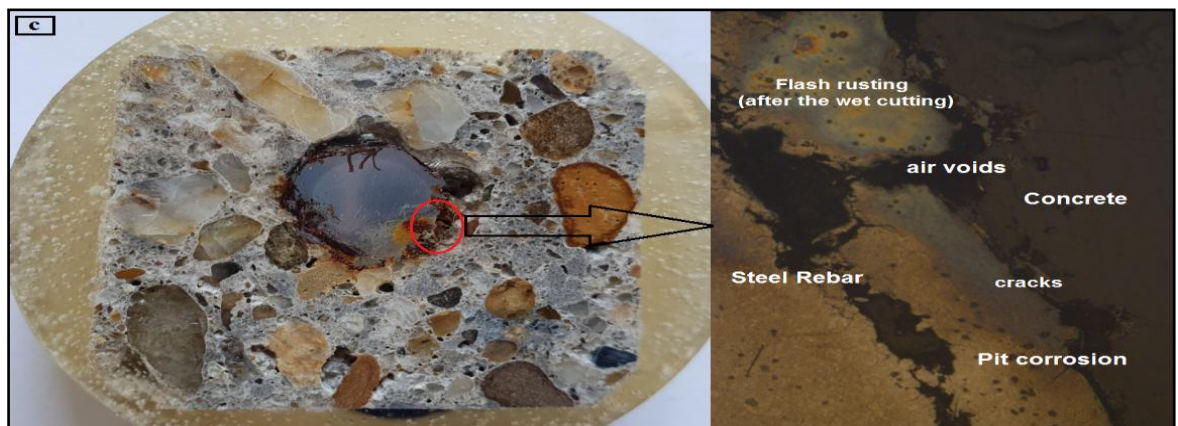
- **B4**
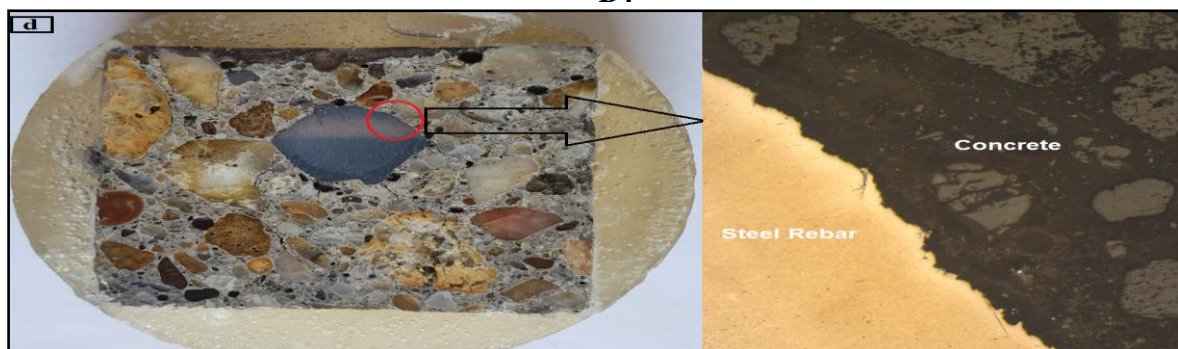
- **C4**

Figure 7.25 Light optical micrographs of the steel-concrete interface sections with magnification 50X of the samples with and without calcium nitrate inhibitor showing the microstructure and the corrosion attack.

The visual examination revealed that in 75% of all cases, corrosion initiated between the rebar ribs or directly at the rib edge as shown in Fig. 7.24a,d (samples A1 and A2) and in Fig. 7.25a,c. Some flash rusting stains (due to wet cutting of the 18-months-old blocks) can also be seen on some of the cut cross sections together with some cracks and air voids.

In Fig. 7.24b (sample B1) there's a steel manufacturing (rolling) defect as well and some slight flash rusting areas (formed after wet cutting the specimen).

Inspection of the steel-concrete interface upon corrosion initiation typically revealed the presence of one distinct corroding spot, which in some cases was surrounded by significantly smaller corrosion pits, all of them within an area of maximum approximately 1 mm^2 as shown in Fig. 7.24e (samples B2). The small corrosion pits were interpreted as sites where corrosion had initiated but was not able to reach stable pit growth (in contrast to the dominating corrosion site), these pits were typically covered with a crust of corrosion products, which occasionally remained even after the chemical cleaning process in inhibited hydrochloric acid.

Inspection of the samples C1, C2 (Fig. 7.24c, f) and C3, C4 (Fig. 7.25b, d) showed there is no pits corrosion or cracks at the steel-concrete interface.

7.11 Composition Analysis of Corrosion Products by XRD test

In Fig. 7.26 all the XRD records measured for the concrete samples with and without green inhibitor at their steel-concrete interfaces are collected and presented from a to f.

X-ray diffraction measurements detected the same products (Portlandite very low content and abundant content from calcite plus corrosion products (Brownmillerite, Biotite, Muscovite, Hydrocalumite, Ettringite, Chlorite) middle content), in concrete at its interface with concrete, as for free inhibitor samples. But the amount of calcite is lower and low or very low content amount of corrosion products in concrete samples containing inhibitor (samples with 1 wt.%, 3 wt.% green inhibitor and samples with 3 wt.% calcium nitrate only) than in the other specimens. Amorphous material was also detected, and is a product of corrosion and is made up by Fe-oxyhydroxides („rust") and Ca-Al-silicate hydrates.

- **A1**

- **B1**
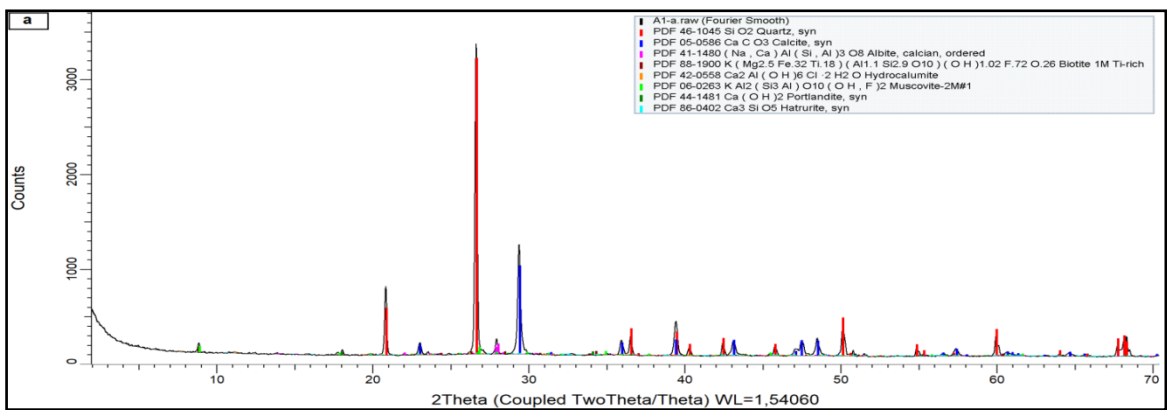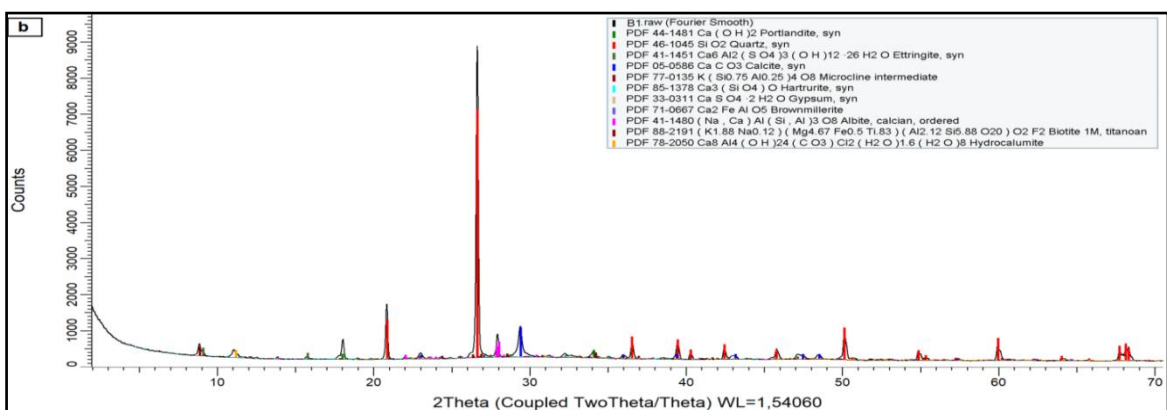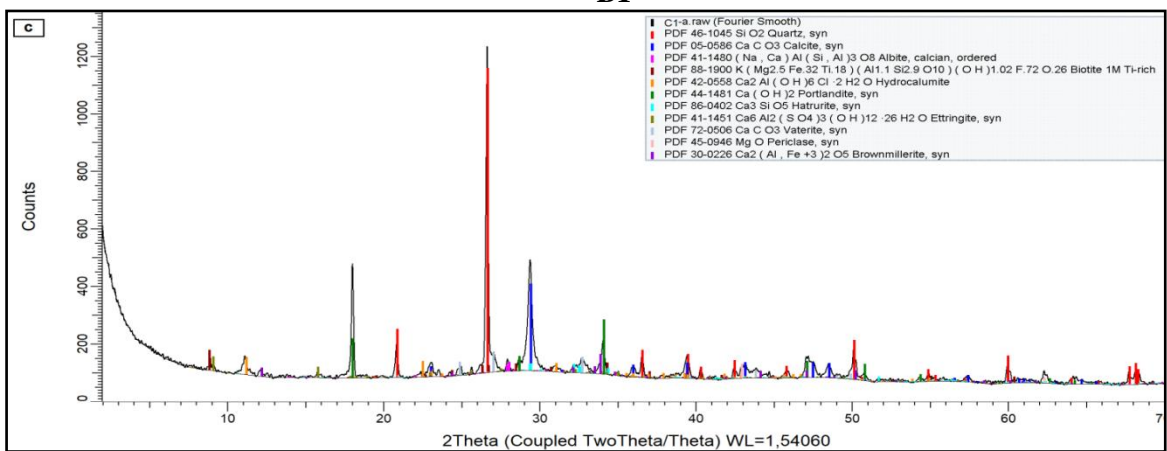
- **C1**
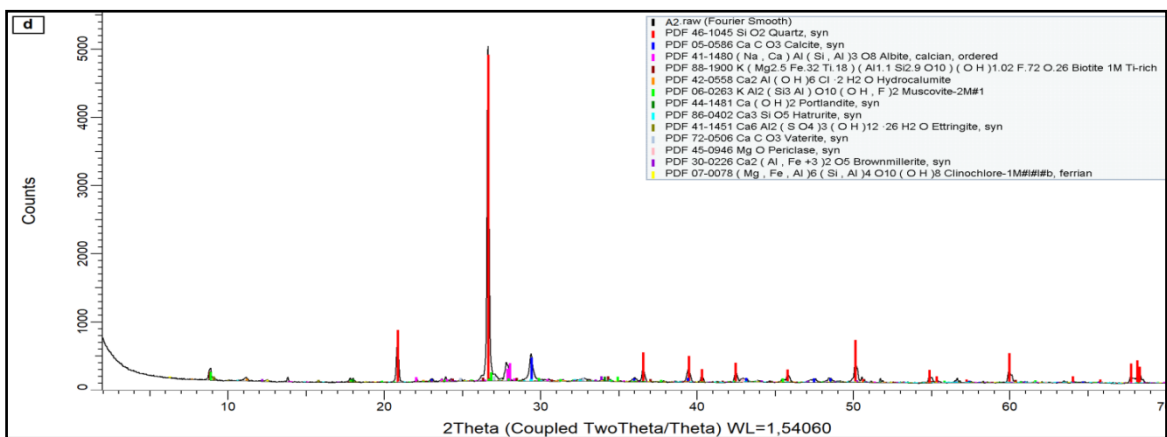
- **A2**
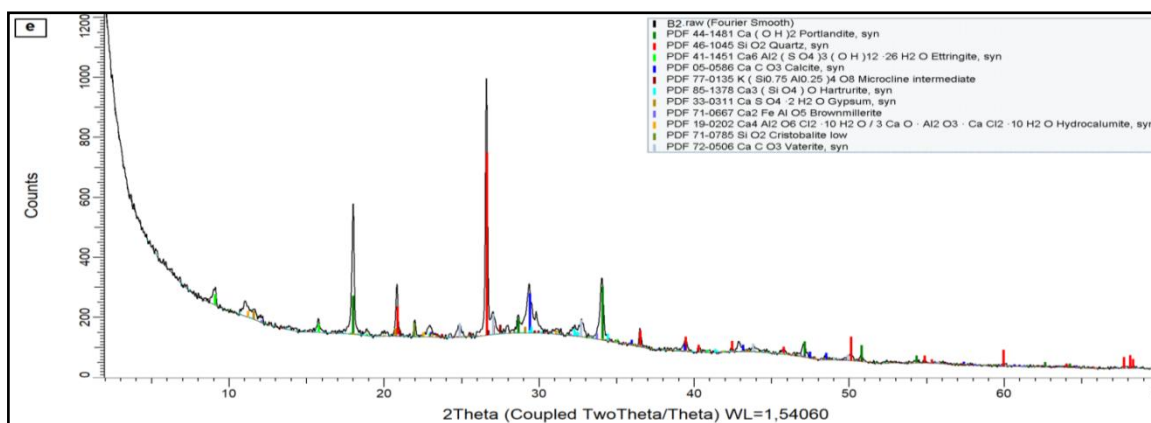
- **B2**
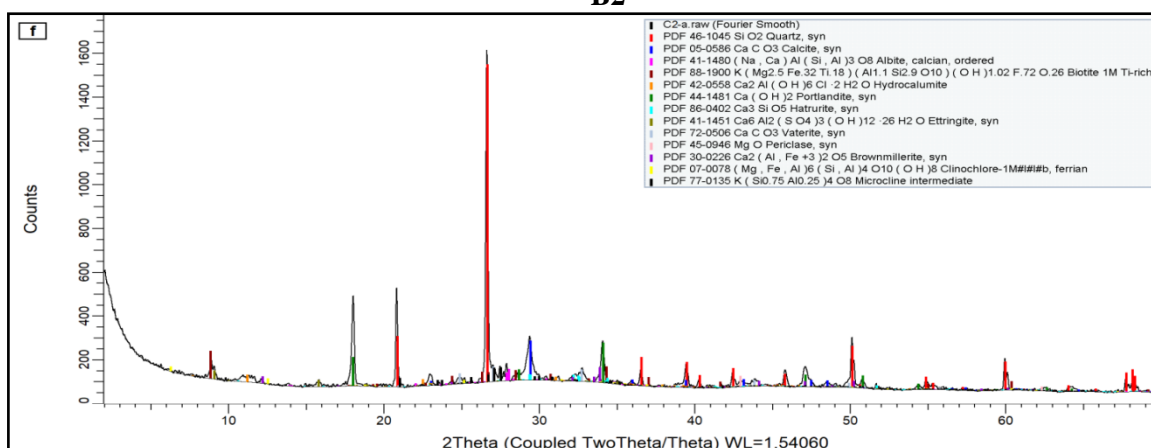
- **C2**

Figure 7.26 XRD pattern of corrosion products in the interface between steel and concrete for samples with and without green inhibitor after immersion in 3.5% NaCl for 18 months

Table 7.5 The qualitative content of the main crystalline hydration products in samples with and without green inhibitor at concrete-steel interface by XRD analysis

Compound Name with Formula	Quantities content of compounds					
	A1	**B1**	**C1**	**A2**	**B2**	**C2**
Portlandite [Ca(OH)$_2$]	+	+++	+++	+	+++	++++
Calcite [CaCO$_3$]	++++	+++	+++	++++	++	+++
Ettringite [Ca$_6$Al$_2$(SO$_4$)$_3$(OH)$_{12}$·26H$_2$O]	+++	+++	++	+++	+++	++
Hydrocalumite [Ca$_2$Al(OH)$_6$Cl·2H$_2$O]	+++	+	++	+++	++	+
Biotite [K(Mg,Fe)$_3$(AlSi$_3$O$_{10}$)(F,OH)$_2$]	+++	+	+	++	+	+
Brownmillerite[Ca$_2$(Al,Fe)$_2$O$_5$]	+++	++	++	+++	+++	+
Muscovite [KAl$_2$(AlSi$_3$O$_{10}$)(FOH)$_2$]	+++	No	No	+++	No	No
Chlorite[(Mg,Fe,Al)$_6$(Si,Al)$_4$O$_{10}$(OH)$_8$]	++	No	No	++	No	No

Notation: ++++: Abundant content; +++: Middle content; ++: Low content; +: Very low content; No: Absence.

Concrete samples with calcium nitrate their XRD records measured at steel-concrete interface presented in Fig. 7.27.
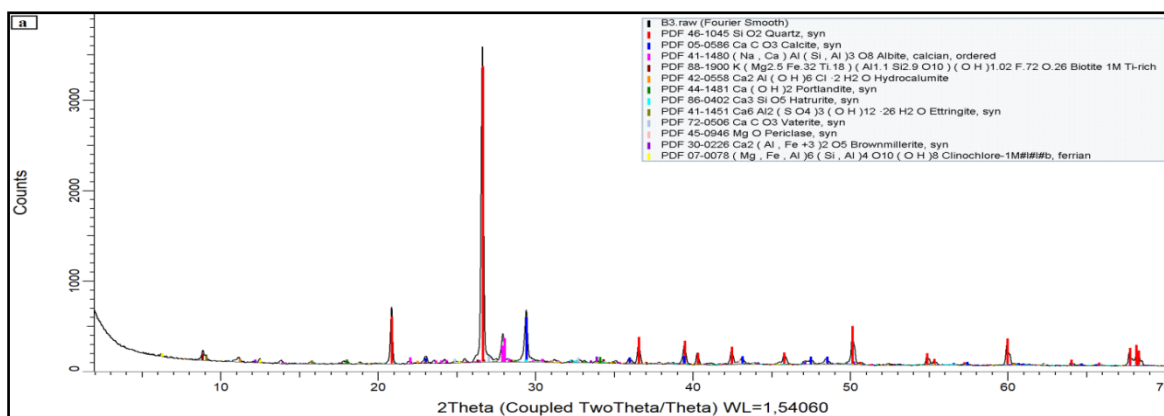
- **B3**
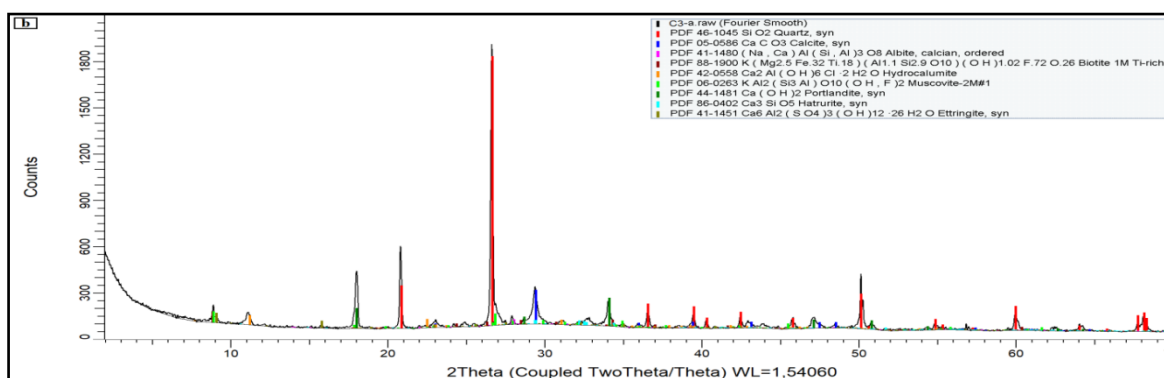
- **C3**
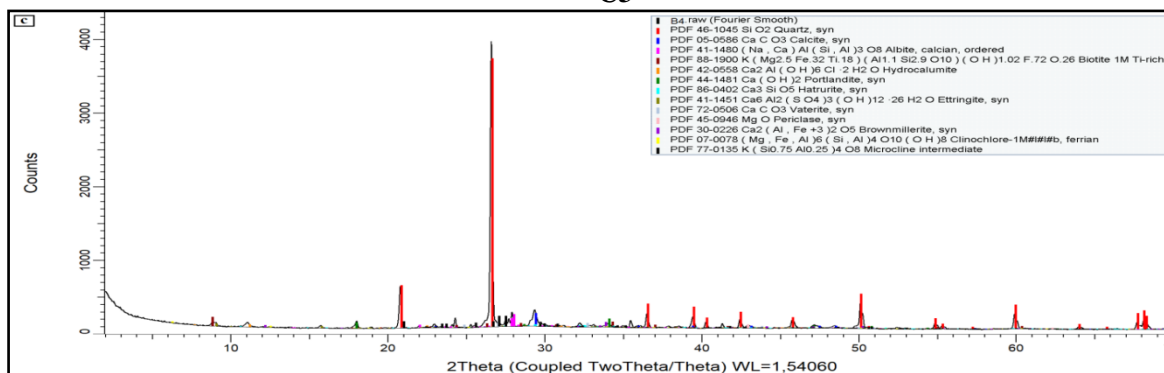
- **B4**
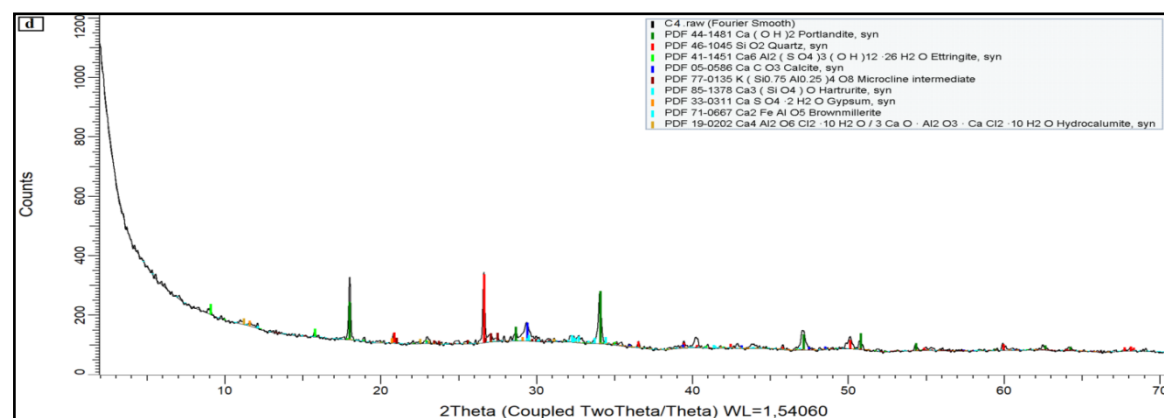
- **C4**

Figure 7.27 XRD pattern of corrosion products in the interface between steel and concrete for samples with calcium nitrate inhibitor after immersion in 3.5% NaCl for 18 months

Table 7.6 The qualitative content of the main crystalline hydration products in samples with calcium nitrate at concrete-steel interface by XRD analysis

Compound Name with Formula	Quantities content of compounds					
	A3 (=A1)	B3	C3	A4 (=A2)	B4	C4
Portlandite [$Ca(OH)_2$]	+	+	+++	+	++	++++
Calcite [$CaCO_3$]	++++	++++	++	++++	+++	+
Ettringite [$Ca_6Al_2(SO_4)_3(OH)_{12}·26H_2O$]	+++	+++	++	+++	+++	+
Hydrocalumite [$Ca_2Al(OH)_6Cl·2H_2O$]	+++	++	+	+++	+++	+
Biotite [$K(Mg,Fe)_3(AlSi_3O_{10})(F,OH)_2$]	+++	++	No	++	+++	No
Brownmillerite [$Ca_2(Al, Fe)_2O_5$]	+++	++	No	+++	+++	+
Muscovite [$KAl_2(AlSi_3O_{10})(FOH)_2$]	+++	++	+	+++	+++	No
Chlorite[$(Mg,Fe,Al)_6(Si, Al)_4O_{10}(OH)_8$]	++	+++	No	++	No	No

Notation: ++++: Abundant content; +++: Middle content; ++: Low content; +: Very low content; No: Absence.

The XRD pattern (Figs. 7.26 and 7.27) for all concrete samples (with and without inhibitors) demonstrates the presence of strong peak is Quartz (SiO_2, deriving from the sand grains in mortar) at about 2θ of 26.5°. The second clear and important peak is Portlandite ($Ca(OH)_2$) at $2\theta = 18°$ and 34° was created by the hydration of calcium silicates. Calcium hydroxide quantity precipitated at the steel surface is important in resist effect of corrosion. The protective effect of calcium hydroxide was attributed to the dissolution of calcium hydroxide crystals close to emerging pits, thereby preventing the pH drop required for the further propagation of the corrosion pit [135].

Calcite ($CaCO_3$) of a small peak at 2θ of 29.5° is attributed to carbonation of hydrates on steel surface. The presence of these two last compounds can be explained by the fact that some traces of concrete materials could remain adhered to the rust during the sampling. Because all the samples were subjected to chloride ingress, the presence of Hydrocalumite ($Ca_2Al(OH)_6Cl·2H_2O$) is justifiable and is confirmed by small peaks at $2\theta = 11°$ and 21° in low and very low content for the samples with inhibitors and in middle content for samples without inhibitors. A little amount of Brownmillerite ($Ca_2(Al, Fe)_2O_5$), Biotite ($K(Mg,Fe)_3(AlSi_3O_{10})(F,OH)_2$), Muscovite ($KAl_2(AlSi_3O_{10})(FOH)_2$), Ettringite ($Ca_6Al_2(SO_4)_3(OH)_{12}·26H_2O$), Chlorite ($(Mg,Fe,Al)_6(Si, Al)_4O_{10}(OH)_8$) as a corrosion products can be observed in different quantities in some of concrete samples as shown in Tables 7.5 and 7.6. However, iron oxides (Hematite (Fe_2O_3) or Maghemite (γ-Fe_2O_3)) cannot be clearly distinguished by this XRD pattern because their diffraction patterns are amorphous phases, only Iron(II) oxide (FeO) I distinguished by SEM-EDS technique.

Samples C2 and C4 has portlandite in high quantity this can explain the resistance of these samples to the attack of chlorides and very little corrosion products because the electrochemical mechanism of pitting corrosion confirms the inhibitive nature of OH⁻ in the pore solution. The pH value of the pore solution in concrete is mainly maintained by the portlandite ($Ca(OH)_2$) from the cement hydration and the alkaline ions (Na^+, K^+) in the pore solution. The inhibitive effect of OH^- on pitting corrosion is enhanced by the concentrated distribution of $Ca(OH)_2$ on the concrete–steel interface. The quality of the concrete–steel interface conditions the electrochemical environment of the pitting corrosion: concentrated CH (calcium hydroxide) can effectively inhibit the initiation, while the air voids and cracks at the interface can favor the formation of macrocells and thus accelerate the initiation. [136]

An increased amount of CH close to the steel in reinforced concrete as observed in this work may be beneficial, in that it may lead to improved local pH-buffering capacity and thus to better protection against carbonation-induced generalized corrosion; that is, it would take a longer time for the larger amount of CH near the interface to react to form calcium carbonate thus delaying the drop in pH associated with complete carbonation. However, it is possible that this potential benefit might not be realized in practice if the CH simply becomes encased in calcium carbonate whilst the surrounding CSH becomes completely carbonated, as has been observed in partially carbonated hardened cement pastes by transmission electron microscopy [137].

Samples A1, A2, B3, B4 have abundant content from calcite and because this component there's no ability to resist the effect of corrosion risk. Concrete carbonation due to atmospheric CO_2 is one of the main environmental aggression leading to steel corrosion. The high pH (~13) of the concrete provides a natural protection against corrosion to the embedded reinforcement by forming a compact insoluble oxide film at the steel surface (passive state). But carbonation (primarily due to the reaction $Ca(OH)_2 + CO_2 = CaCO_3 + H_2O$) leads concrete pH to decrease to about 9 and active steel corrosion to start [137]. Corrosion of steel in carbonated concrete is assumed to be uniform. If this is the case, the anodic and cathodic areas form corrosion microcells which are not separated spatially, leading to a uniform steel loss. However, in reinforced concrete structures the CO_2 penetration in the concrete cover is a complex process. Gradients in concrete humidity content affect a lot the carbonation rate, mechanical damage of concrete subjected to excessive tension can also lead to a CO_2 penetration increase. The quality of the concrete cover (strength, porosity, permeability, etc.) can also be very different in regard to the

location in the structure as it was clearly observed by us at the end of our laboratory experiments; although our steel reinforced sample blocks were not exposed to all the above mentioned various external mechanical and chemical "impacts" during the 18-months testing period when they were just kept stay immersed in stagnant aqueous solutions of NaCl open to the laboratory atmosphere (air). As the actual corrosion degradation of the reinforcing steel rebar can only occur in the so-called steel-concrete contact zone, the pores and voids at or near to the concrete–steel interface are conveying the greatest impact on corrosion initiation. Moreover, the pores are not always saturated by pore solutions and the availability of oxygen (gas phase), the pore solution (liquid phase) actual composition as well as its inhibitor content are all such factors which influence the transport rate and influx of those chemically aggressive reactants which can initiate and maintain, i.e. propagate the corrosion of the reinforcement steel. Accordingly, highly saturated, compact and very dry concretes should have higher resistance to chloride initiation of corrosion and the structural degradation of the concrete matrix, which phenomena could be well observed and characterized by the stated results of the experimental work for the important XD3 concrete system with embedded steel reinforcement bars.

Conclusions

After testing the reinforced concrete samples with or without corrosion inhibitors and two types of admixtures we can conclude the following points:

1. The concrete samples without any inhibitors had high porosity and lower corrosion resistance. Still, the samples prepared with admixing superplasticizer admixture (sample A1=A3) showed better resistance to corrosion than samples prepared with water-resisting admixture (sample A2=A4).

2. The lower concentration of infiltrated/ingressed Cl⁻ ions in the outer and depth samples were in samples C1, C2, C3, and C4 after immersion in 3.5 wt.% NaCl solution for six months to the other samples. Also, these samples showed lower porosity and the best corrosion resistance.

3. Electrical resistivity for all concrete samples (with both types of admixtures) increased with increased orange peels extract inhibitor concentration. In the case of calcium nitrate inhibitor, it increased only at a 3 wt.% concentration with two kinds of admixtures used in this work.

4. Half-cell potential became less negative values for concrete samples with increased the concentration of green inhibitor for both types of admixtures. It was also less negative values with samples containing 3 wt.% calcium nitrate with both kinds of admixtures used in this work.

5. Adding the orange peels extract inhibitor to the fresh concrete mixes showed a good ability in corrosion resistance with water-resisting admixture (as in sample C2) than the superplasticizer admixture. The concrete samples with calcium nitrate became better to resist corrosion only at a 3 wt.% concentration from this inhibitor.

6. Calcium nitrate inhibitor, which was added by 1 wt.% to the samples B3 and B4, was not worked as an inhibitor and not improving any properties of concrete samples.

7. Corrosion products (containing iron oxides and chlorides) have been observed in rising quantities with decreasing inhibitor concentration by SEM-EDS and optical microscopy and also by XRD analysis on the steel rebar surface after removal from the concrete blocks (as at a 1 wt.% orange peel extract inhibitor and at a 1wt.% calcium nitrate inhibitor). The minimum amount of corrosion products was observed in the surface points tested at the samples C1, C2, C3, and C4 (these specimens often tended to be the least corroded (almost corrosion-free) surface by merely looking at the surface).

New Scientific Results

During 18 months testing period of the concrete samples immersed in 3.5 wt.% NaCl aqueous solution at room temperature the following novelties were found:

Claim 1:

High corrosion reduction rates were obtained with the concrete mix prepared with water-resisting admixture and 3 wt.% orange peels extract inhibitor, where the Cl⁻ induced corrosion rates were measured on the hardened samples immersed in 3.5 wt.% NaCl aqueous solution at room temperature for 18 months.

This comparison with all the other tested concrete mix compositions under the specified conditions is shown in the Figure.
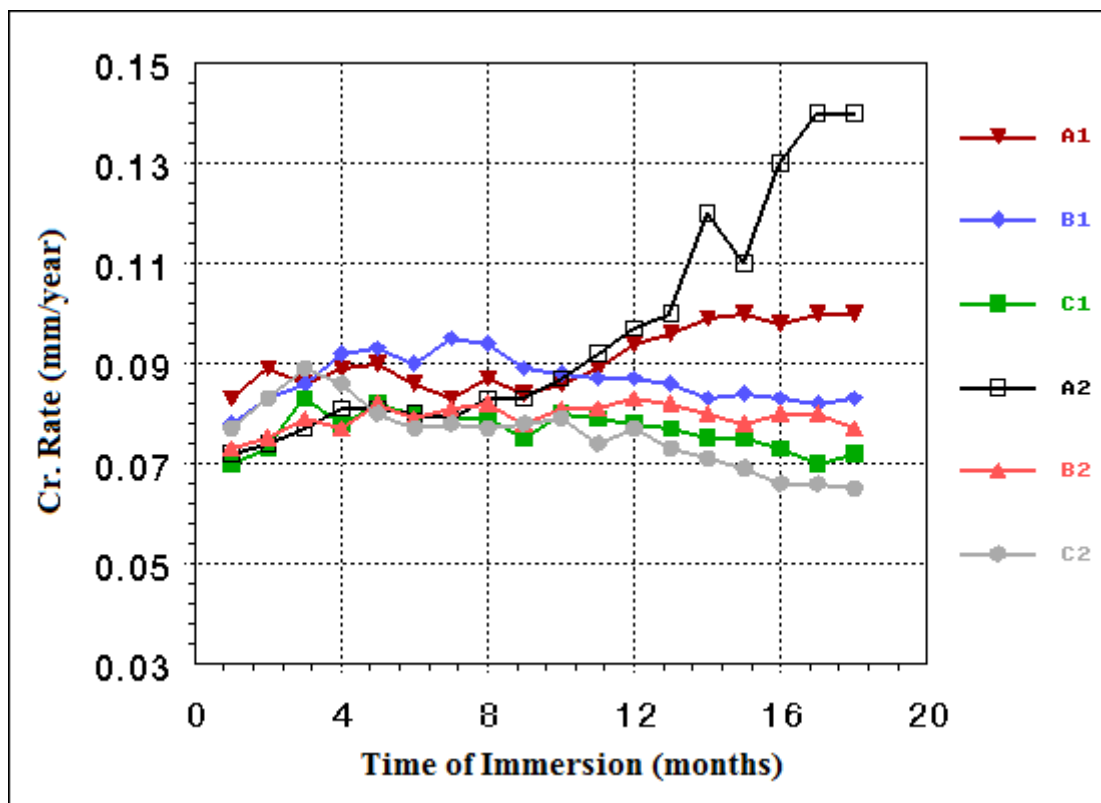
Figure to Claim 1: Corrosion rates of steel rebars in the reinforced concrete samples prepared with orange peels extract inhibitor and tested in 3.5 wt.% NaCl aqueous solution at room temperature, where A1: was prepared with superplasticizer and without orange peels extract inhibitor, B1: with superplasticizer and 1 wt.% orange peels extract inhibitor, C1:with superplasticizer and 3 wt.% orange peels extract inhibitor, A2: with water-resisting admixture and without orange peels extract inhibitor, B2:with water-resisting admixture and 1 wt.% orange peels extract inhibitor, C2: with water-resisting admixture and 3 wt.% orange peels extract inhibitor.

Claim 2:

The orange peels extract inhibitor can reduce the chloride induced corrosion rate more if it is applied together with water-resisting admixture in comparison to the case when it is applied only with superplasticizer admixture. As the water-resisting admixtures can alone

reduce the porosity and so the ingress of chlorides towards the steel bars, this retardation effect becomes stronger when we apply it together with the orange peels extract inhibitor.

Claim 3:

Calcium nitrate inhibitor can work effectively as a corrosion reducing agent with two types of admixtures (superplasticizer and water-resisting admixture) at 3 wt.%, which was proved with the steel reinforced concrete samples immersed in 3.5% NaCl solution and tested for 18 months.

The Cl^- induced corrosion rates reduction at 3 wt.% calcium nitrate inhibitor is shown in the Figure.
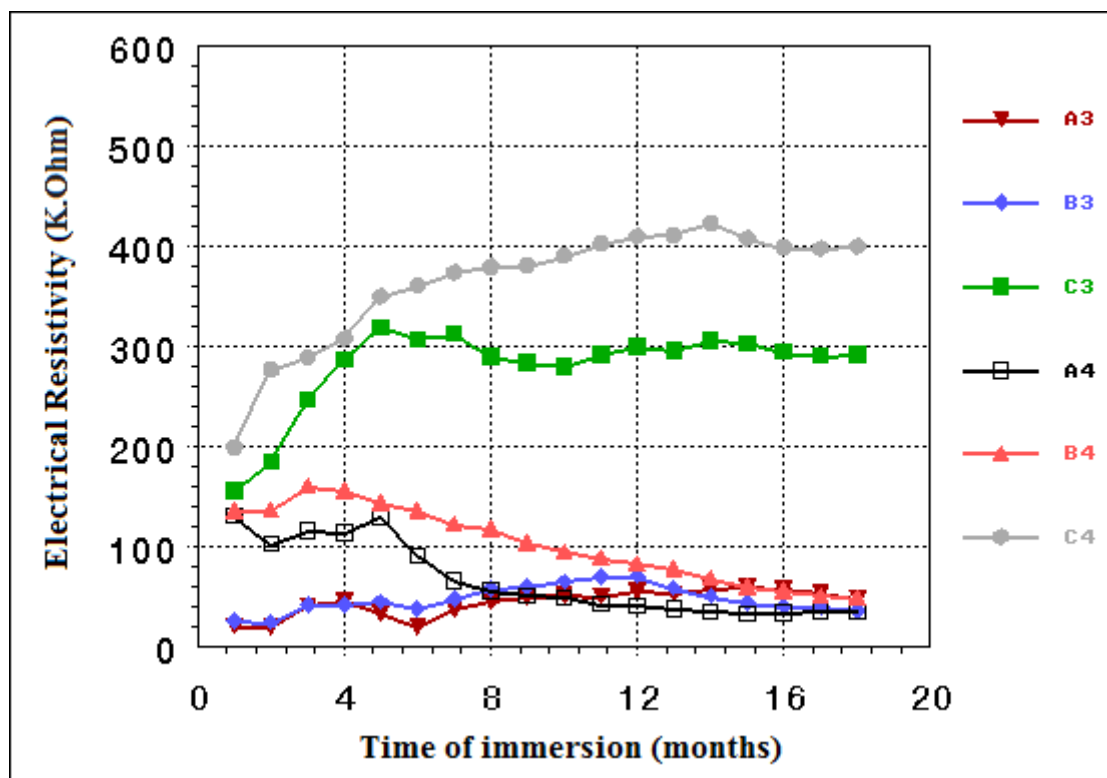
Figure to Claim 3: Electrical resistivity of steel rebars in the reinforced concrete samples prepared with calcium nitrate inhibitor and tested in 3.5 wt.%NaCl aqueous solution at room temperature, where A3: was prepared with superplasticizer and without calcium nitrate inhibitor, B3: with superplasticizer and 1 wt.% calcium nitrate inhibitor, C3:with superplasticizer and 3 wt.% calcium nitrate inhibitor, A4: with water-resisting admixture and without calcium nitrate inhibitor, B4:with water-resisting admixture and 1 wt.% calcium nitrate inhibitor, C4: with water-resisting admixture and 3 wt.% calcium nitrate inhibitor.

Claim 4:

Calcium nitrate inhibitor can work together with the water resisting admixture with better efficiency and can reduce the chloride induced corrosion rate more if we compare the test results obtained on the reinforced concrete samples prepared with the orange peels extract inhibitor and investigated up to 18 months immersion time in 3.5 wt.% NaCl aqueous solution at room temperature.

Claim 5:

At 3 wt.% concentration both orange peels extract inhibitor and calcium nitrate inhibitor were effective in mitigating the Cl⁻ induced corrosion for the superplasticizer admixture and water-resisting admixture, which was demonstrated by the corrosion measurements and after comparing the results at 1 wt.% orange peels extract inhibitor and at 1 wt.% calcium nitrate inhibitor during 18 months time period of immersion the concrete samples in 3.5 wt.% NaCl aqueous solution at room temperature.

References

[1] Y. Bellal, F. Benghanem, S. Keraghel, A new corrosion inhibitor for steel rebar in concrete: Synthesis, electrochemical and theoretical studies, Journal of Molecular Structure, 1225, 129257, 2021. https://doi.org/10.1016/j.molstruc.2020.129257

[2] S.A. Abdulsada, R. Bak, A. Heczel, T.I. Török, Corrosion studies on XD3 reinforced concrete samples prepared by using calcium nitrate as inorganic corrosion inhibitor with different superplasticizers, Koroze a ochrana materiálu, 64, 11-18, 2020. https://doi.org/10.2478/kom-2020-0002

[3] S.A. Abdulsada, É. Fazakas, T.I. Török, Corrosion testing on steel reinforced XD3 concrete samples prepared with a green inhibitor and two different superplasticizers, Materials and Corrosion, 70, 1262-1272, 2019. https://doi.org/10.1002/maco.201810695

[4] S.A. Abbas, T.I. Török, É. Fazakas, Preliminary Corrosion Testing of Steel Rebar Samples in 3.5%NaCl Solution with and without a Green Inhibitor, Építőanyag-Journal of Silicate Based and Composite Materials, 70, 48-53, 2018. https://doi.org/10.14382/epitoanyag-jsbcm.2018.10

[5] S.A. Abbas, É. Fazakas, T.I. Török, Corrosion Studies of steel rebar samples in neutral sodium chloride solution also in presence of a bio-based (green) inhibitor, International Journal of Corrosion and Scale Inhibition, 7, 38-47, 2018. http://dx.doi.org/10.17675/2305-6894-2018-7-1-4

[6] S. Abbas Abdulsada, I. Tamás Török, Studying chloride ions and corrosion properties of reinforced concrete with a green inhibitor and plasticizers, Structural Concrete, WILEY, 21(5), 1894-1904, 2020. https://doi.org/10.1002/suco.201900580

[7] S. A. Abdulsada, T. I. Török, Investigations on the resistivity of XD3 reinforced concrete for chloride ions and corrosion with calcium nitrate inhibitor and superplasticizers, Cement Wapno, Beton, 25, 330-343, 2020.

https://doi.org/10.32047/cwb.2020.25.4.7

[8] H.S. Ryu, S.H. Shin, C.G. Lim, T.W. Kang, S.Lim and H.T. Kim, Evaluation of Corrosion Resistance of Corrosion Inhibitors for Concrete Structures by Electrochemical Testing in Saturated $Ca(OH)_2$ Solutions with NaCl and Na_2SO_4, Advances in Materials Science and Engineering, Volume 2019, Article ID 8294360, 11 pages. https://doi.org/10.1155/2019/8294360

[9] G.M. Akshatha, B.G. Jagadeesha and H. Pushpa, Effect of Corrosion Inhibitors in Reinforced Concrete, International Journal of Innovative Research in Science, Engineering and Technology, 4(8) 6794-6801, 2015. https://doi.org/10.15680/IJIRSET.2015.0408013

[10] J. Damborenea, A. Conde, M.A. Arenas, 3-Corrosion inhibition with rare earth metal compounds in aqueous solutions, Rare Earth-Based Corrosion Inhibitors, Woodhead Publishing Series in Metals and Surface Engineering, 84-116, 2014. https://doi.org/10.1533/9780857093585.84

[11] M. Sangeetha, S. Rajendran, and T.S Muthumegala, A. Krishnaveni, Zašt. Mate., 52, 3, 2011. http://idk.org.rs/wp-content/uploads/2013/12/ZM_52_1_3.pdf

[12] M.L.S. Rivetti, J.S.A. Neto, N.S.A. Júnior, D.V. Ribeiro, Corrosion Inhibitors for Reinforced Concrete, Chapter 2, IntechOpen Limited, London, 2018.
 http://dx.doi.org/10.5772/intechopen.72772

[13] Z. Marta, Effectiveness of Calcium Nitrate as Corrosion Inhibitor in Concrete, Master Thesis, Politecnico Di Milano, School of Industrial and Information Engineering, Department of Chemistry, Materials and Chemical Engineering, 2017.

[14] F. Bolzoni, S. Goidanich, L. Lazzari and M. Ormellese, Corrosion inhibitors in reinforced concrete structures Part 2 – Repair system, Corrosion Engineering, Science and Technology, 41(3), 212-220, 2006. http://dx.doi.org/ 10.1179/174327806X111234

[15] Y. Tang, , S. Wang, Y. Xu, J. Ni, , Influence of calcium nitrite on the passive films of rebar in simulated concrete pore solution, Anti-Corrosion Methods and Materials, 64(3), 265-272, 2017. https://doi.org/10.1108/ACMM-05-2016-1667

[16] C. Sun, M. Chen, H. Zheng, P. Zhang, L. Yantao, H. Baorong, The effect of amino-alcohol-based corrosion inhibitors on concrete durability, Canadian Journal of Civil Engineering, 46(9), 771-776, 2019.https://doi.org/10.1139/cjce-2018-0482

[17] D.G. Eyu, H. Esah, C. Chukwuekezie, J. Idris, I. Mohammad, Effect of green inhibitor on the corrosion behavior of reinforced carbon steel in concrete, ARPN Journal of Engineering and Applied Sciences, 8(5) 326-332, 2013.

[18] J. Herbert Sinduja, G. Ganesh kumar, Effect of green corrosion inhibitors on the corrosion behaviour of reinforced concrete, International Research Journal of Engineering and Technology, 6(1), 1656-1661, 2019.

[19] V. Helbert, L. Gaillet, T. Chaussadent, V. Gaudefroy, J. Creus, Rhamnolipids as an eco-friendly corrosion inhibitor of rebars in simulated concrete pore solution: evaluation of conditioning and addition methods, Corrosion Engineering, Science and Technology, 2019. https://doi.org/10.1080/1478422X.2019.1672008

[20] R. Anitha, S. Chitra, V. Hemapriya, I. Chung, M. Prabakaran, S. Kim, Implications of eco-addition inhibitor to mitigate corrosion in reinforced steel embedded in concrete, Construction and Building Materials, 213, 246–256, 2019.

https://doi.org/10.1016/j.conbuildmat.2019.04.046

[21] L. Bertolini, B. Elsener, P. Pedeferri, and R. Polder, Corrosion of Steel in Concrete: Prevention, Diagnosis, Repair. Weinheim: Wiley, 2004.

[22] J. P. Broomfield, Corrosion of Steel in Concrete: Understanding, Investigation and Repair, Second Edition. Taylor & Francis, 2006.

[23] V. K. Gouda, "Corrosion and Corrosion Inhibition of Reinforcing Steel: I. Immersed in Alkaline Solutions," Br. Corros. J., 5(5) 198–203, 1970.

[24] A. Rossi, G. Puddu, and B. Elsener, The surface of iron and Fe10Cr alloys in alkaline media, in Proc. Eurocorr 2001.

[25] P.K. Mehta, P. J. M. Monteiro, Concrete: microstructure, properties, and materials. 2006.

[26] B. Elsener, Corrosion Inhibitors for Steel in Concrete: State of the Art Report. 2001.

[27] European Standard EN 206-1, Concrete – Part 1: Specification, performance, production and conformity, 2000, European Committee for Standardization.

[28] European Standard EN 1990, Eurocode - Basis of structural design, 2010, European Committee for Standardization.

[29] European Standard EN 197-1, Cement - part 1: Composition, specifications and conformity criteria for common cements, 2000, European Committee for Standardization.

[30] J. Bensted, P. Barnes (Eds.), Structure and Performance of Cements, 2nd Ed., 2002, Spon Press, London.

[31] W. Jaap, Understanding the tensile properties of concrete, Woodhead Publishing Series in Civil and Structural Engineering: Number 48, Woodhead Publishing Limited, 2013.

[32] S.J. Preece, J. Billinghamand, A.C. King, On the initial stages of cement hydration, School of Mathematics and Statistics, University of Birmingham, Edgbaston, Birmingham B152TT, 2000. https://www.maths.nottingham.ac.uk/plp/pmzjb1/cem.pdf

[33] F.W. Locher, W. Richartz, S. Sprung, Setting of Cement–Part I: Reaction and Development of Structure, Zement-Kalk-Gips INTERN, 29(10), 435 – 442, 1976 .

[34] U. Angst, Chloride induced reinforcement corrosion in concrete, PhD Thesis, Department of Structural Engineering, Faculty of Engineering Science and Technology, Norwegian University of Science and Technology, 2011.

[35] P.A. Claisse, Transport Properties of Concrete, Concrete International, 27(1), 43-48, 2005.

[36] J. Kim, W.J. McCarter, B. Suryanto, S. Nanukuttan, P.A.M. Basheer, T.M. Chrisp, Chloride ingress into marine exposed concrete: A comparison of empirical- and physically-based models, Cement and Concrete Composites, 72, 133-145, 2016 .
 https://doi.org/10.1016/j.cemconcomp.2016.06.002

[37] D. Breysse, in Non-Destructive Evaluation of Reinforced Concrete Structures: Deterioration Processes and Standard Test Methods, Vol. 1 in Woodhead Publishing Series in Civil and Structural Engineering, 28-56, 2010. https://doi.org/10.1533/9781845699536.1.28

[38] C.R. Bayliss, B.J. Hardy, Transmission and Distribution Electrical Engineering (Fourth Edition), Chapter 15 - Substation and Overhead Line Foundations, 615-632, 2012. https://doi.org/10.1016/B978-0-08-096912-1.00015-0

[39] M.A. Guowei, L.Wang, A critical review of preparation design and workability measurement of concrete material for large scale 3D printing, Frontiers of Structural and Civil Engineering, 12(3), 382-400, 2018. https://doi.org/10.1007/s11709-017-0430-x

[40] K. Soudki, in Service Life Estimation and Extension of Civil Engineering Structures, Chapter 2 in Woodhead Publishing Series in Civil and Structural Engineering, 75-95, 2011. https://doi.org/10.1533/9780857090928.1.75

[41] M. Pourbaix, Atlas d'équilibres électrochimiques, Centre Belge d'Etude de la Corrosion Cebelcor / Gauthier-Villars & Cie, Paris, 1963.

[42] K.Y. Ann, H.W. Song, Chloride threshold level for corrosion of steel in concrete, Corrosion Science, 49, 4113–4133, 2007. http://dx.doi.org/10.1016/j.corsci.2007.05.007

[43] U. Angst, Ø. Vennesland, Critical chloride content in reinforced concrete – State of the art, Concr. Repair Rehabil. Retrofit, Taylor Francis Group Lond. ISBN 978-0-415-46850-3, 311–318, 2009.

[44] H. Böhni, Corrosion in Reinforced Concrete Structures, Woodhead Publishing Ltd, Cambridge, UK, 2005.

[45] D. Trejo, P.J. Monteiro, Corrosion performance of conventional (ASTM A615)and low-alloy (ASTM A706) reinforcing bars embedded in concrete and exposed to chloride environments, Cement and Concrete Research, 35, 562–571, 2005. http://dx.doi.org/10.1016/j.cemconres.2004.06.004.

[46] M. Manera, Ø. Vennesland, L. Bertolini, Chloride threshold for rebar corrosion in concrete with addition of silica fume, Corrosion Science, 50, 554–560, 2008. http://dx.doi.org/10.1016/j.corsci.2007.07.007.

[47] U. Angst, B. Elsener, C.K. Larsen, Ø. Vennesland, Critical chloride content in reinforced concrete — a review, Cement and Concrete Research, 39, 1122–1138, 2009. http://dx.doi.org/10.1016/j.cemconres.2009.08.006.

[48] C.L. Page, K.W.J. Treadaway, Aspects of the electrochemistry of steel in concrete, Nature, 297, 109–115, 1982. http://dx.doi.org/10.1038/297109a0.

[49] H. Yu, K.-T.K. Chiang, L. Yang, Threshold chloride level and characteristics of reinforcement corrosion initiation in simulated concrete pore solutions, Constr. Build. Mater., 26, 723–729, 2012. http://dx.doi.org/10.1016/j.conbuildmat.2011.06.079.

[50] Minimum Concrete Cover for Reinforcement, The Constructor - Civil Engineering Home, 2019. https://theconstructor.org/practical-guide/concrete-cover-for-reinforcement/6014/

[51] M. Mckenzie, The use of embedded probes for monitoring reinforcement corrosion rates, 5th Int. Conf. on Bridge Management, Surrey Univ., 11–13 April 2005.

[52] Ramboll, SAMCO Final report, F04 Case studies, Skovdiget bridge superstructure, Denmark, Ramboll, 2006.

[53] D. Breysse, S. Yotte, M. Salta, E. Pereira, J. Ricardo, A. Povoa, Influence of spatial and temporal variability of the material properties on the assessment of a RC corroded bridge in marine environment, ICASP 10, Tokyo, 31 July–3 August 2007.

[54] M.G .Alexander, H. Beushausen, M.B. Otieno, Corrosion of steel in reinforced concrete: Influence of binder type, water / binder ratio, cover and cracking, Research Monograph NO. 9, Concrete Materials and Structural Integrity Research Unit, Department of Civil Engineering, University of Cape Town, 2012.

[55] R.O. Heckroodt, Guide to deterioration and failure of building materials, Thomas Telford Ltd, 1 Heron Quay, London E14 4JD, 2002.

[56] E. Sola, Experimental and numerical study of chloride induced corrosion in reinforced concrete, PhD thesis, Institute for Materials in Construction at the University of Stuttgart, Italy, 2017.

[57] D.V. Ribeiro, M.P. Cunha, Deterioração das estruturas de concreto armado. In: Ribeiro DV, editor. Corrosão em estruturas de concreto armado: Teoria, Controle e Métodos de Análise. 1st ed. Rio de Janeiro: Elsevier, 87-118, 2014.

[58] A. Poursaee, Corrosion of Steel in Concrete Structures, Woodhead Publishing Series in Civil and Structural Engineering: Number 61, 2016.

[59] R. Edwards, Corrosion of Steel in Concrete, Corrosion Engineering Solutions Ltd, Document No: CN12-X02-GN-0003, 2012, on the web:
 https://www.corrosionengineering.co.uk/knowledge-library/corrosion-of-steel-in-concrete/index.php

[60] L. Bertolini, M. Carsana, M. Gastaldi, F. Lollini, E. Redaelli, Corrosion of Steel in Concrete and Its Prevention in Aggressive Chloride-Bearing Environments, 5th International Conference on Durability of Concrete Structures, Jun 30–Jul 1, 2016 in Shenzhen University, Shenzhen, Guangdong Province, P.R.China.
https://docs.lib.purdue.edu/cgi/viewcontent.cgi?article=1153&context=icdcs

[61] Z. Ahmad, in Principles of Corrosion Engineering and Corrosion Control, 57-119, 2006. https://doi.org/10.1016/B978-075065924-6/50004-0

[62] M. Luna Sousa Rivetti, J. Silva Andrade Neto, N. Santana de Amorim Júnior, R. Daniel Véras, Corrosion Inhibitors for Reinforced Concrete, Corrosion Inhibitors, Principles and Recent Applications, Mahmood Aliofkhazraei, IntechOpen, 2017. http://dx.doi.org/10.5772/intechopen.72772

[63] M. James Gaidis, Chemistry of corrosion inhibitors, Cement & Concrete Composites 26, 181–189, 2004. http://dx.doi.org/10.1016/S0958-9465(03)00037-4

[64] Annual Book of ASTM Standards, vol. 04.02. Philadelphia: American Society for Testing and Materials, 1989.

[65] A.M. Rosenberg, J.M., Gaidis, Corrosion inhibiting concrete composition. US Patent No. 4,285,733, 25 August 1981.

[66] P. Finnerty, Stewart V, Meyers R. HPC Bridge Views, vol. 18. Nov/Dec 2001. p. 1.

[67] S.L. Amey, D.A. Johnson, M.A. Miltenberger, H. Farzam, Predicting the service life of concrete marine structures: an environmental methodology. ACI Struct J., 95(2), 205–214, 1998. doi:10.14359/540

[68] K. Tuutti, Corrosion of steel in concrete. CBI research report no 4.82. Swedish Cement and Concrete Research Institute, Stockholm, Sweden, 1982.

[69] J. P. Broomfield, Corrosion of Steel in Concrete: Understanding, Investigation and Repair, Second Edition. Taylor & Francis, 2006.

[70] M. Zerbi, Effectiveness of Calcium Nitrate as Corrosion Inhibitor in Concrete, Master Thesis, School of Industrial and Information Engineering, Department of Chemistry, Materials and Chemical Engineering "G. Natta", Politecnico DI Milano, 2017.

[71] B. Elsener, Corrosion Inhibitors for Steel in Concrete: State of the Art Report. 2001.

[72] J. Mietz, B. Elsener, R. Polder, Corrosion of reinforcement in concrete: monitoring, prevention and rehabilitation: papers from EUROCORR '97, Trondheim, Norway, 1997, Routledge publisher, 2017.

[73] C.Venkatesh, S.K. Mohiddin, N. Ruben, Corrosion Inhibitors Behavior on Reinforced Concrete - A Review. In: Das B., Neithalath N. (eds) Sustainable Construction and Building Materials. Lecture Notes in Civil Engineering, 25, 2019. https://doi.org/10.1007/978-981-13-3317-0_11

[74] A.S. Abdulrahman, I. Mohammad, S.H. Mohammad, Corrosion inhibitors for steel reinforcement in concrete: A review, Scientific Research and Essays, 6(20), 4152-4162, 2011. https://doi.org/0.5897/SRE11.1051

[75] C. Lisha, M. Rajalingam, S. George, Corrosion Resistance of Reinforced Concrete With Green Corrosion Inhibitors, International Journal of Engineering Science Invention Research & Development, III(XI), 687-691, 2017.

[76] U. Maeder, A New Class of Corrosion Inhibitors for Reinforced Concrete, Spec. Publ., 163, 215–232, 1996.

[77] ikipedia.org, "Nitrate." [Online]. Available: https://en.wikipedia.org/wiki/Nitrate. [Accessed: 17-Decmber-2019].

[78] M. V. Diamanti, B. Del Curto, M. Ormellese, F. Bolzoni, and G. Cilluffo, "On the use of nitrates as corrosion inhibitors for concrete rebars, La Metall. Ital., 109, 11–14, 2017.

[79] H. Justnes and E. C. Nygaard, Technical calcium nitrate as set accelerator for cement at low temperatures, Cement and Concrete Research, 8, 1766–1774, 1995.

[80] Y.U.K. D'yachenko, S.G. Enisherlova, G.D. Kucheryaeva, V.B. Rationov, and S.D. Semenova, Effect of Chloride, Nitrate, and Nitrite on the Corrosion of Prestressed Rebars in Heavy Concrete, Zashch. Met, 23(4), 655–659, 1987.

[81] H. Justnes, E.C. Nygaard, The influence of technical calcium nitrate additions on the chloride binding capacity of cement and the rate of chloride induced corrosion of steel embedded in mortars, in Corrosion protection of steel in concrete, 491–502, 1994.

[82] H. Justnes, Concrete Corrosion Problems solved by Calcium Nitrate, in 25th Conference on Our World in Concrete and Structures, 349–356, 2000.

[83] D. Talbot and J. Talbot, Corrosion Science and Technology. Boca Raton, FL: CRC Press LLC, 1998.

[84] H. Verbruggen, H. Terryn, and I. De Graeve, Inhibitor evaluation in different simulated concrete pore solution for the protection of steel rebars, Constr. Build. Mater., 124, 887–896, 2016.

[85] R.M. Brown, M.M. Sprinkel, R.E. Weyers, Solution Tests of Corrosion-Inhibiting Admixtures for Reinforced Concrete, Mater. J., 99(4), 371–378, 2002.

[86] P. Saura, E. Zornoza, C. Andrade, and P. Garcés, Steel corrosion-inhibiting effect of sodium nitrate in simulated concrete pore solutions, Corrosion, 67(7), 2011.

[87] H. Justnes, Accelerator Blends for Portland Cement, in Second International Symposium on Cement and Concrete Technology in the 2000s, 1, 433–442, 2000.

[88] W. Franke, C. Thiel, F. Duran, and C. Gehlen, Effect of Calcium Nitrate on the freeze- thaw-resistance of concrete, Betonw. und Fert. Plant Precast Technol., 81(10), 2015.

[89] N. Chikh, M. Cheikh-Zouaoui, S. Aggoun, and R. Duval, Effects of calcium nitrate and triisopropanolamine on the setting and strength evolution of Portland cement pastes, Mater. Struct. Constr., 41(1), 31–36, 2008.

[90] W. Franke, D. Weger, J. Skarabis, and C. Gehlen, Study on Calcium Nitrate impact on Carbonation of Concrete, in 1st International Conference on Grand Challenges in Construction Materials, 2016.

[91] CEMMAC Company, Cement CEM II/B-M (S-V) 32,5 R, on this web: http://www.cemmac.sk/en/cement-cem-iib-m-s-v-325-r.

[92] EN 12620, Aggregates for Concrete, European Standard was Approved by CEN National Members on September 2002.

[93] EN 934-2, Admixtures for concrete, mortar and grout., European Standard was Approved by BSI on 30 June 2009.

[94] MAPEI Company, Admixtures for Concrete: DYNAMON SR31, on this web: http://www.mapei.com/CN-EN/Admixtures-for-Concrete/Dynamon-System/DYNAMON-SR31

[95] Mineral Cement Technology, Oxydtron, on this web: http://function.oxydtron.hu/

[96] RPI, " EN ISO 18753 : 2017, Fine ceramics (advanced ceramics, advanced technical ceramics) - determination of absolute density of ceramic powders, Committee European de Normalisation, 2017.

[97] C. Hall, Water Transport in Brick, Stone and Concrete, ed. W.D. Hoff., London: London : E. & F. N. Spon, 2000.

[98] ISO 1920-5: 2018, Testing of concrete - Part 5: Density and water penetration depth, International Standard was published in Switzerland, Second edition 2018-06.

[99] EN 13396, Products and systems for the protection and repair of concrete structures. Test methods. Measurement of chloride ion ingress, European Standard was Approved by CEN National Members on 12 July 2004.

[100] Standard: BIS - IS 3025: PART 32, Methods Of Sampling And Test (Physical And Chemical) For Water And Wastewater : Part 32 Chloride, Bureau of Indian Standards, 1988, on this web: http://standards.globalspec.com/std/1484098/bis-is-3025-part-32

[101] M.G. Richardson, Fundamentals of Durable Reinforced Concrete, Spon Press, London, UK, 2002.

[102] Concrete Society, Repair of concrete Damaged by reinforced corrosion, Technical Report No.26, London, 1984.

[103] D.V. Ribeiro, J.A. Labrincha, M.R. Morelli, Effect of red mud addition on the corrosion parameters of reinforced concrete evaluated by electrochemical methods, IBRACON Structures and Materials Journal, 5, 451-467, 2012.
 http://dx.doi.org/10.1590/S1983-41952012000400004

[104] K. Falah Matlob, A. Abeer Mohammed, H. Nada, Effect of Using Corrosion Inhibitors on Concrete Properties and Their Activity, Journal of Kerbala University, 6(4), 121-139, 2008.

https://www.iasj.net/iasj?func=fulltext&aId=50963&fbclid=IwAR1hssaJPJ_kM7GvQa1YxANtcpyrQ3prnLp0lANP-Mhefn4BMeA2f4m28Fk

[105] BS EN 1504, Basics of Concrete Repair and Structural Strengthening, Structural Concrete Alliance, Concrete Repair Association, on this web:

http://www.sca.org.uk/pdf_word/Penrith%202015/Basics%20of%20Concrete%20Repair%20and%20Structural%20Strengthening.pdf

[106] Gu Ping and J.J. Beaudoin, Obtaining Effective Half-Cell Potential Measurements in Reinforced Concrete Structures, Construction Technology Update No. 18, Institute for Research in Construction, National Research Council of Canada, July 1998, ISSN 1206-1220.

[107] E. Mahallati and M. Saremi, An assessment on the mill scale effects on the electrochemical characteristics of steel bars in concrete under DC-polarization, Cement and Concrete Research, 36(7), 1324-1329, 2006.
https://doi.org/10.1016/j.cemconres.2006.03.015

[108] M. Esthaku Peter, P. Ramasam, Structural, Growth and Characterizations of NLO Crystal: Triglycinium Calcium Nitrate, Adv. Mater. Lett., 7, 83-88, 2016.
 https://doi.org/10.5185/amlett.2016.5944

[109] A Kičaitė, I Pundienė, G Skripkiūnas,The influence of calcium nitrate on setting and hardening rate of Portland cement concrete at different temperatures, IOP Conf. Series: Materials Science and Engineering, 251, 12-17, 2017. https://doi.org/10.1088/1757-899X/251/1/012017

[110] Karagöl F, Demirboğa R, Kaygusuz M A, Yadollahi M M and Polat R, The influence of calcium nitrate as antifreeze admixture on the compressive strength of concrete exposed to low temperatures, Cold Regions Science and Technology, 89, 30-35, 2013. https://doi.org/10.1016/j.coldregions.2013.02.001

[111] Popovics S, Concrete materials, properties, specifications and testing, 2nd edition, William Andrew Publishing Noyes, 1992.

[112] V.S. Ramachandran, Concrete Admixtures Handbook, 2nd edition, Publishing Noyes, 1995.

[113] H. Justnes and E.C. Nygaard, The Influence of Technical Calcium Nitrate Additions on the Chloride Binding Capacity of Cement and the Rate of Chloride Induced Corrosion of Steel Embedded in Mortars, International conference, Corrosion and corrosion protection of steel in concrete; 1994; Sheffield, Sheffield Academic Press, 491-502.
https://www.tib.eu/en/search/id/BLCP%3ACN004860901/The-Influence-of-Technical-Calcium-Nitrate-Additions/

[114] Cti Technical Note C2, Chlorides In Concrete, Cti Consultants Pty Ltd, 1-3, 2018, on the web: https://cticonsultants.com.au/wp-content/uploads/2019/03/CTI-TN2-Chlorides-in-Concrete.pdf

[115] R.B., Polder, Test methods for onsite measurement of resistivity of concrete - a RILEM TC-154 technical recommendation, Construction and Building Materials, 15, 2011, 125-131. https://doi.org/10.1016/S0950-0618(00)00061-1

[116] D.A. Whiting, M.A. NAGI, Electrical Resistivity of Concrete − A Literature Review, Illinois, USA: Portland Cement Association, 2003, pp.57, (R&D Serial No. 2457).

[117] P.A.M. Basheer et al., Monitoring electrical resistance of concretes containing alternative cementitious materials to assess their resistance to chloride penetration, Cement and Concrete Composites, 24, 437-449, 2002.https://doi.org/10.1016/S0958-9465(01)00075-0

[118] W.J. Mccarter, G. Starrs, T.M. Chrisp, Electrical conductivity, diffusion, and permeability of Portland cement-based mortars, Cement and Concrete Research, 30(9), 1395-1400, 2000. https://doi.org/10.1016/S0008-8846(00)00281-7

[119] M.A. El-Reedy, Steel-Reinforced Concrete Structures: Assessment and Repair of Corrosion, Second Edition, CRC Press, Taylor & Francis, London, 2018.

[120] H. Justnes, Calcium nitrate as corrosion inhibitor for reinforced concrete, Innovations and Developments In Concrete Materials And Construction: Proceedings of the International Conference held at the University of Dundee, Scotland, UK on 9–11 September 2002, 391-401.

https://www.icevirtuallibrary.com/doi/abs/10.1680/iadicmac.31791.0038

[121] R. F. Stratfull, Corrosion Autopsy of a Structurally Unsound Bridge Deck, Highway Research Record 433, Highway Research Board, National Research Council, Washington, DC, 1973,1-11. (52nd Annual Meeting of the Highway Research Board held in Washington District of Columbia, United States during 22 to 26 January 1973).

[122] C. Naish, A. Harker, R.F.A. Carney, Concrete inspection: Interpretation of potential and resistivity measurements, Proceedings from Corrosion of Reinforcement in Concrete, Elsevier Applied Science, 1990, 314-332. 3rd International Symposium on Corrosion of Reinforcement in Concrete Construction, Wishaw, England, 21-24, 1990

[123] C. Andrade, C. Alonso, On-Site Measurements of Corrosion Rate of Reinforcements, Construction and Building Materials, 15, 141-145, 2001. https://doi.org/10.1016/S0950-0618(00)00063-5

[124] B. Eisener, H. Bohni, ASTM STP 1065, Potential Mapping and Corrosion of Steel in Concrete, ASTM, Philadelphia, 143-156, 1990. http://doi.org/10.1520/STP25021S

[125] S. Jefremczuk, Chloride Ingress and Transport in Cracked Concrete, MSc thesis, Mc Gill University, Canada, pp.97, 2004. http://digitool.library.mcgill.ca/R/?func=dbin-jump-full&object_id=82603&local_base=GEN01-MCG02

[126] S.Y. Qian, Reinforcing Decay, Canadian Consulting Engineer.

https://www.canadianconsultingengineer.com/features/reinforcing-decay/

[127] A.H. Nielsen, T. Hvitved-Jacobsen and J. Vollertsen, Effect of Sewer Headspace Air-Flow on Hydrogen Sulfide Removal by Corroding Concrete Surfaces, Water Environmental Research, 84, 265, 2012. https://doi.org/10.2175/106143012X13347678384206

[128] I. Yakub , N.M. Sutan, C.S. Kiong, Characterization of calcium silicate hydrate and calcium hydroxide in nanosilica binder composites, Nano Studies, 7, 57, 2013. https://www.researchgate.net/publication/263738702_Characterization_of_calcium_silicate_hydrate_and_calcium_hydroxide_in_nanosilica_binder_composites

[129] H. Justnes, Concrete Corrosion Problems Solved by Calcium Nitrate, in 25th Conference on Our World in Concrete and Structures, 349–356, 2000.

[130] P. Saura, E. Zornoza, C. Andrade, and P. Garcés, Steel corrosion-inhibiting effect of sodium nitrate in simulated concrete pore solutions, Corrosion, 67, 075005-1-075005-15, 2011. https://doi.org/10.5006/1.3613642

[131] P. Saura, E. Zornoza, C. Andrade, and P. Garcés, Steel corrosion-inhibiting effect of sodium nitrate in simulated concrete pore solutions, Corrosion, 67, 075005-1-075005-15, 2011. https://doi.org/10.5006/1.3613642

[132] C. Andrade and C. Alonso with contributions from J. Gulikers, R. Polder, R. Cigna, Ø. Vennesland, M. Salta, A. Raharinaivo and B. Elsener, Test methods for on-site corrosion rate measurement of steel reinforcement in concrete by means of the polarization resistance method, Materials and Structures / Matériaux et Constructions, 37, 623-643, 2004. https://doi.org/10.1007/BF02483292

[133] P. Montes-Garcia, H. Z. López-Calv, and T. W. Bremner, Effectiveness of calcium nitrate inhibitor (CNI) in cracked concrete, Revista Ingeniería de Construcción, 24, 233-244, 2009. http://dx.doi.org/10.4067/S0718-50732009000300002

[134] A. Magdy Abd El-Aziz, H. Waleed Sufe, Effect of sewage wastes on the physico-mechanical properties of cement and reinforced steel, Ain Sha. Eng. Jou., 4, pp.390, 2013. https://doi.org/10.1016/j.asej.2012.04.011

[135] P. Sandberg, , The effect of defects at the steel - concrete interface, exposure regime and cement type on pitting corrosion in concrete. (Report TVBM; Vol. 3081). Division of Building Materials, LTH, Lund University, 1998. https://portal.research.lu.se/portal/en/publications/the-effect-of-defects-at-the-steel-concrete-interface-exposure-regime-and-cement-type-on-pitting-corrosion-in concrete(fa981216-1745-49c7-b73b-f6d7e03659ca).html

[136] L. Kefei, Durability Design of Concrete structures, 1st edition, John Wiley & Sons, Singapore Pte. Ltd., 2016.

[137] A.T. Horne, I.G. Richardson, R.M.D. Brydson, Quantitative analysis of the microstructure of interfaces in steel reinforced concrete, Cement and Concrete Research, 37, 1613– 1623, 2007. https://doi.org/10.1016/j.cemconres.2007.08.026